

May 2023

Hydrogel and Soluble Polymers to Support Metal Ion Chemosensors

Rebecca Adel Dominguez
University of Wisconsin-Milwaukee

Follow this and additional works at: <https://dc.uwm.edu/etd>



Part of the [Chemistry Commons](#)

Recommended Citation

Dominguez, Rebecca Adel, "Hydrogel and Soluble Polymers to Support Metal Ion Chemosensors" (2023).
Theses and Dissertations. 3134.
<https://dc.uwm.edu/etd/3134>

This Thesis is brought to you for free and open access by UWM Digital Commons. It has been accepted for inclusion in Theses and Dissertations by an authorized administrator of UWM Digital Commons. For more information, please contact scholarlycommunicationteam-group@uwm.edu.

HYDROGEL AND SOLUBLE POLYMERS TO SUPPORT METAL ION CHEMOSENSORS

by

Rebecca A. Dominguez

A Thesis Submitted in
Partial Fulfillment of the
Requirements for the Degree of

Master of Science

in Chemistry

at

The University of Wisconsin-Milwaukee

May 2023

ABSTRACT

HYDROGEL AND SOLUBLE POLYMERS TO SUPPORT METAL ION CHEMOSENSORS

by

Rebecca A. Dominguez

The University of Wisconsin-Milwaukee, 2023

Under the Supervision of Professor Alexander (Leggy) Arnold and Professor Emeritus Alan W. Schwabacher

Most water systems contain metal ions. Some of these ions, such as lead, arsenic, and mercury, are extremely toxic. It is of great concern when those ions make their way into drinking water. There is a need for a device that can detect small amounts of dissolved metal ions in real-time. The Schwabacher group has designed such a device, based on azo dyes as the chemo sensors that change color in the presence of metal ions. These sensors can detect very small concentrations of metal ions into the parts per billion range. The sensor dyes are connected with covalent bonds to a hydrogel polymer solid support. The work herein describes the continuing development of hydrogel polymers for this application. These hydrogels are transparent and attached to glass for stability. The previous prototype worked but had some undesirable variability that can be improved upon. The length of the synthesis of the hydrogel components has been reduced while achieving higher stability and better replicability.

© Copyright by Rebecca A. Dominguez, 2023
All Rights Reserved

To myself. I finally made it through and it's time for the next adventure!

TABLE OF CONTENTS

LIST OF FIGURES	vi
LIST OF TABLES	viii
LIST OF ABBREVIATIONS	ix
ACKNOWLEDGEMENTS	xiii
Chapter 1. Introduction	1
1.1 Sensor Project Background	1
1.2 Polymers	11
1.2.1 - Structures and Synthesis	11
1.2.2 Polymerization	13
1.2.3 Free vs Controlled Radical Polymerization	17
1.2.4 Hydrogel Polymers	18
1.2.5 Hydrogels as a Solid Support for Azo Dyes	22
Chapter 2. Results and Discussion	24
2.1 Hydrogel Solid Support for a Metal Ion Chemosensor	24
2.1.1 Fenske-Hagemann Hydrogel Sensor	24
2.1.2 Synthesis of an Amine Terminated Monomer	25
2.1.3 Polymerization to Form a Hydrogel	27
2.1.4 Synthesis of an Azide Terminated Monomer.....	30
2.1.5 Cross-linker Optimization.....	31
2.1.6 4-Vinylbenzyl Azide and Relevant Polymers.....	34
2.1.7 Addressing Hydrogel Inconsistencies	35
2.1.8 Silanization of Glass	41
2.2 Soluble Polymers	48
2.2.1 – Azide Based Soluble Polymers	48
2.2.2 4-Vinylbenzyl Phthalimide and Soluble Polymers	53
2.3 Hydrogels From Soluble Polymer	61
2.4 RAFT reactions	67
2.5 Conclusion	69
Chapter 3. Experimental	71
Bibliography/Works Cited/References	113
Appendix : Spectra	118

LIST OF FIGURES

<i>Figure 1: Generalized schematic diagram of the sensor array.</i>	2
<i>Figure 2: General structure of an azo dye [ex: 4-(2-pyridylazo)resorcinol (PAR)].</i>	3
<i>Figure 3: Azo dyes of different colors and similar structures. Disperse Orange 3, Methyl Yellow, and Disperse Black¹⁴.</i>	4
<i>Figure 4: PAR Zinc association and color change.</i>	5
<i>Figure 5: Acidic method for generating azo dyes.</i>	5
<i>Figure 6: Basic method for generating azo dyes.</i>	6
<i>Figure 7: Degradation of solution based dyes over time (Joe Labeots)¹⁹.</i>	7
<i>Figure 8: Current method for attachment of azo dye to solid support.</i>	8
<i>Figure 9: Metal ion response of the high affinity sulfonamide sensor array (Trevor Hagemann)¹⁸.</i>	8
<i>Figure 10: Response of an azo dye to zinc ions; in solution and on polymer (Trevor Hagemann)¹⁸.</i>	9
<i>Figure 11: Regeneration of polymer dots via acid rinse and a period of buffering. (Joe Labeots)¹⁹.</i>	10
<i>Figure 12: Polymer architectural guide. The three main aspects of polymer architecture—composition, topology, and function—are shown separately and in combination.²³</i>	12
<i>Figure 13: Free radical polymerization of styrene with AIBN.</i>	13
<i>Figure 14: Mechanisms of controlled radical polymerization (CRP) (a) dissociation-combination, (b) degenerative chain transfer, and (c) atom transfer.</i>	14
<i>Figure 15: ATRP scheme for poly methyl methacrylate-block-styrene.</i>	15
<i>Figure 16: RAFT scheme for poly styrene-block-methyl methacrylate.</i>	15
<i>Figure 17: Example of a Chain Transfer Agent (CTA)</i>	16
<i>Figure 18: RAFT mechanism featuring polystyrene.</i>	16
<i>Figure 19: Comparison of polydispersity in traditional radical polymerization and controlled radical polymerization.</i>	18
<i>Figure 20: Classification of hydrogels flowchart²⁹.</i>	19
<i>Figure 21: Three sizes of a spherical hydrogel (Orbeez) before and after swelling⁴³.</i>	20
<i>Figure 22: A render showing water and oxygen inside the pores of a hydrogel (ex: contact lens).</i>	21
<i>Figure 23: Hydrogel volume in the uncrosslinked, relaxed, swollen, and dry states⁴⁶.</i>	22
<i>Figure 24: General reaction scheme for the formation of the hydrogel polymer supported heavy metal ion sensor - Fenske-Hagemann Hydrogel Sensor.</i>	24
<i>Figure 25: Synthesis of N-boc amine tetra(ethylene glycol) methacrylamide [5] from tetra(ethylene glycol) (TEG).</i>	25
<i>Figure 26: Free radical polymerization to form the Fenske Hydrogel [6A].</i>	27
<i>Figure 27: Application of Kapton tape mold to a hydrophobic C18 glass slide [30].</i>	28
<i>Figure 28: Filling the polymer mold.</i>	28
<i>Figure 29: Deprotection of 6A to obtain 6B, and general scheme for functionalization with the desired sensor dye and perturbation moieties.</i>	29
<i>Figure 30: Synthesis of azide tetra(ethylene glycol) methacrylamide [7] from TEG.</i>	30
<i>Figure 31: Poly(ethylene glycol) dimethacrylate (average MW 750).</i>	31
<i>Figure 32: Synthesis of bis(4-vinylbenzyl) poly(ethylene glycol) (av. MW 850) [8].</i>	32

Figure 33: Polymerization of azide monomer [7], cross-linker [8], and DEGMEMA to form hydrogels attached to glass.....	33
Figure 34: Synthesis of 4-vinylbenzyl azide [10] from 4-vinylbenzyl chloride.	34
Figure 35: Polymerization inhibitors MEHQ and BHT and their silylated analogs.	36
Figure 36: Hydrogel synthesis in the presence of BSA and with varying cross-link densities.....	37
Figure 37: Cleaning the surface of glass microscope slides.	41
Figure 38: Glass silanization in solution with TMSPM.	42
Figure 39: Gas phase silanization of glass with APTMS and subsequent reaction with methacryloyl chloride to obtain a polymerizable handle.	44
Figure 40: Large crystallization dish and lid with a rack of 5 glass slides inside.	46
Figure 41: Co-polymerization of 4-vinylbenzyl azide [10] and DEGMEMA.....	48
Figure 42: Homo-polymerization of 4-vinylbenzyl azide [10].	50
Figure 43: Reaction of poly(4-vinylbenzyl azide) [13] with triphenylphosphine.....	51
Figure 44: Hydrogenation of poly(4-vinylbenzyl azide) [13].....	52
Figure 45: Synthesis of 4-vinylbenzyl phthalimide [15] via Sn2 reaction.....	53
Figure 46: Synthesis of 4- vinylbenzyl amine HCl salt.....	54
Figure 47: Five different lengths of poly(ethylene glycol) bis(carbonyl imidazole) [17a-e].....	56
Figure 48: Homo-polymerization of 4-vinylbenzyl phthalimide [15].....	57
Figure 49: Co-polymerization of 4-vinylbenzyl phthalimide and DEGMEMA.	58
Figure 50: Synthesis of poly(4-vinylbenzyl amine) [20] from poly(4-vinylbenzyl phthalimide) [18].	58
Figure 51: 4-Vinylbenzyl amine HCl [16] polymerization to poly(4-vinylbenzyl amine HCl) [21].	59
Figure 52: Co-polymerization of 4-vinylbenzyl amine HCl [16] and HEMA.	60
Figure 53: Minimum crosslinker length; Qualitative gel tests with poly(4-vinylbenzyl amine) and poly(ethylene glycol) bis(carbonyl imidazole) [17a-e].....	61
Figure 54: Timed gel tests with poly(4-vinylbenzyl amine) and poly(ethylene glycol) bis(carbonyl imidazole) [17c-e].....	62
Figure 55: Timed gel tests with poly(4-vinylbenzyl amine HCl) and poly(ethylene glycol) bis(carbonyl imidazole) [17c,e].....	64
Figure 56: Amine terminated sillanized glass slides [31C].	65
Figure 57: Hydrogel dots attached to glass; from soluble polymer [21] and cross-linker [17c].66	
Figure 58: Grignard reaction to synthesise 1-phenylethyl dithiobenzoate [27].	67
Figure 59: RAFT polymerization of 4-vinylbenzyl amine HCl [16].....	68

LIST OF TABLES

<i>Table 1: Reagent ratios for the polymerization of hydrogels [11a-e].</i>	38
<i>Table 2: Hydrogel formations tests with free amine polymer [20]</i>	63
<i>Table 3: Hydrogel formations tests with amine HCl polymer [21]</i>	64

LIST OF ABBREVIATIONS

AAS	Atomic Absorption Spectroscopy
Abs	absorbance
AcOH	acetic acid
AIBN	azobisisobutyronitrile
APTMS	(3-aminopropyl)trimethoxysilane
aq.	aqueous
ATRP	Atom Transfer Radical Polymerization
Av.	average
BHT	butylated hydroxytoluene
Boc	tert-butoxycarbonyl
BSA	N,O-bis(trimethylsilyl)acetamide
C18	Octadecyltrichlorosilane
CI	Color Index
CDI	carbonyldiimidazole
CRP	Controlled Radical Polymerization
CTA	Chain Transfer Agent
d	doublet (NMR)
dd	doublet of doublets (NMR)
DEGMEMA	di(ethylene glycol) methyl ether methacrylate
DMF	dimethylformamide
DMSO	dimethyl sulfoxide
DNA	Deoxyribonucleic acid
DTRP	degenerate-transfer radical polymerization
EDTA	ethylenediaminetetraacetic acid
EPA	Environmental Protection Agency
Eq.	equivalent
EtOH	ethanol
h	hour

HBTU	hexafluorophosphate benzotriazole tetramethyluronium
HEMA	2-hydroxyethyl methacrylate
HPLC	High-performance liquid chromatography
Hz	Hertz
ICP-MS	Inductively Coupled Plasma Mass Spectrometry
IR	Infrared
ITP	iodine transfer polymerization
J	Coupling constant (NMR)
K _d	Dissociation Constant
LCMS	Liquid Chromatography Mass Spectrometry
M	Molar concentration
MEHQ	4-methoxyphenol / Methyl Ether of Hydroquinone
MeOH	methanol
min	minute
MOPS	3-(N-morpholino)propanesulfonic acid
MS	Mass Spectrometry
MsCl	mesyl chloride
MW	molecular weight
NMP	N-methyl-2-pyrrolidone
NMR	Nuclear Magnetic Resonance
NMRP	nitroxide-mediated (radical) polymerization
OMRP	organometallic-mediated radical polymerization
PAR	4-(2-pyridylazo)resorcinol
Pd/C	Palladium on carbon
PDI	polydispersity index
PE	polyethylene
PEG	poly(ethylene glycol)
PEGDMA 750	poly(ethylene glycol) dimethacrylate (av. MW 750)
Ph	phenyl

pH	$-\log[H^+]$, acidity
pKa	$-\log(K_a)$
PMMA	poly(methyl methacrylate)
ppm	part per million
ppb	part per billion
PS	polystyrene
PVC	poly vinyl chloride
RAFT	reversible-addition-fragmentation chain-transfer polymerization
RDRP	reversible-deactivation radical polymerization
R _f	retention factor
rt	room temperature
rxn	reaction
s	singlet (NMR)
sol	solution
SRMP	stable-radical-mediated polymerization
t	triplet (NMR)
<i>t</i>	Time
tBuOH	tert-butanol
TEG	tetra(ethylene glycol)
TEMPO	(2,2,6,6-Tetramethylpiperidin-1-yl)oxyl
TFA	trifluoroacetic acid
THF	tetrahydrofuran
TLC	thin layer chromatography
TMOF	trimethyl orthoformate
TMS	trimethylsilyl
TMSPM	3-(trimethoxysilyl)propyl methacrylate
TsCl	tosyl chloride
UV	Ultraviolet
UV-Vis	Ultraviolet-Visible spectroscopy

VBA	4-vinylbenzyl amine
VBAZ	4-vinylbenzyl azide
VBC	4-vinylbenzyl chloride
VBP	4-vinylbenzyl phthalimide
v/v	Volume/Volume
X-link	Cross-link

POLYMER NAMING – Prefixes and Connectives	
<i>poly-</i>	Polymer
Connectives for co-polymer (polymer made of different monomers) structures	
<i>-co-</i>	unspecified or unknown monomer sequence
<i>-ran-</i>	random (has Bernoullian distribution) monomer sequence
<i>-graft-</i>	side chains polyB linked to main chains polyA
Connectives or prefixes for non-linear polymers and polymer assemblies	
<i>-comb-</i>	Comb – main chain (backbone) with multiple trifunctional branch points from each of which a linear side-chain emanates
<i>net-</i>	Network – highly branched polymer in which essentially each constitutional unit is connected to each other constitutional unit by many permanent paths through the macromolecule
<i>-v-</i>	Cross-linked [Ex: poly(A-crosslinked by-B) is poly(A-v-B)]

ACKNOWLEDGEMENTS

Thank you to everyone who's accompanied me on this journey! To my partner Geno for being endlessly kind and understanding. To my friends for their encouragement, support, and advice; Robert, Katryna, Vila, Megan, Luke, Rob, Elli, Kory, Cassie, Bory, Trevor, Gabrielle, and my D&D group. To my Mom, Dad, and my siblings David and Sarah for always having my back. I couldn't have done this without you all!

Thank you to my advisors, Dr. Schwabacher for your contagious enthusiasm for chemistry and Dr. Arnold for your support and understanding, and for helping me edit this thesis. Thank you so much!

Chapter 1. Introduction

1.1 Sensor Project Background

Metal ions are present in all ecosystems, though which ones are most common vary with the local geography¹. Some metal ions such as iron, copper, and magnesium, are necessary for life while others, such as lead, arsenic, and mercury, are toxic at low concentrations^{1,2}. The presence of metal ions in drinking water has been of increasing concern as their negative effects on human health have been discovered^{1,2,3}. For example, lead was once commonly used for water pipes due to its durability⁴. It is now known that lead ions are extremely toxic and can cause decreased kidney function, reproductive problems, and negative cardiovascular effects^{2,3,5}. Lead ions accumulates in the body over time as it is stored in bones like calcium⁵. The United States Environmental Protection Agency (EPA) has accordingly set the maximum containment level goal for lead in drinking water at zero⁵. Though the most toxic metal ions are of particular concern, any metal ion can be harmful in high concentrations².

The detection and subsequent removal of heavy metal ions in drinking water is a public health concern. The EPA has set legal limits for over 90 contaminants in drinking water, including metal ions^{1,2}. However, there are issues with compliance, and multiple cities and towns are in severe violation of the EPA regulations¹. Some of this is due to issues with infrastructure and the large cost of repairing old plumbing. Another difficulty is water testing and accurately treating it to EPA standards. The removal of metal ions from water relies on polymers and sedimentation^{6,7}. Many industries conduct their own water treatment but rely on outside labs for testing⁸. Testing for contaminants involves taking a sample, sending it off for

analysis, and waiting for results to get sent back. This is inherently a slow process. The testing itself is also costly, relying on specialized analytical instruments, such as flame AAS and ICP-MS⁸.

A system with faster quantification of metal ions that can be done on site is highly desirable. The Schwabacher group in collaboration with Aqua Metals, a local startup company, conceptualized a sensor system that would quantify metals in real-time. The system would be placed in a continuous flow of water constantly sampling and outputting the concentration of the target analyte. Rather than using ICP-MS or AAS, the design would take advantage of UV spectroscopy. This would decrease the cost of instrumentation and increase the speed of measurement to the speed of light.

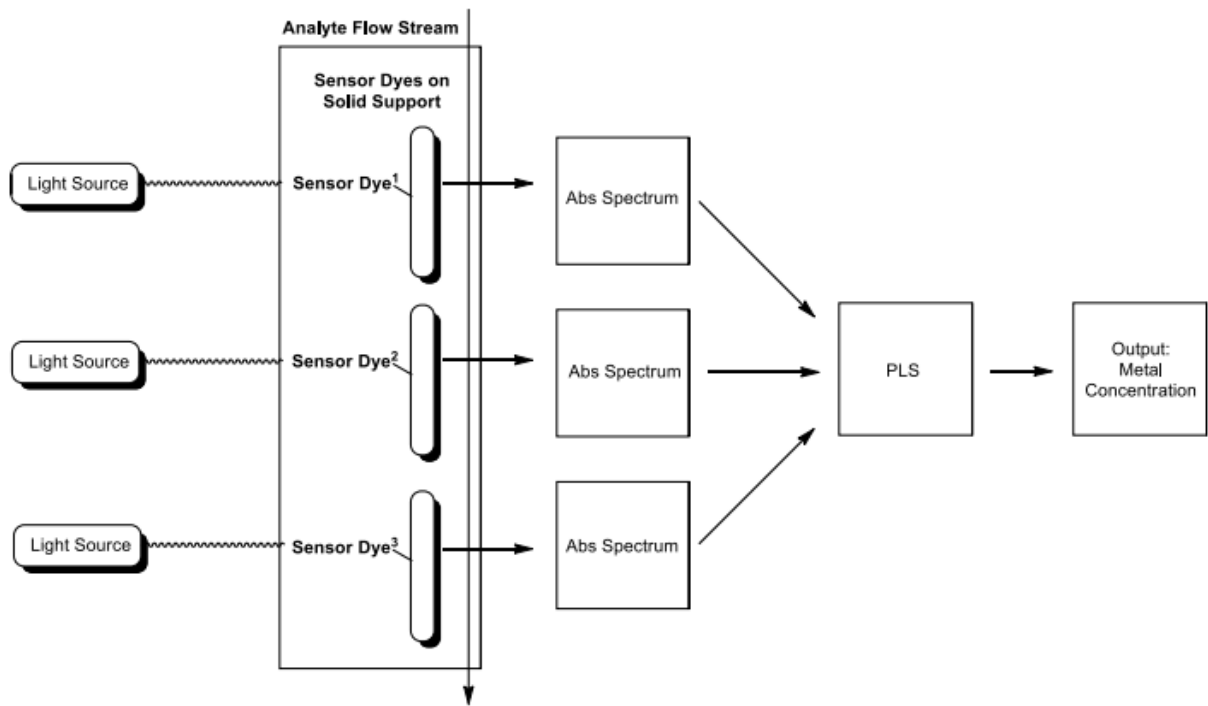


Figure 1: Generalized schematic diagram of the sensor array.

This system was designed as an array of sensors each detecting and differentiating different metal ions. For this to work there were several key requirements; first a sensor that would have a measurable change in absorbance in the presence of heavy metal ions, and second a support that the sensor would be attached to so it would not be washed away. The support also needed to be transparent to avoid interference with the UV spectroscopy measurements.

The class of sensors chosen were azo dyes, which have been widely used as colorants in a variety of industries and are known to chelate metals in some cases^{9,10}. The composition of an azo dye includes at least one azo bond and aromatic groups, either phenol or aniline based.

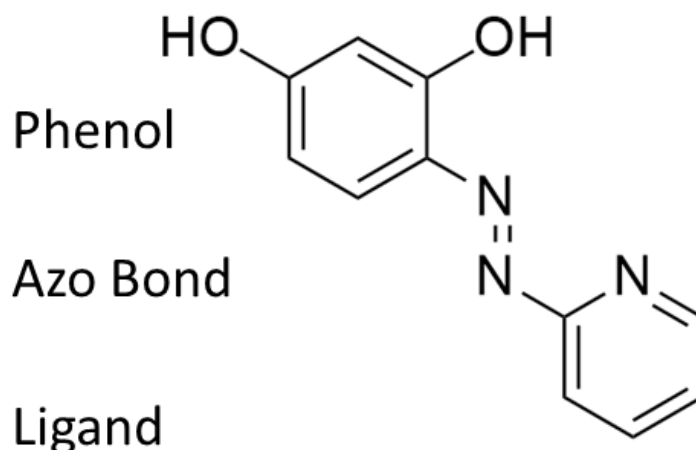


Figure 2: General structure of an azo dye [ex: 4-(2-pyridylazo)resorcinol (PAR)].

The properties of azo dyes vary, as small variations in their structure can result in widely different functionality¹¹. There are thousands of different azo dyes, each one with distinct properties. In the Color Index (CI) system (a dye classification system developed by the society of dyers and colorists) azo dyes are supplied with numbers ranging from 11,000 to 39,999 in correspondence with the chemical structure^{12,13}. Dyes with a single azo bond are given numbers

11,000 to 19,999. Figure 3 shows a few examples of azo dyes that are relatively similar in structure but vary in color from orange to yellow to black¹⁴.

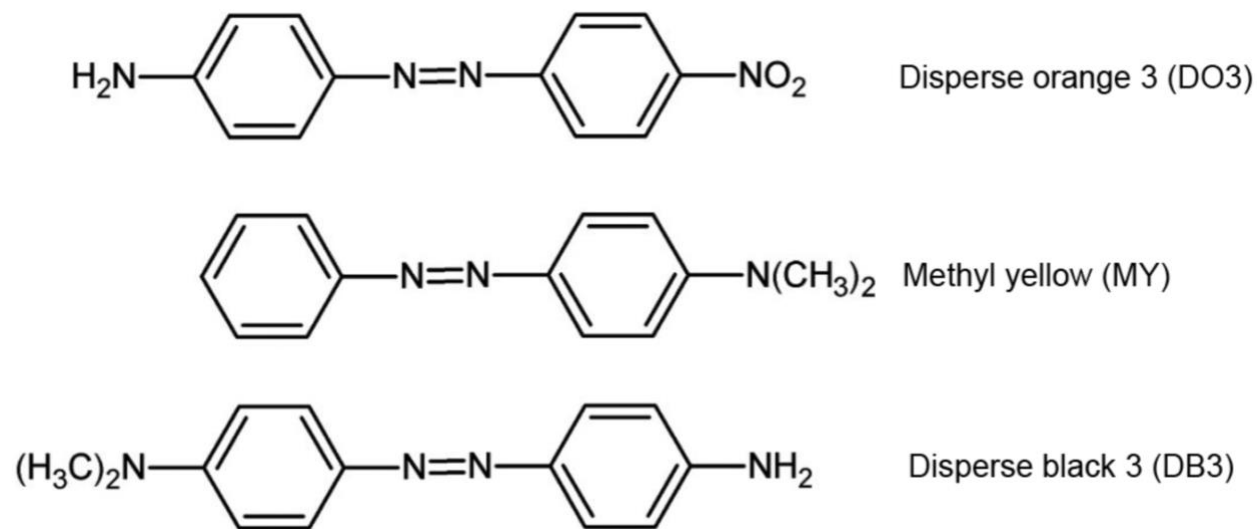


Figure 3: Azo dyes of different colors and similar structures. Disperse Orange 3, Methyl Yellow, and Disperse Black¹⁴.

Among the azo dyes known to chelate metals, the most well-known example is 4-(2-pyridylazo)resorcinol (PAR)¹⁰. PAR tends to ligate divalent metal ions, changing color and absorbance in response to doing so. The response can be measured by UV-Vis spectroscopy and has been associated with the formation of a 2:1 complex of 2 PAR:1 metal ion. PAR isn't selective for all divalent metal ions; only resulting in absorbance changes for Ni, Cu, Zn, and Co. For these ions, the concentrations can be determined down to ppb levels using UV-Vis spectroscopy.



Figure 4: PAR Zinc association and color change.

Azo dyes can be synthesized in multiple ways^{11,15-17} but the majority fall into one of two categories, the acidic method via a diazonium compound or the basic method via a diazotate.

Acidic Method - Diazonium

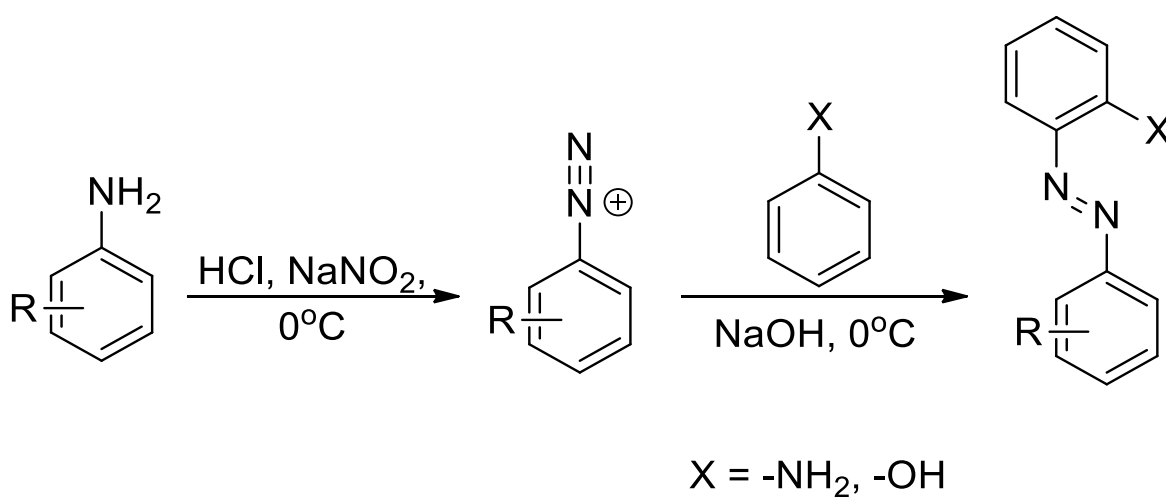


Figure 5: Acidic method for generating azo dyes.

The acidic method generally involves combining an aniline with acid and nitrate to form a diazonium salt, which is then used in an electrophilic aromatic substitution reaction with a phenol or aromatic amine. This method works best with electron rich aromatic amines. The reaction generally does not proceed with electron poor aromatic amines under these conditions.

Basic Method - Diazotate

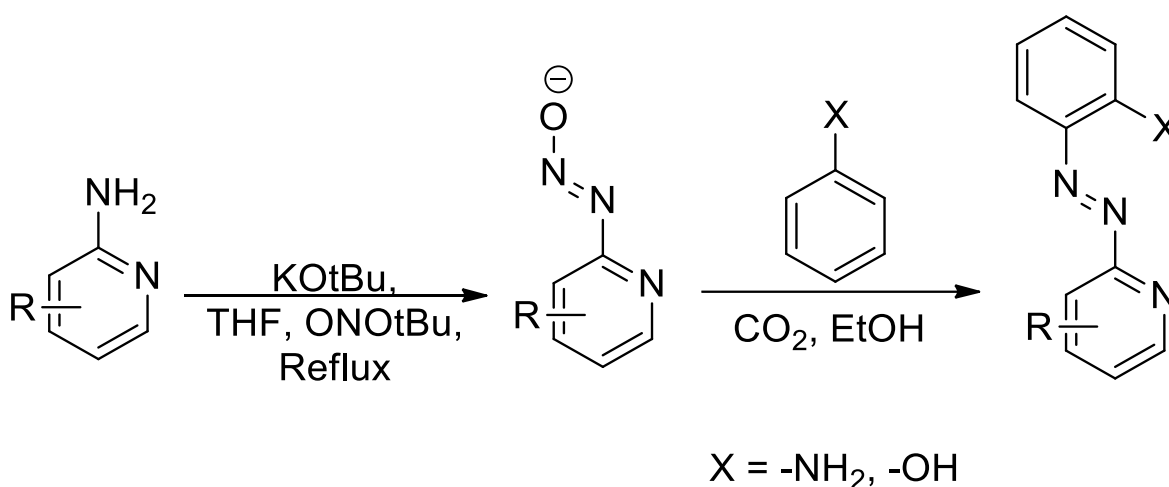


Figure 6: Basic method for generating azo dyes.

Electron poor aromatic amines require harsher conditions in order to form azo dyes, such as those used in the basic method.

This reaction works by deprotonation of 2-aminopyridine followed by substitution of the *tert*-butyl nitrite to form a diazotate. The diazotate is then suspended in EtOH containing the phenol/aromatic amine and CO₂ is bubbled through the reaction mixture over multiple days as a coolant and buffer. This allows for the slow conversion of diazotate to diazonium under slightly basic conditions and facilitates the coupling. This process is unfortunately incredibly

slow and often poor yielding, on the order of 20 – 50 % and occasionally above 70% after multiple days.¹⁸

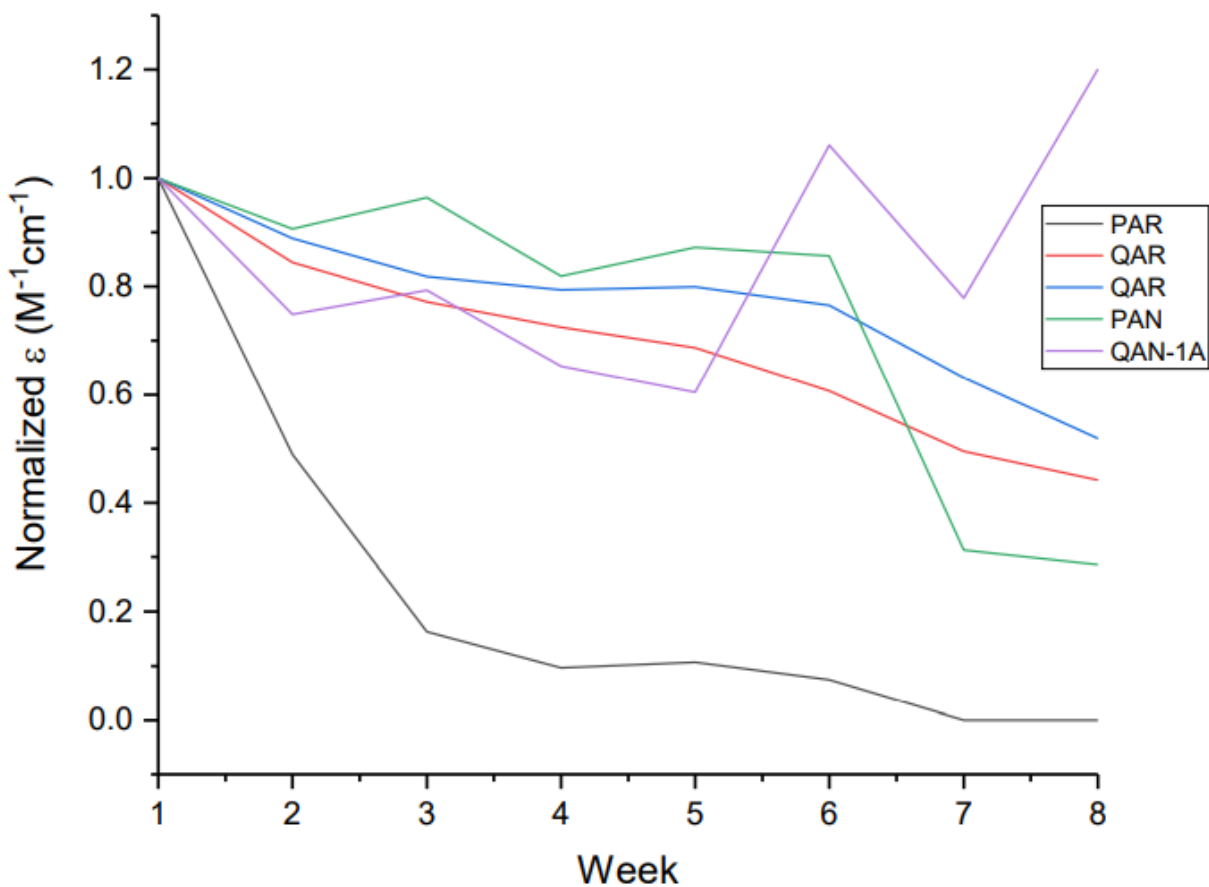


Figure 7: Degradation of solution based dyes over time (Joe Labeots)¹⁹.

A large library of azo dyes were synthesized by Trevor Hagemann¹⁸ and Katryna Williams²⁰. Unfortunately, azo dyes tend to isomerize or degrade over time as depicted in Figure 7. However, when covalently attached to a solid support the azo dyes are much more stable. A cellulose solid support was initially investigated by Sarah Oehm²¹, but the translucency proved to be an issue. A hydrogel on glass solid support was developed by Tyler Fenske²², and further modified by myself as described in this work. Further information will be given in the second chapter.

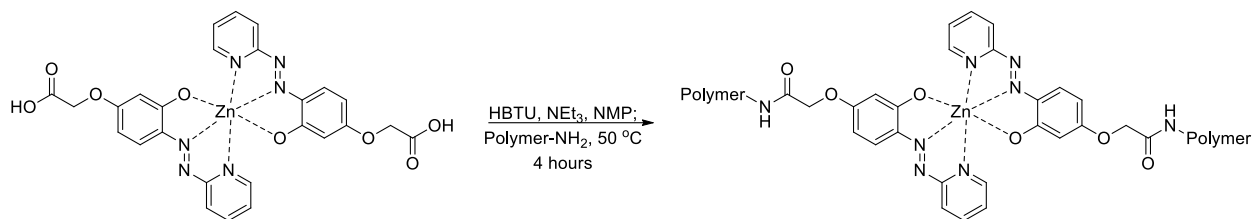


Figure 8: Current method for attachment of azo dye to solid support.

The azo dyes were modified by Trevor Hagemann to have a carboxylic acid functionality; which facilitated coupling reactions using HBTU to attach the dye to the polymer solid support. The dyes are very sensitive to their environment, resulting in a very visible color change as well as a change in absorbance in response to changes in the surrounding conditions. The dyes were studied in solution by Joe Laboets (Aldstadt group), who found them to respond to changes in solvent and pH in addition to different metal ions and different ion concentrations¹⁹.

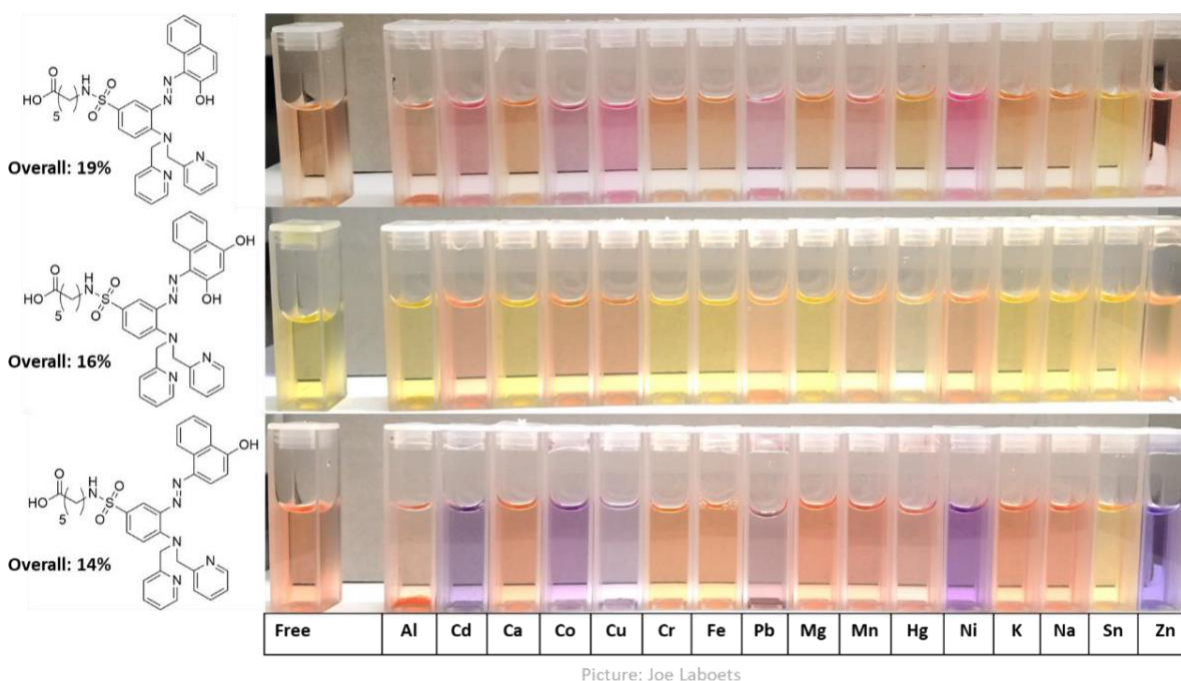


Figure 9: Metal ion response of the high affinity sulfonamide sensor array (Trevor Hagemann)¹⁸.

Each of the azo dyes has a different selectivity and response to different metal ions. A small selection of dyes and their responses are shown in Figure 9. The different responses can be taken advantage of in the design of the sensor array. Though each dye response to multiple metals, in theory, cross-referencing the absorbance readings from several different dyes allows for differentiation and determination of which metal ions are in solution.

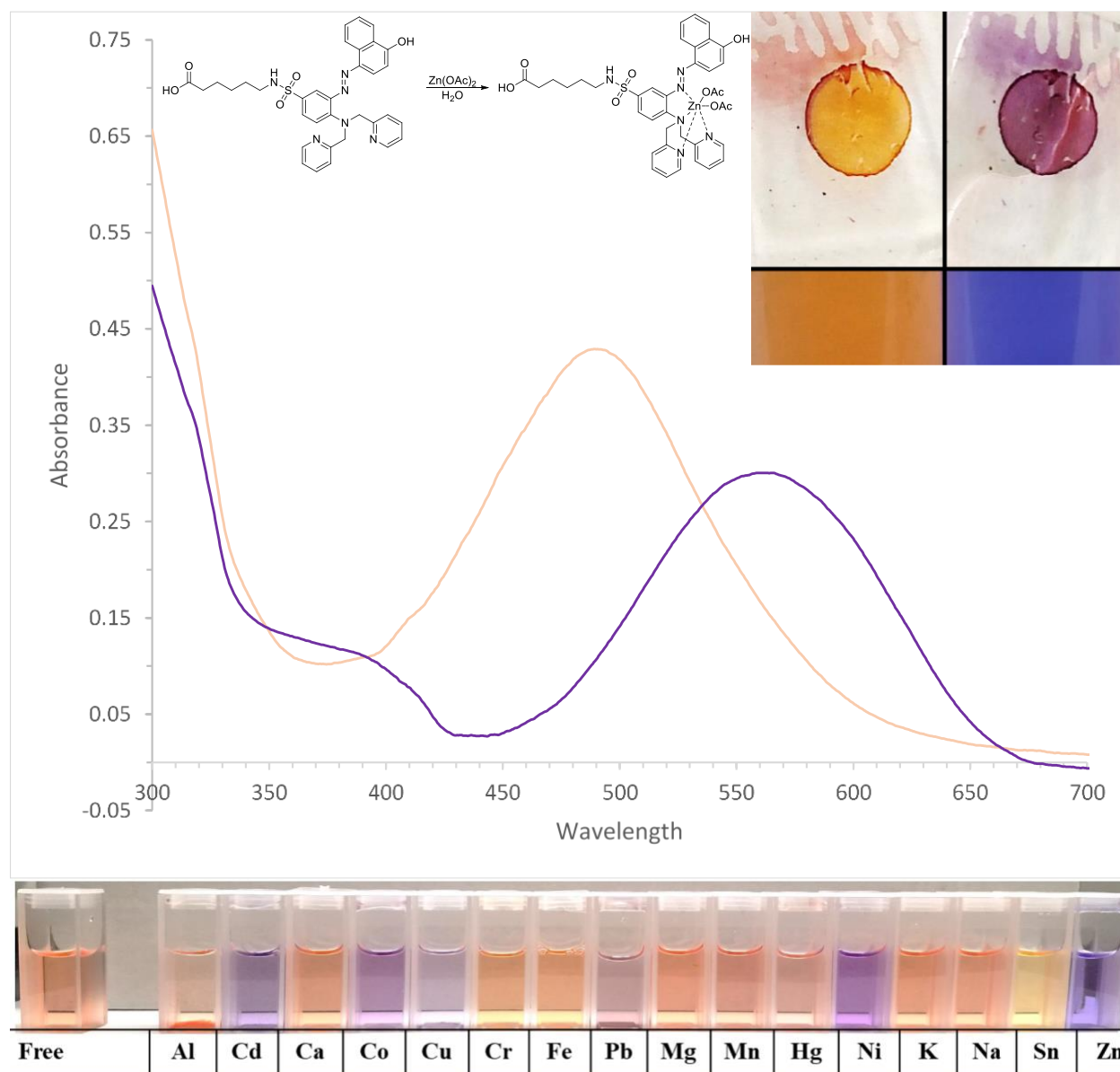


Figure 10: Response of an azo dye to zinc ions; in solution and on polymer (Trevor Hagemann)¹⁸.

Figure 10 shows an example of the visible color change of a dye both attached to a polymer and in free solution when in the presence of zinc ions. The absorbance spectrum of the dye changes drastically after ligating zinc ions.

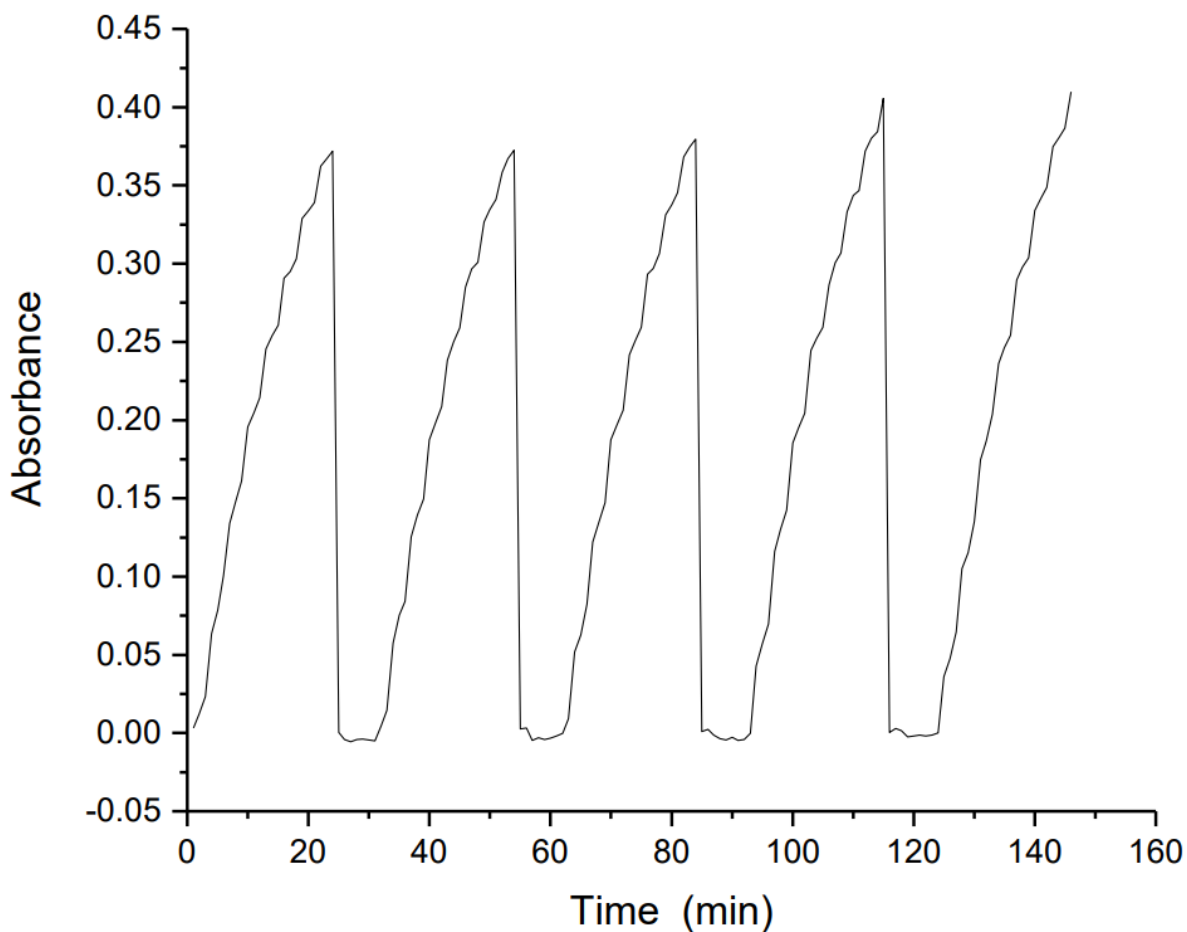


Figure 11: Regeneration of polymer dots via acid rinse and a period of buffering. (Joe Labeots)¹⁹.

The low affinity sensor dyes synthesized by Trevor Hagemann as well as the dyes optimized for lead detection synthesized by Katryna Williams could have the metal ions washed out from them with mild acid. The sensors could then be reused and continue detecting metal ions. Joe Labeots¹⁹ showed that the absorbance measurements were repeatable between acid wash cycles. This shows the sensor dyes to be stable and reusable when attached to a solid support. This is further supported by the fact that some sensors given to Aqua Metals were still

providing consistent measurements for over a year, and in one case (sensor 008) over 2 years. The useful lifetime of the sensor gels has not been determined, as degradation of azo dyes attached to polymer has yet to be observed to date.

1.2 Polymers

Polymers are a class of substances, natural and/or synthetic, that are composed of macromolecules which in turn are composed of smaller chemical units called monomers. Naturally occurring polymers include proteins, nucleic acids such as DNA, and starch. The most common synthetic polymers are plastics such as acrylic/poly methyl methacrylate (PMMA), polyethylene (PE), and polyvinyl chloride (PVC), and rubbers such as latex, polybutadiene, neoprene, and silicone. Polymers are used in clothing, paints, glue, cookware, tires, electronics, machinery, and many other implementations. Polymers are very ubiquitous and remain a very active field of chemical research as more uses for them are discovered.

1.2.1 - Structures and Synthesis

The larger structures of polymers are composed of monomers as the smaller building blocks. There are several aspects of polymer architecture. The first is chain composition, how the individual monomer units are arranged. A polymer composed of a single type of monomer is a homo-polymer, and a polymer composed of two or more monomer types is a co-polymer. Monomer units within a co-polymer can be arranged in many ways. Block co-polymers contain multiple homo-polymer subunits. Periodic co-polymers have a repeating pattern. Gradient co-polymers have a monomer sequence that gradually changes along the chain length. Statistical co-polymers have a random monomer distribution that follows a statistical rule.

A polymer's topology describes the spatial arrangement of the polymer chains. Some examples are linear polymers which are straight chains, and cyclic polymers which have a ring-like structure. Branched polymers encompass anything that has at least one branch point; specific types are usually named according to the overall shape such as comb, brush, star, etc. graft polymers are specifically where side polymer chains of type B are linked to the main chains (backbone) that are type A. Networks have all of the polymer chains interconnected with each other; this can be by cross-links, entanglements, etc. A functionality within the polymer architecture describes the placement of reactive functional groups. General examples of the architectural elements both individually and combined are shown in Figure 12.

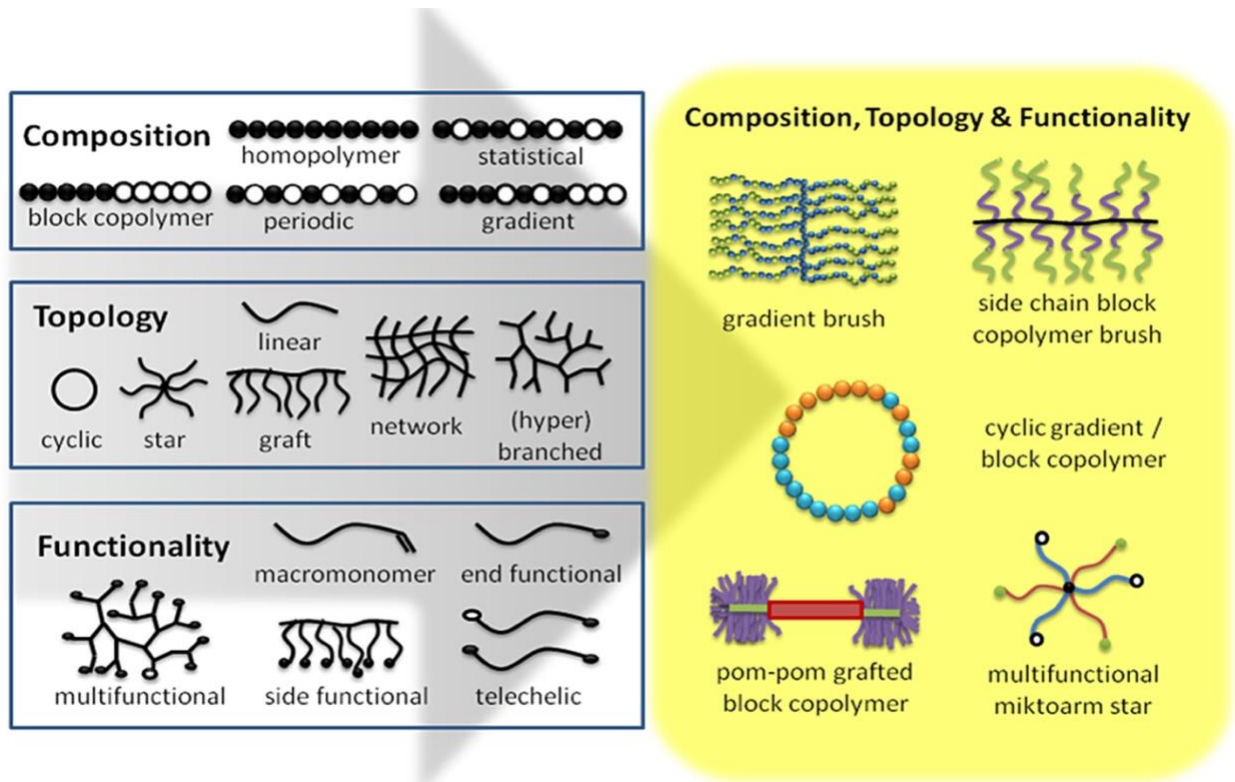


Figure 12: Polymer architectural guide. The three main aspects of polymer architecture—composition, topology, and function—are shown separately and in combination.²³

1.2.2 Polymerization

There are over a dozen types and subtypes of polymerization. We will be focusing specifically on radical polymerization. The mechanism of free radical polymerization consists of 3 parts, initiation (the generation of free radicals), propagation (a chain reaction that increases the polymer chain length), and termination (the destruction of radicals). A mechanistic scheme for the radical polymerization of styrene with radical initiator AIBN is shown below.

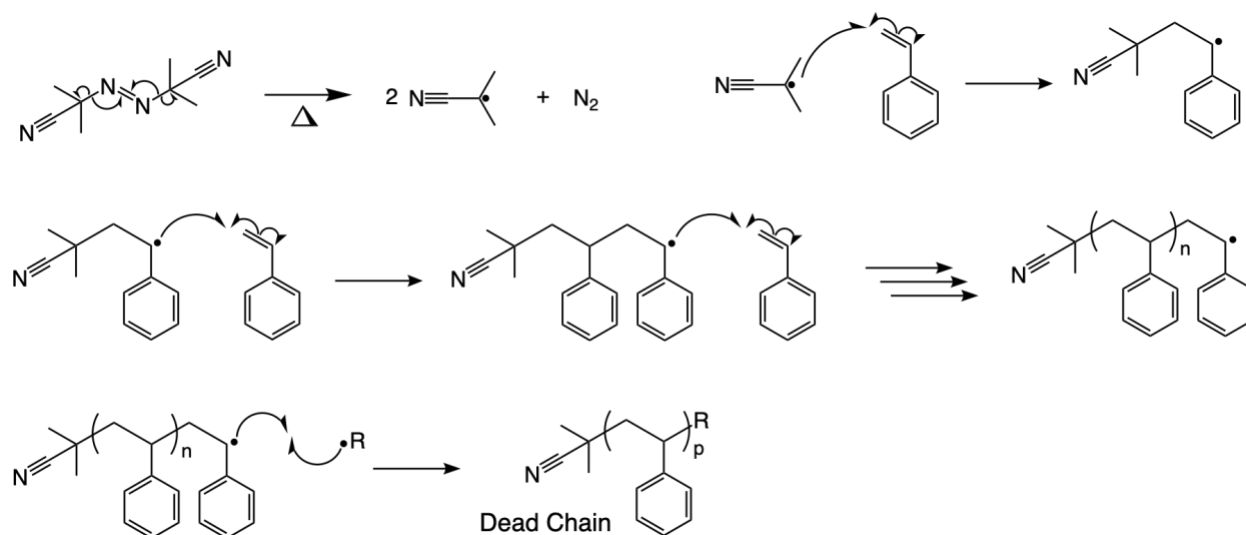


Figure 13: Free radical polymerization of styrene with AIBN.

Free radical polymerization works but has several drawbacks. These drawbacks include uncontrolled molecular weight distribution and monomer sequencing. One of the factors that impacts the physical properties of polymers is molecular weight. Higher molecular weight improves the polymers mechanical properties (break and impact strength) and increases the glass transition temperature and melting point. An increase in the width of the molecular weight distribution curve and polydispersity negatively impacts the tensile strength. It also increases the variability of results when repeating a reaction.

The alternative is Controlled (“Living”) Radical Polymerization (CRP) or Reversible-Deactivation Radical Polymerization, (RDRP), which has seen ever increasing interest over the past two decades^{24,25}. There are three main types of RDRP; Stable-Radical-Mediated Polymerization (SRMP) which includes Nitroxide-Mediated (Radical) Polymerization (NMRP) and Organometallic-Mediated Radical Polymerization (OMRP); Atom-Transfer Radical Polymerization, (ATRP); and Degenerate-Transfer Radical Polymerization (DTRP), which includes Reversible-Addition-Fragmentation chain-Transfer polymerization (RAFT) and Iodine Transfer Polymerization (ITP)²⁶.

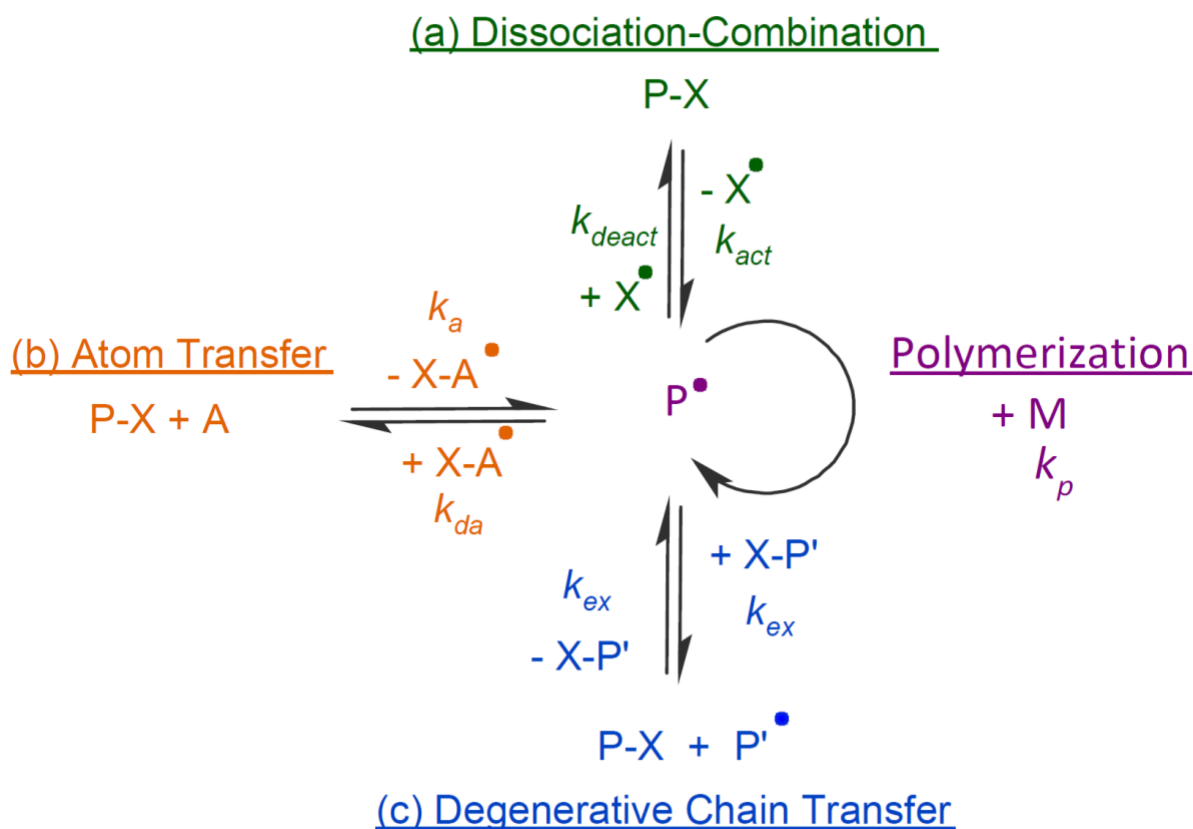


Figure 14: Mechanisms of controlled radical polymerization (CRP) (a) dissociation-combination, (b) degenerative chain transfer, and (c) atom transfer.

SRMP, particularly NMRP, is the oldest method but is less versatile than the others. It takes advantage of radical traps such as TEMPO to cap the end of the propagating polymer chain and control the kinetics via the dissociation-combination mechanism in Figure 14. This method would work for polymerizing the monomers synthesized herein. It was not used in this case as suitable nitroxide radicals were unable to be obtained due to cost.

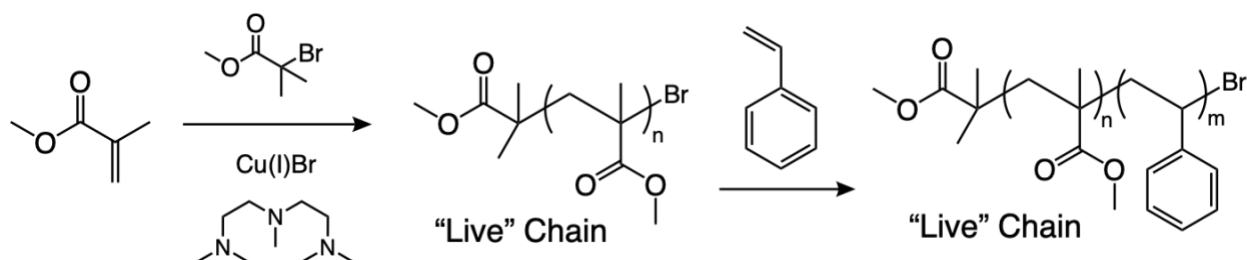


Figure 15: ATRP scheme for poly methyl methacrylate-block-styrene.

ATRP has a dormant polymer chain and a transition metal complex that are passing a halide back and forth. When the polymer chain is not bearing a halide, it is an activated radical and can propagate briefly before returning to being dormant again. ATRP is not ideal for this application because of the metal initiator. Any trace amount of initiator that is not removable from the polymer would become a source of interference in the final sensor as the azo dyes are designed to chelate metal ions.

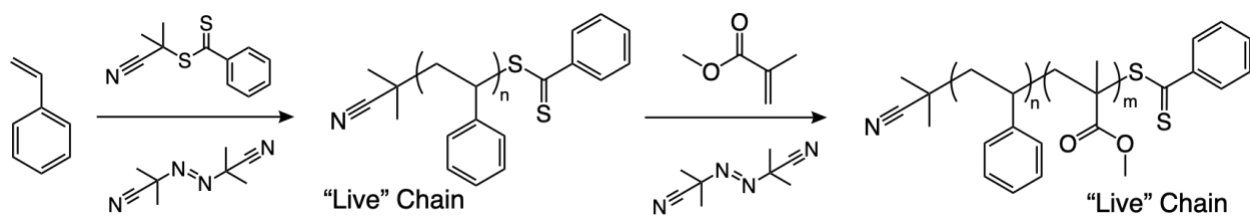
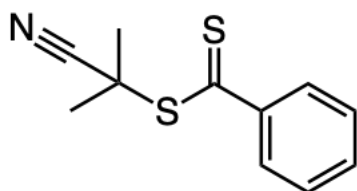


Figure 16: RAFT scheme for poly styrene-block-methyl methacrylate.

The third type of CRP is Degenerate-Transfer Radical Polymerization (DTRP). The most studied version of DTRP is Reversible Addition/Fragmentation Chain Transfer Polymerization (RAFT). An example RAFT synthesis scheme is shown in Figure 16. The key to polymerization control is the chain transfer agent (CTA).



Chain Transfer Agent (CTA)

Figure 17: Example of a Chain Transfer Agent (CTA)

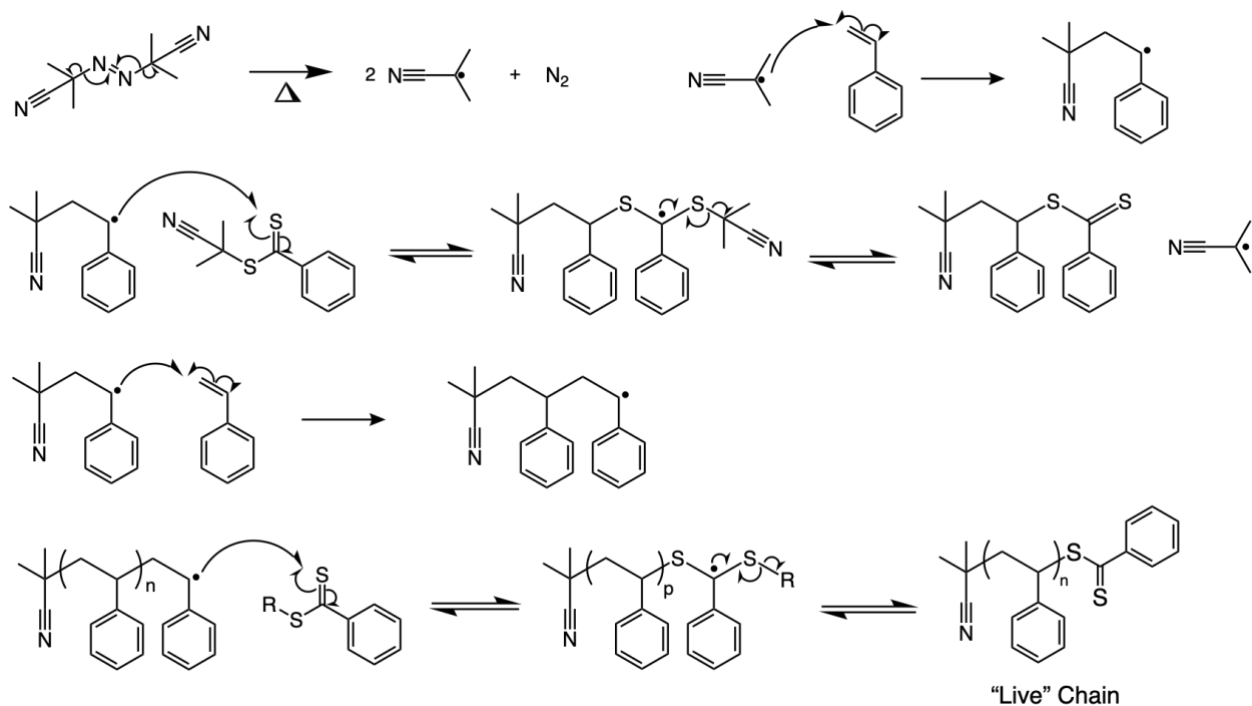


Figure 18: RAFT mechanism featuring polystyrene.

The main propagation in RAFT is an equilibrium between the propagating polymer chain radical, the RAFT radical CTA adduct, and the dormant chain.

1.2.3 Free vs Controlled Radical Polymerization

Each of the controlled radical polymerizations adds extra steps to the propagation cycle so that most of the polymer chains are dormant at any particular time. This limits the number of active radicals and therefore the number of unwanted termination steps. The amount of radical initiator in a CRP is much lower than in a regular radical polymerization, barely enough to start the reaction. The main source of radicals that begin the polymer chains are from the chain transfer agents, initiating all the polymer chains at about the same time. Ideally the number of polymer chains should be equal to the number of chain transfer agent molecules. This gives a great degree of control over the length and molecular weight of the polymer chains. Because the propagating chains are in equilibrium with chain transfer agent adduct the dormant chains of the polymer chains are growing at the same rate. This, combined with the minimalization of termination steps and mass initiation at the beginning of the reaction, produces polymer chains that are all roughly the same length. Contrast to the regular free radical polymerization where termination steps are more common, initiation of new chains happens throughout the entire reaction. As free radical polymerization goes on and the concentration of monomers available in solution decreases, the number of short chains increases since new chains are still being initiated. The number of termination steps cause chains to stop growing somewhat randomly throughout the entire duration of the polymerization reaction. These differences are reflected in the molecular weight distribution and polydispersity index (PDI). PDI is M_w/M_n , where M_w and M_n are the weight average and number average molecular weight, respectively. PDI is also the width of the molecular weight distribution curve at half height.

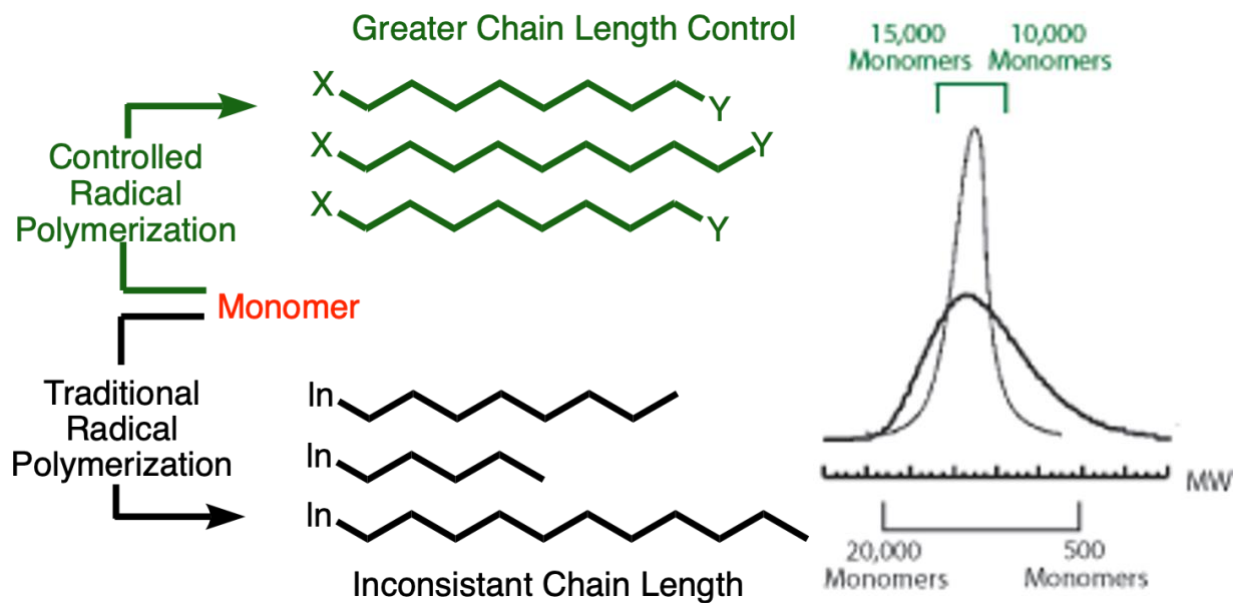


Figure 19: Comparison of polydispersity in traditional radical polymerization and controlled radical polymerization.

Figure 19 shows a visual comparison of controlled radical polymerization (CRP) and traditional radical polymerization. The two molecular weight distribution curves on the right are very different though the average molecular weight appears to be the same for both polymers.

1.2.4 Hydrogel Polymers

A hydrogel polymer is a three-dimensional polymer network where water fills the space between macromolecules. These networks are usually cross-linked in some way, so they don't dissolve in water. Cross-links can be either chemical, usually via covalent bonds, or physical such as chain entanglements or other physical interactions including hydrogen bonds, ionic interactions, and hydrophobic interactions²⁷. Hydrogels can be further classified based on source, composition/preparation, physical properties, ionic charge, response to stimuli, and biodegradability²⁸. These classifications are summarized in Figure 20.

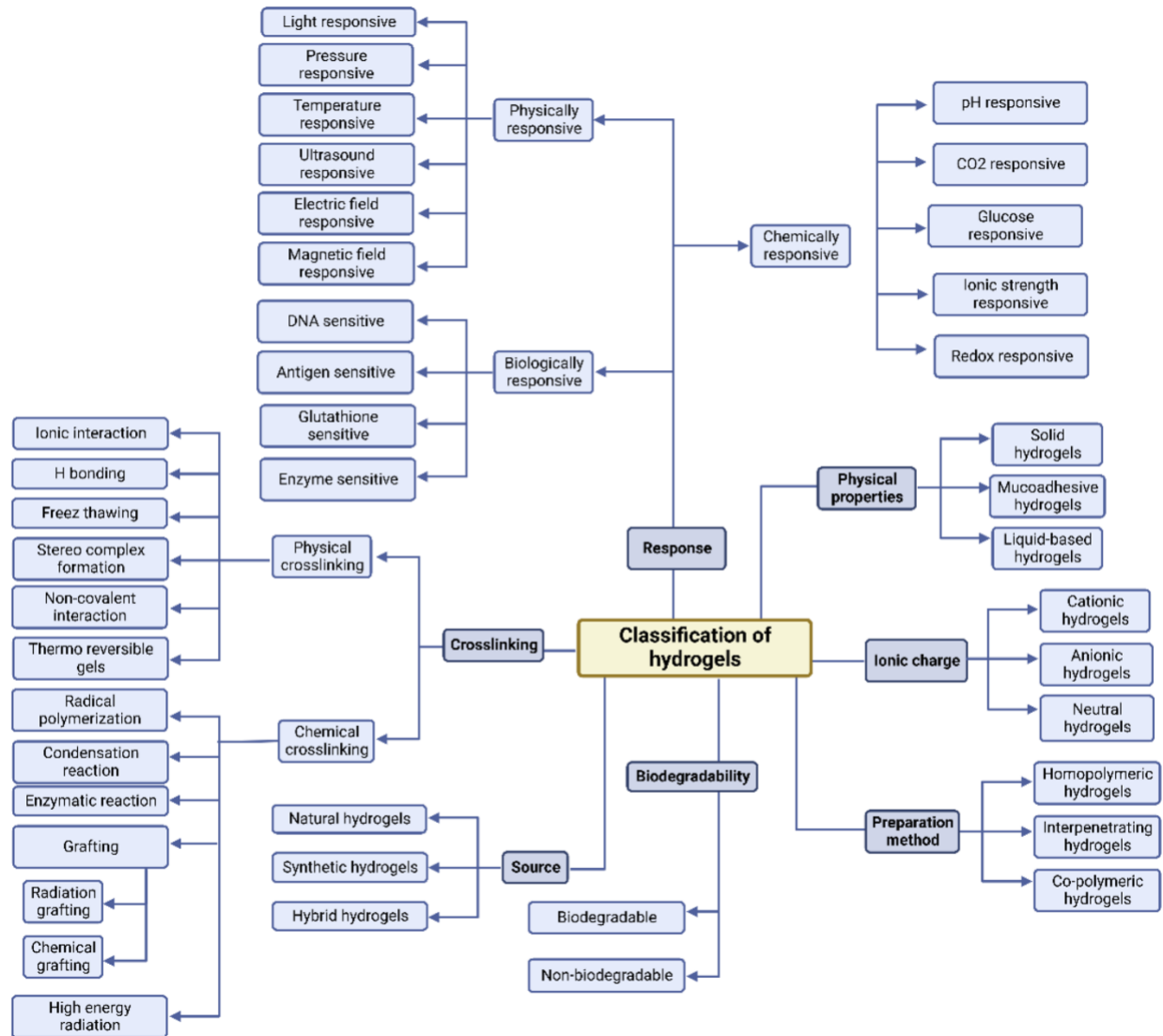


Figure 20: Classification of hydrogels flowchart²⁹.

The first hydrogels were recorded in 1960³⁰, resulting from the need for a plastic that could remain in contact with living tissue. Hydrogels have remained an active field of research for the past 6 decades. As opposed to the many polymers that are hard plastics, hydrogel polymers have several distinguishing characteristics. Hydrogels are permeable, flexible, and absorb and retain water while maintaining the network structure. Hydrogels are also extremely customizable; physiochemical properties such as strength, toughness, conductivity, anti-

adhesion, elasticity, stretch ability, adhesiveness, self-healing, etc. can be manipulated to meet the requirements of the desired application. The development of stimuli responsive hydrogel polymers has further increased their appeal^{31,32}. Biomedical applications for hydrogels encompass a large scope³³, including contact lenses³⁴, wound dressing, drug delivery³⁵, tissue engineering³⁶, dental materials, cell therapy, and sanitary pads³⁷. Other applications include agriculture³⁵, fake snow, food additives, energy storage³⁸, soft robotic devices, construction, textiles³⁹, actuators⁴⁰, and sensors^{41,42}.

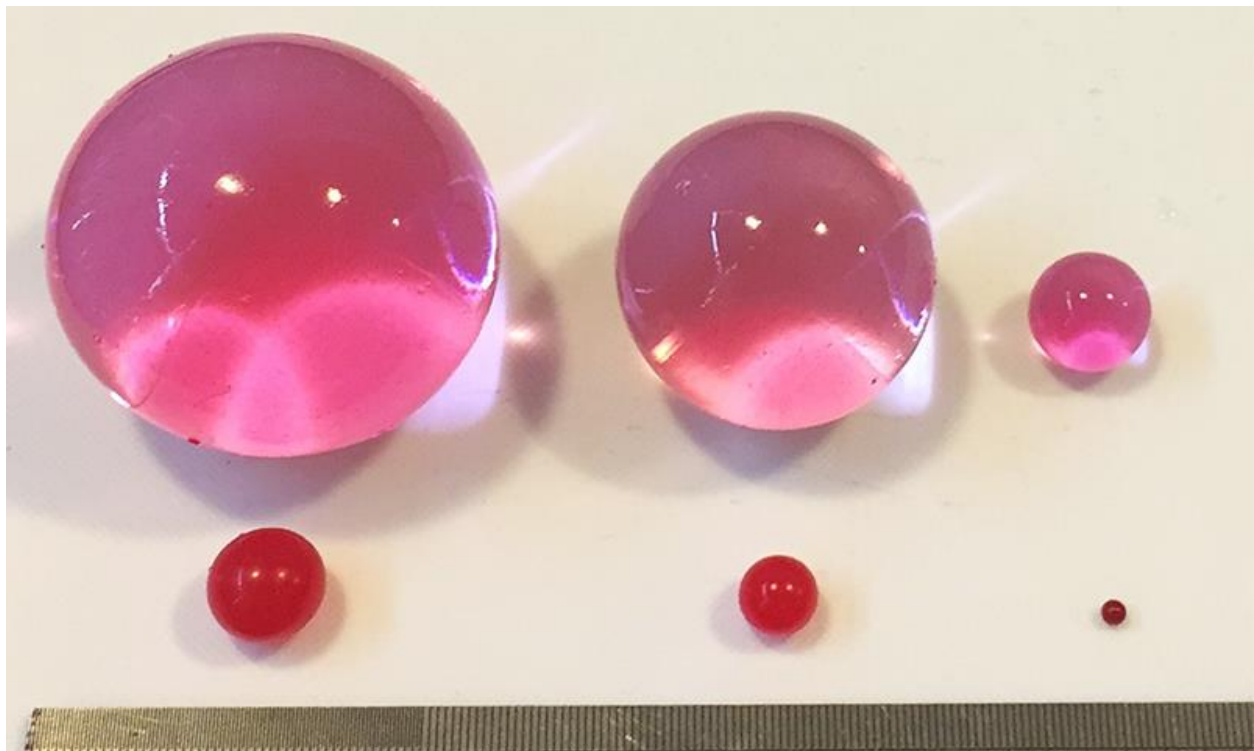


Figure 21: Three sizes of a spherical hydrogel (Orbeez) before and after swelling⁴³.

The main feature of a hydrogel is water absorption and retention, with water comprising anywhere between 10% to 90% of the total mass⁴⁴. Swelling refers to the change in volume of a gel as it absorbs a solvent. The elements of the polymer network that affect the properties of the hydrogel, including swelling, are the monomers, monomer concentration,

cross-link density, cross-link type, and porosity^{27,32}. External factors, such as solvent, pH, temperature, pressure, and ionic strength^{32,45}, among others⁴⁴ also influence said properties (see the “response” branch in Figure 20). The ability of a hydrogel to absorb water is due to the presence of hydrophilic functional groups in the polymer network. Cross-linking helps maintain the network structure and control water absorption.

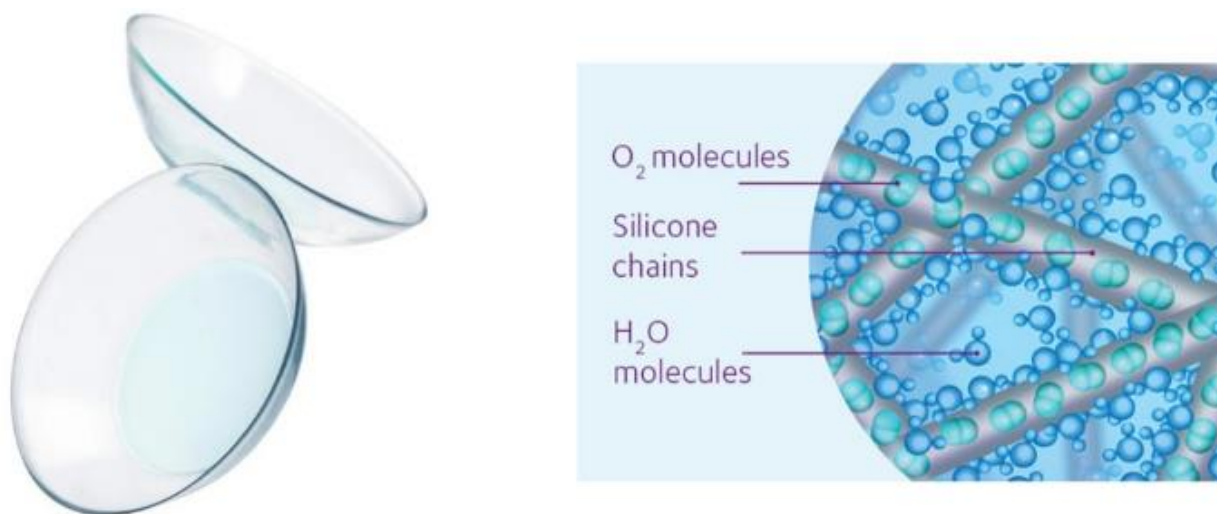


Figure 22: A render showing water and oxygen inside the pores of a hydrogel (ex: contact lens).

As depicted in Figure 22, the water molecules inside a hydrogel are associated with the hydrophilic polymer chains and fill in the pores in the gel. When the hydrogel network is first formed it's generally in a relaxed state, the space between the molecule chains dependent on the original monomer concentration. When introduced to excess water, the hydrogel will swell until it reaches equilibrium. Water will continue to be absorbed until the network is stretched out in the pores can't expand any further to absorb more water. Cross-linking causes the formation of the gel network and pores; thus, a higher cross-link density results in more pores that are smaller in size. The cross-links limit the mobility of the polymer chains, allowing for less

expansion and less swelling. Conversely, removing the water by drying the hydrogel decreases the volume and swelling until the pores are completely compressed.

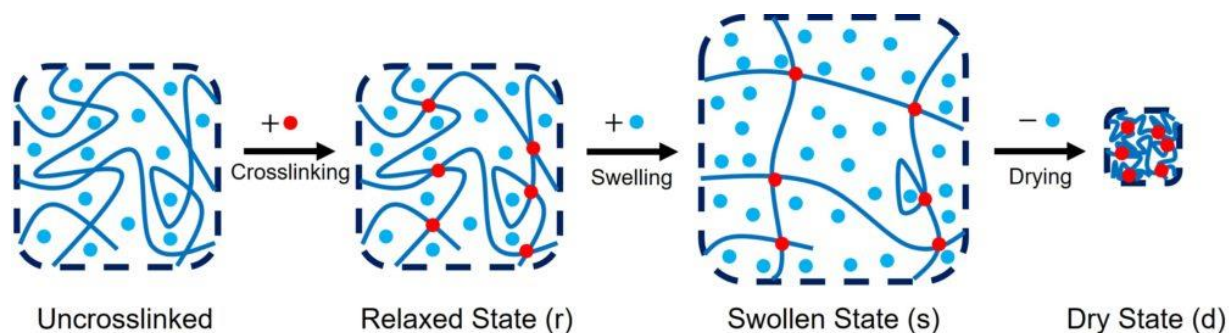


Figure 23: Hydrogel volume in the uncrosslinked, relaxed, swollen, and dry states⁴⁶.

1.2.5 Hydrogels as a Solid Support for Azo Dyes

Several qualities are necessary in the support for the sensor dyes; water compatibility; transparency for UV spectroscopy; high enough porosity to allow a continuous flow of water; hydrolytic stability; and ability to be handled. The customizability and water compatibility makes a hydrogel polymer ideal as a solid support for the sensor dyes. Hydrogels are water compatible, with transparency and porosity fully customizable. Choosing appropriate monomers and cross-linker provides hydrolytic stability and functional groups to attach the dye to. The only caveat is that most mechanical properties are a tradeoff. The hydrogel needs to be thin for both water flow and transparency. A high porosity gel has higher elasticity and transparency but less tensile strength; a thin film would be very delicate and hard to handle. There are several ways to reinforce a hydrogel, such as a dual network where 2 polymer networks with symmetrical properties (one strong but brittle and one weak but flexible) are woven together⁴⁷. However, the most straightforward method is adding another layer of support. The hydrogel sensor is stationary and does not need to bend or stretch aside from

swelling. Immobilizing the gel on a rigid support would allow it to be handled without sacrificing any of the desired properties. The best options for a clear solid support are the same materials used for cuvettes, glass, PMMA, and PS. Surface modification methods are known for all three⁴⁸⁻⁵⁰, but glass was chosen for its higher heat tolerance and scratch resistance.

Chapter 2. Results and Discussion

2.1 Hydrogel Solid Support for a Metal Ion Chemosensor

2.1.1 Fenske-Hagemann Hydrogel Sensor

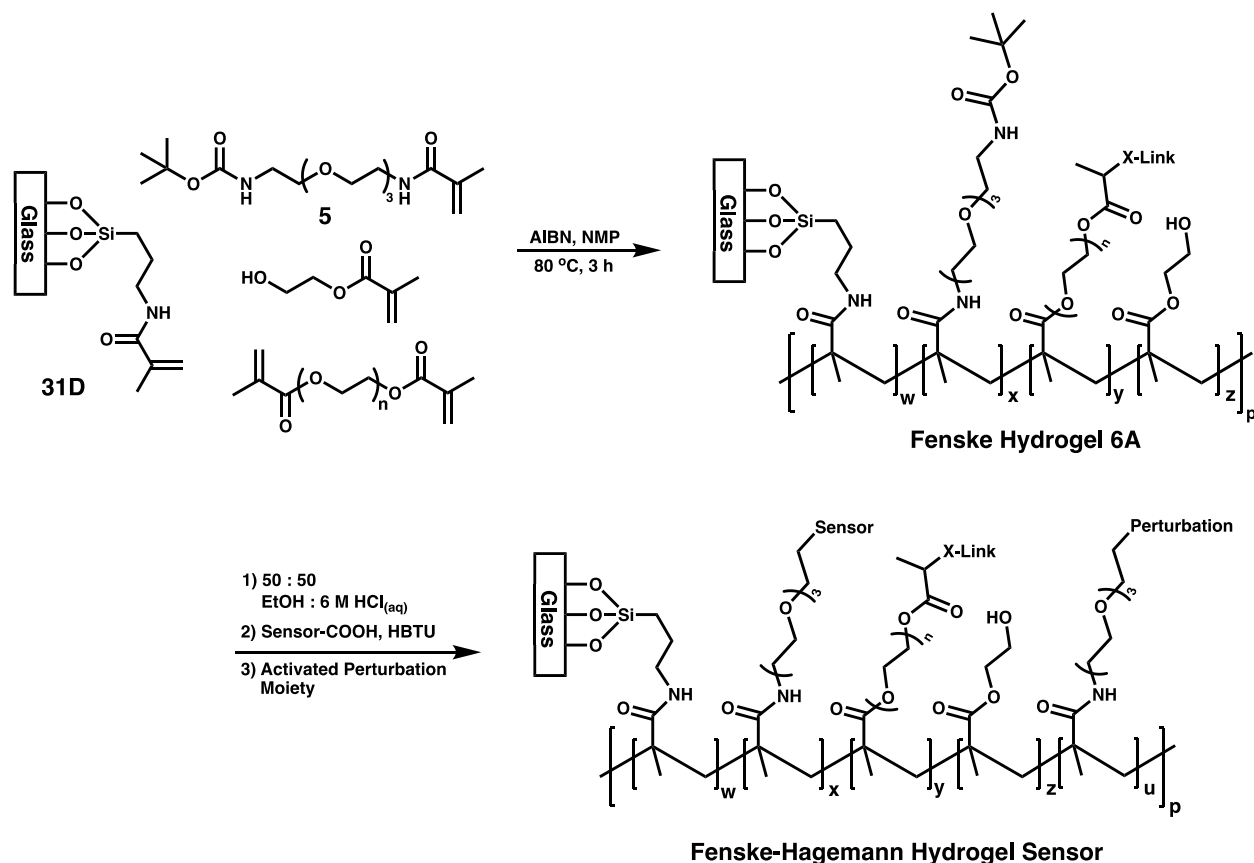


Figure 24: General reaction scheme for the formation of the hydrogel polymer supported heavy metal ion sensor - Fenske-Hagemann Hydrogel Sensor.

The polymer developed for the sensor project was the Fenske hydrogel [6A], consisting of 2 monomers, N-boc-amine tetra(ethylene glycol) methacrylamide [5] and 2-hydroxyethyl methacrylate (HEMA), with a cross-linker, poly(ethylene glycol) dimethacrylate (av. MW 750) (PEGDMA 750), all polymerized on a glass slide silanized with N-(3-(trimethoxysilyl)propyl) methacrylamide.

The boc-amine terminated side chains can be deprotected under acidic conditions, a solution of 50:50 EtOH:6M HCl. The inclusion of the amine group in the final polymer allowed for the desired azo dye sensor and perturbation moieties to be efficiently acylated onto the polymer with hexafluorophosphate benzotriazole tetramethyl uranium (HBTU), with a method originally developed for peptide coupling⁵¹. The inclusion of HEMA, a monomer also used in contacts⁵², was to assist with transparency and water compatibility. The cross-linker is necessary for hydrogel formation and its length is the determining factor in the transparency of the final gel. Using a cross-linker based on poly(ethylene glycol) (PEG) also helped with water compatibility, as PEG is hydroscopic. The glass slide was the chosen solid support; maintaining transparency while allowing for the sensor gel system to be handled, as the hydrogel by its own is fragile regarding any applied pressure.

While the Fenske hydrogel is a robust working system, there are improvements that can be made. The experiments described herein aim to improve the efficiency of the overall synthesis as well as precise replicability.

2.1.2 Synthesis of an Amine Terminated Monomer

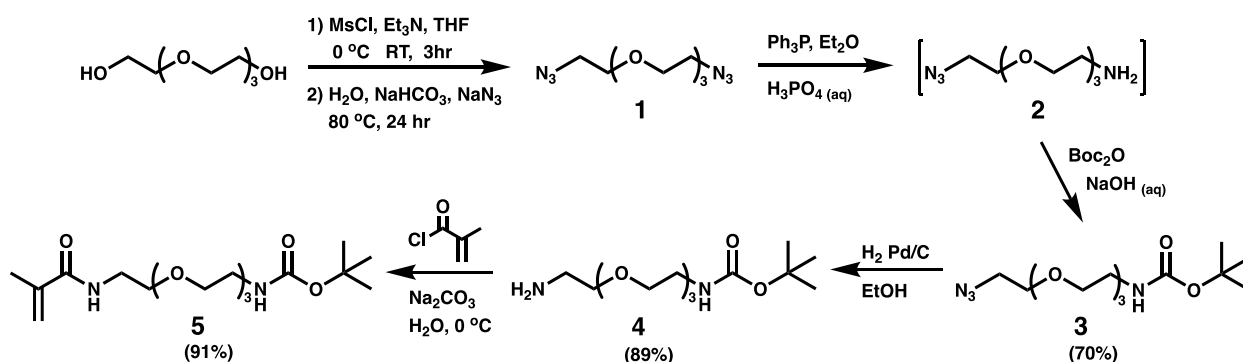


Figure 25: Synthesis of N-boc amine tetra(ethylene glycol) methacrylamide [5] from tetra(ethylene glycol) (TEG).

The functional amine monomer is derivatized from tetra(ethylene glycol) (TEG). The key to the synthesis is the 2nd reaction which involves the selective reduction of tetra(ethylene glycol) diazide [1], using a procedure that was developed by the Schwabacher group⁵³. Tetra(ethylene glycol) diazide [1] is formed by first activating the terminal hydroxyl groups of TEG with methane sulfonyl chloride and triethylamine; and subsequently substituting them with sodium azide. The selective reduction of diazide [1] uses a biphasic solution consisting of triphenyl phosphine in ether and aqueous phosphoric acid. Diazide [1] is soluble in ether, and triphenyl phosphine reduces one of the terminal azides to an amine, forming intermediate [2]. Intermediate [2] is quickly protonated by the phosphoric acid and then extracted into the aqueous phase of the solution, preventing any further contact with triphenyl phosphine and thus also preventing reduction of the other terminal azide. Intermediate [2] is not isolated as it is very difficult to extract out of aqueous solution (roughly 16 extractions are necessary⁵³). Instead, the aqueous layer is made alkaline with sodium hydroxide and the terminal amine of intermediate [2] is boc protected by heating the solution in the presence of Boc₂O. This allows for the extraction and isolation of N-boc-amine tetra(ethylene glycol) azide [3]. The boc protection also protects any small amount of diamine impurity rendering it inert for the rest of the reaction sequence. This prevents the formation of any tetra(ethylene glycol) dimethacrylamide during the last reaction step, which would cause issues during the polymerization of the hydrogel. The remaining terminal azide in compound [3] is reduced to an amine using hydrogenation over catalytic palladium on carbon, forming N-boc tetra(ethylene glycol) diamine [4]. The free amine in compound [4] is converted to a methacrylamide using

methacryloyl chloride, producing the protected amine monomer, N-boc-amine tetra(ethylene glycol) methacrylamide [5].

2.1.3 Polymerization to Form a Hydrogel

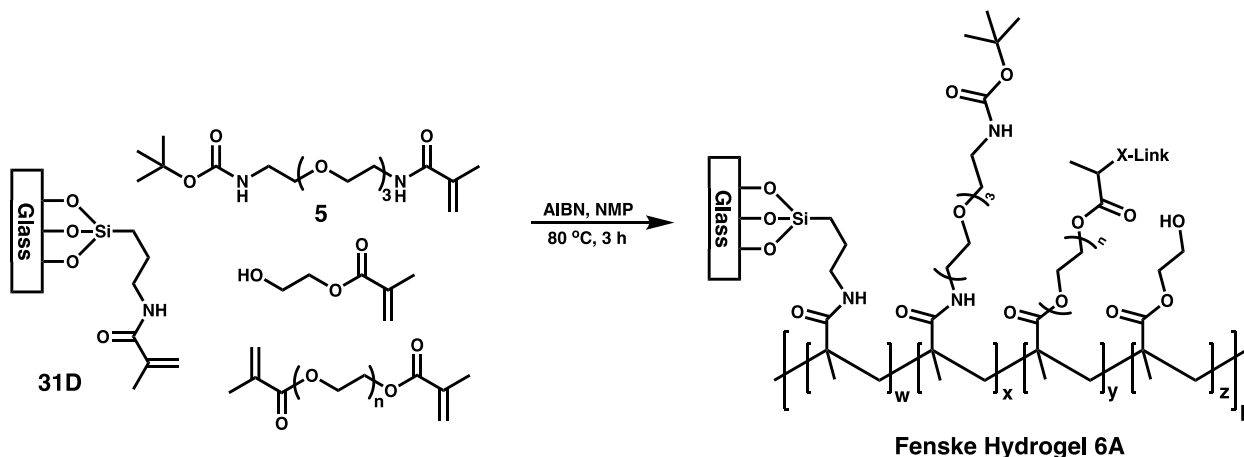


Figure 26: Free radical polymerization to form the Fenske Hydrogel [6A].

Monomer [5] can be polymerized with poly(ethylene glycol) dimethacrylate and 2-hydroxyethyl methacrylate on a silanized glass slide [31D] to form the Fenske hydrogel [6A]. Both monomers and the cross-linker are mixed and the polymerization inhibitor that was present as a stabilizer is removed via a mini column. The radical initiator AIBN is added, then the solution is degassed and used immediately.

Ratios: Monomer [5] and HEMA had a concentration of 0.917 M each (2.75 mmol each in 3mL). PEGDMA 750 had a concentration of 0.33 M (1.0 mmol in 3 mL). The AIBN concentration was 0.25 M.

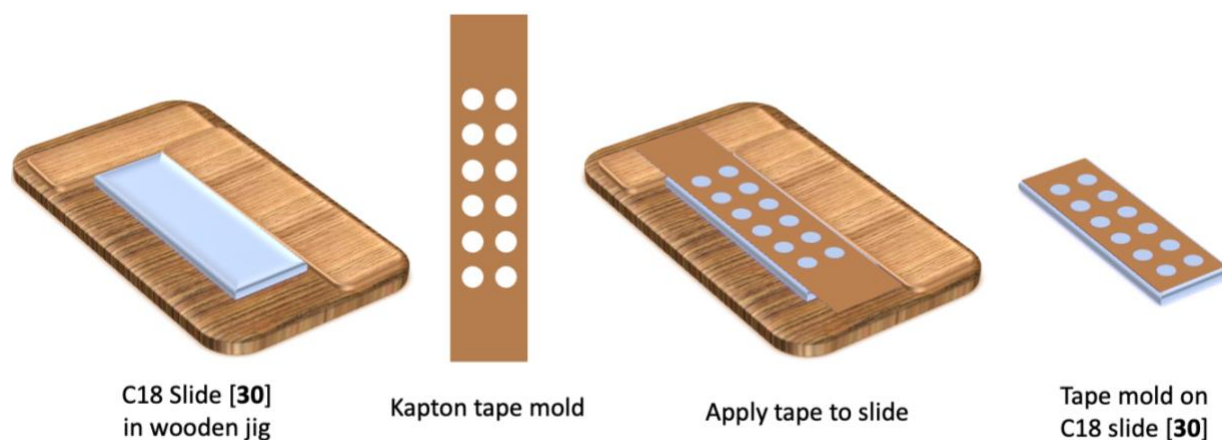


Figure 27: Application of Kapton tape mold to a hydrophobic C18 glass slide [30].

The polymer mold is custom and consists of 2 glass slides and a piece of tape. The tape is 1 mil (0.001 inches or 0.0254 mm) Kapton tape with 12 evenly spaced holes in it, which determines the height and diameter of the hydrogel disks. The slide the Kapton tape is applied to is hydrophobic [30], allowing for the hydrogels to be cleanly demolded. The other slide is silanized and modified so the surface has polymerizable handles covalently attached [31A-D]. During polymerization, the polymerizable handles are incorporated into the hydrogel, adhering it to the glass slide. The glass silanization process is discussed later in section 2.1.8.

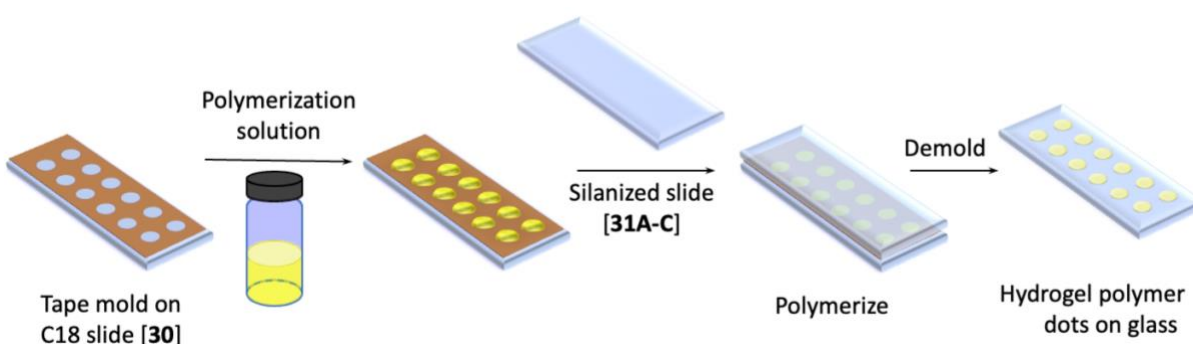


Figure 28: Filling the polymer mold.

The slide with the tape mold is placed tape up and in excess amount of polymerization solution is placed in each of the tape wells. The excess helps ensure that each well is filled

completely. The other slide [31A-D] is placed on top and then adjusted so that there are no visible air bubbles present in the polymer mold. Any overflow of the polymerization solution is wiped off the sides. The slides are then clamped together and polymerized in an 80°C oven for 3 hours, while keeping the slides level.

After polymerization, the whole setup is cooled, unclamped, and soaked in NMP overnight. The polymers are then demolded, transferred to a solution of 50:50 water: EtOH and stored until used. Water/EtOH is safer than NMP and less likely to breach the seal of the container (50 mL centrifuge tube). Water/EtOH also roughly matches the acidic deprotection solution of the next step.

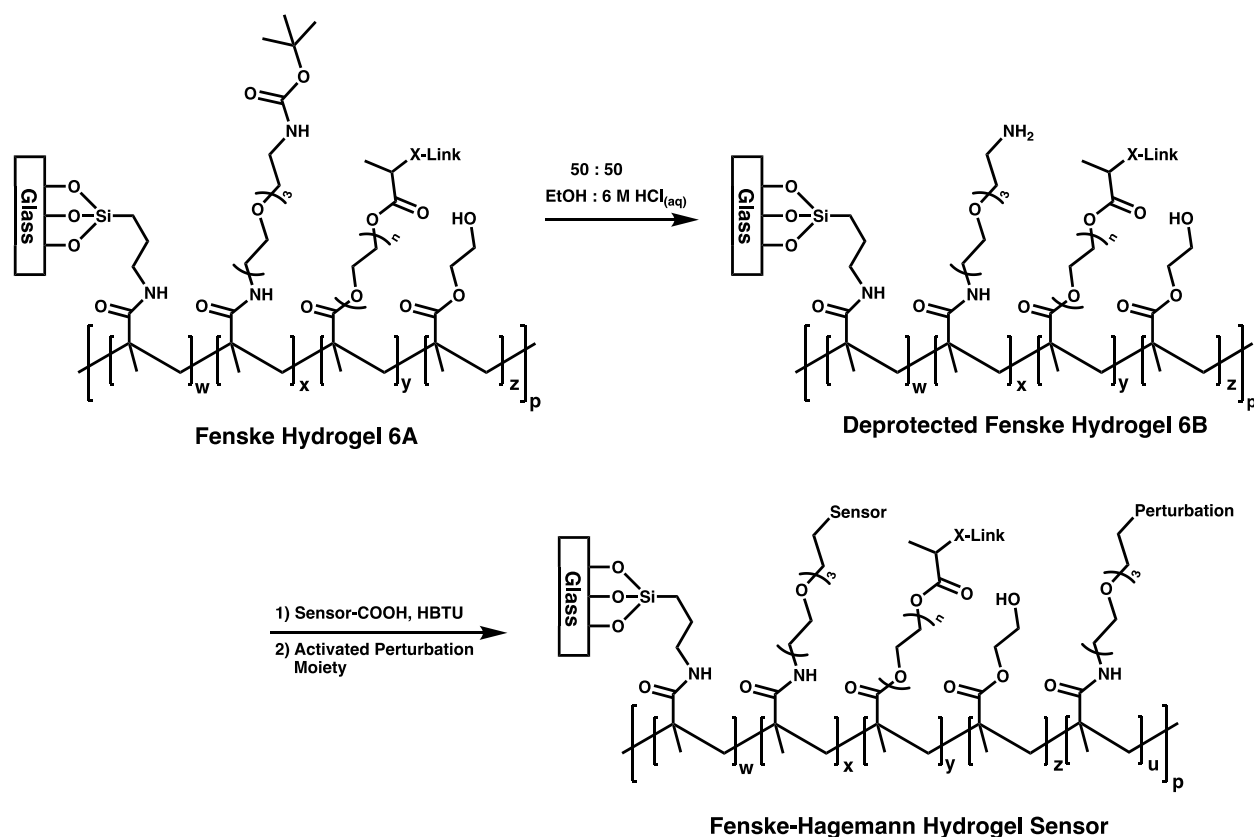


Figure 29: Deprotection of 6A to obtain 6B, and general scheme for functionalization with the desired sensor dye and perturbation moieties.

Hydrogel [6A] can be deprotected using a 50-50 mixture of aqueous 6M HCl and ethanol, removing the boc protecting groups. This gives a hydrogel with free amines [6B], that can now have the desired azo dye and perturbation moieties attached. The attachment of said azo dye and perturbation moieties utilizes an amide formation reaction originally developed for peptide coupling⁵¹.

2.1.4 Synthesis of an Azide Terminated Monomer

It was hypothesized that Fenske's functional monomer synthesis could be made shorter and more efficient, while keeping the final hydrogel polymer the same, by changing the terminal functional group to an azide rather than a boc-protected amine. Assuming the cross-linker and co-monomer were kept the same, reduction of the azide groups after polymerization would yield hydrogel polymer 6B, which is the same polymer obtained after boc deprotection.

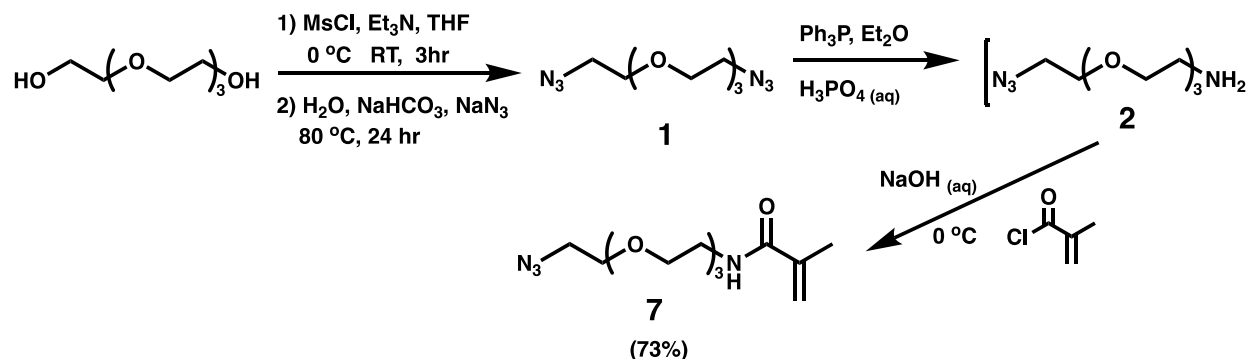


Figure 30: Synthesis of azide tetra(ethylene glycol) methacrylamide [7] from TEG.

As in the original scheme and the literature⁵³, the terminal hydroxyl groups of tetra(ethylene glycol) (TEG) were mesylated with methane sulfonyl chloride and subsequently substituted with sodium azide, giving tetra(ethylene glycol) diazide [1]. Diazide [1] was selectively reduced using a biphasic solution of triphenylphosphine in ether and aqueous phosphoric acid, producing intermediate [2]. Instead of boc-protection, the terminal amine

group was reacted with methacryloyl chloride to form azide tetra(ethylene glycol) methacrylamide [7]. [7] was stored at -20 °C with a small amount of 4-methoxyphenol (MEHQ) to inhibit polymerization. Without the boc protection, there may be small amounts of tetra(ethylene glycol) dimethacrylamide present as an impurity. This doesn't interfere with subsequent reactions on a small scale, but it could become an issue on a commercial scale.

2.1.5 Cross-linker Optimization

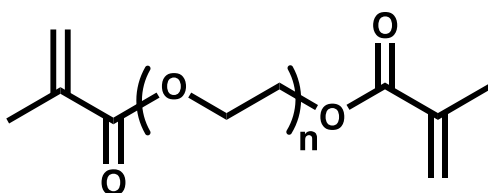


Figure 31: Poly(ethylene glycol) dimethacrylate (average MW 750).

There were concerns that the original cross-linker used in the hydrogel, poly(ethylene glycol) dimethacrylate (av. MW 750), would be vulnerable to hydrolysis, negatively impacting the long-term stability of the hydrogel.

This is especially important for the cross-linker as it is a stoichiometrically small amount of the polymer's composition, but critical to keeping the polymer together in its gel form. Hydrolysis of the cross-linker would break the links between chains, and if enough of said links were broken the hydrogel would lose its structure. The co-monomers used in these polymers, 2-hydroxyethyl methacrylate and di(ethylene glycol) methyl ether methacrylate, also contain methacrylate groups that are less hydrolytically stable. However, the co-monomer is much less structurally important than the cross-linker. The hydrolysis of the co-monomer results in the loss of that sidechain but leaves the main polymer backbone intact. Thus, co-monomer hydrolysis mildly increases the size of the polymer pores but doesn't damage the overall

structure. The functional monomer uses methacrylamide, which is more hydrolytically stable than a methacrylate group. Preventing hydrolysis of the functional monomer is important not because of hydrogel structural integrity, but because functional monomer hydrolysis would result in the loss of sensor dye molecules. This would change the dye concentration in the hydrogel and result in incorrect absorbance readings and heavy metal ion concentrations.

Rather than changing the terminal ends of the cross-linker to methacrylamides, they were changed to vinylbenzyl groups. This makes the only hydrolytic vulnerability in the cross-linker the ether groups within poly(ethylene glycol). Ethers are more hydrolytically stable than either methacrylamides or methacrylates. Obtaining greater hydrolytic stability than ether groups is not necessary or practical, as conditions that would hydrolyze ethers would also affect the functional monomer, co-monomer, and the connection of the hydrogel to glass, destroying the structural integrity of the entire polymer.

A poly(ethylene glycol) based cross-linker with terminal groups that were more hydrolytically stable was thus developed.

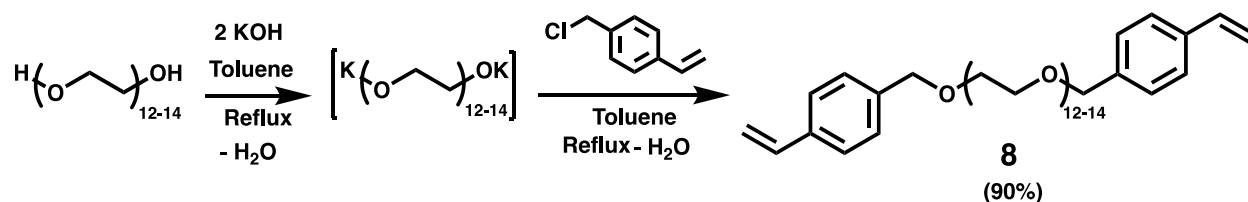


Figure 32: Synthesis of bis(4-vinylbenzyl) poly(ethylene glycol) (av. MW 850) [8].

Poly(ethylene glycol) (av. MW 600) was reacted with potassium hydroxide in toluene to form the PEG alkoxide, with water continually removed from the system via a Dean Stark trap. A substitution (S_N2) reaction with 4-vinylbenzyl chloride produced bis(4-vinylbenzyl) poly(ethylene glycol) (av. MW 850) [8]. The product **8** polymerizes upon concentration (when

2.1.6 4-Vinylbenzyl Azide and Relevant Polymers

As the addition of vinylbenzyl groups in the cross-linker did not negatively affect the optical transparency or water compatibility of the final hydrogel, it was hypothesized that it might be possible to change the tetra(ethylene glycol)-based monomer to one based on styrene without sacrificing transparency or water compatibility.

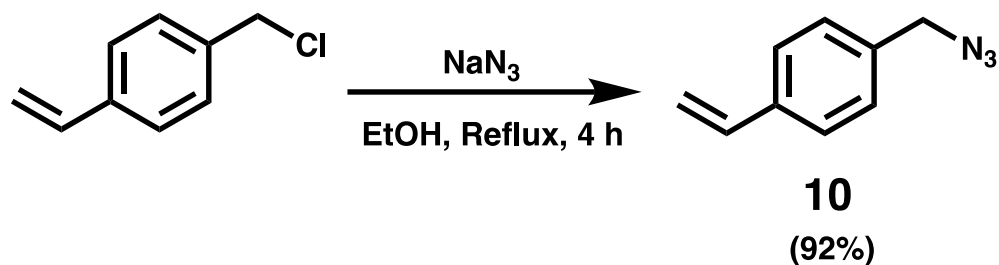


Figure 34: Synthesis of 4-vinylbenzyl azide [10] from 4-vinylbenzyl chloride.

A substitution reaction was performed with 4-vinylbenzyl chloride and an excess of sodium azide in refluxing ethanol. This produced 4-vinylbenzyl azide [10], a yellow-orange oil to which a small amount of MEHQ was added. 4-vinylbenzyl azide [10] proved to not be bench stable, as it was completely unusable after a day exposed to light at room temperature. The previous viscous liquid became a hard amorphous solid containing many bubbles, which proved to be mostly insoluble in the most commonly available organic solvents. It is only very sparingly soluble in toluene. An NMR of the extract showed it was composed of 4-vinylbenzyl azide [10] and many other impurities. As this occurred in the presence of a polymerization inhibitor it is vital that 4-vinylbenzyl azide [10] be stored away from heat and light. It is stable stored in the dark at $-20\text{ }^\circ\text{C}$ (freezer temp) in the presence of a polymerization inhibitor. It is also important to track the reaction progress via TLC, as continuing to heat the reaction solution after reaction

completion results in the slow formation of the same unwanted solid, greatly reducing yield (41% yield after 72 h/weekend, vs 90+% after 4 h).

Changing the solvent to acetonitrile more than tripled the reaction time (14 h but still 94% yield). Switching the solvent to DMF at 80°C, shortened the reaction time (~1.5 to 2.5 h) but complicated the workup as the DMF was extremely difficult to remove from the final product (traces of DMF remained after a few days under reduced pressure on the Schlenk line). The best observed conditions remain the original reflux in ethanol.

2.1.7 Addressing Hydrogel Inconsistencies

There was some variation between each batch of hydrogels. One reason for this was how the polymerization inhibitors/radical traps were removed. Commercial compounds with vinyl groups have trace amounts of a polymerization inhibitor added as a stabilizer, so that the compound is less vulnerable to polymerization and degradation during storage. These inhibitors are usually a phenolic molecule, such as 4-methoxyphenol (MEHQ) or butylated hydroxytoluene (BHT) or a mixture of both. A small amount of MEHQ is purposefully added to all synthesized monomers and cross-linker as with vinyl groups for the same reason. This is demonstrably necessary, as compound **[8]**, bis(4-vinylbenzyl) poly(ethylene glycol) (av. MW 850), polymerizes in under 30 min when neat without MEHQ present. The hydrogel polymerization method thus calls for the mixture to be polymerized (sans AIBN) to be made up in toluene, passed through a column to remove polymerization inhibitor, concentrated, combined with AIBN, and dissolved in NMP to the desired concentration. The mixture is then used immediately. The issue with this is that the initial ratio of reagents is not the same as what comes out of the column and is actually used. An NMR of the final mixture could be taken to determine the ratios, but although

this solves the problem of the actual ratios of monomer and cross-linker being unknown, it does not provide the desired level of control over said ratios.

It was hypothesized that removing the inhibitors chemically rather than physically might provide a solution. MEHQ and BHT are both radical traps that function in the same way. In the presence of radicals, the phenolic hydrogen is abstracted, and the resulting radical is stabilized through resonance and aromaticity. This prevents further reaction with any vinyl groups present, and thus inhibits polymerization. The presence of enough radicals will eventually exceed the ability of MEHQ/BHT to trap radicals, and polymerization will then occur. This is a plausible scenario in the case of AIBN being added and purposefully heating the mixture.

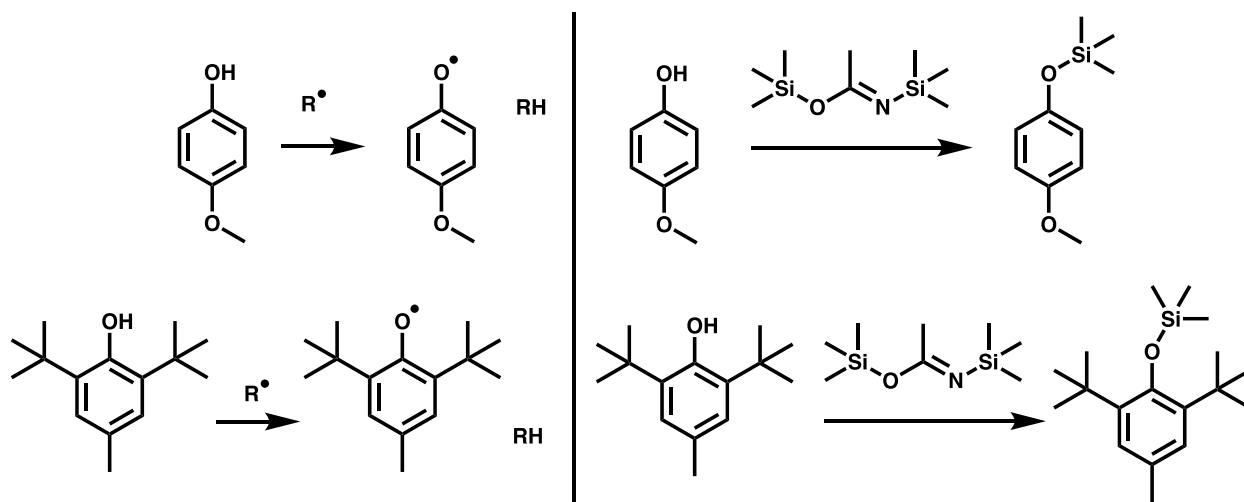


Figure 35: Polymerization inhibitors MEHQ and BHT and their silylated analogs.

Alternatively, protecting the phenolic hydroxyls would prevent BHT/MEHQ from acting as a radical trap, thus rendering the inhibitor chemically inert regarding polymerization. This could be accomplished by silylating BHT/MEHQ with bis(trimethylsilyl)acetamide (BSA). BSA should not cause any undesired reactions, provided that there are no hydroxyl groups in the monomers or cross-linker. DEGMEMA was thus used instead of HEMA in all reactions with BSA

because HEMA has a terminal hydroxyl group that would be silylated by BSA while the ether in DEGMEMA would not. In theory, this method would allow for the polymerization solution to be prepared in advance and stored for longer without risk of polymerization, as the inhibitor would still be present. AIBN and BSA could be added directly before the solution was used.

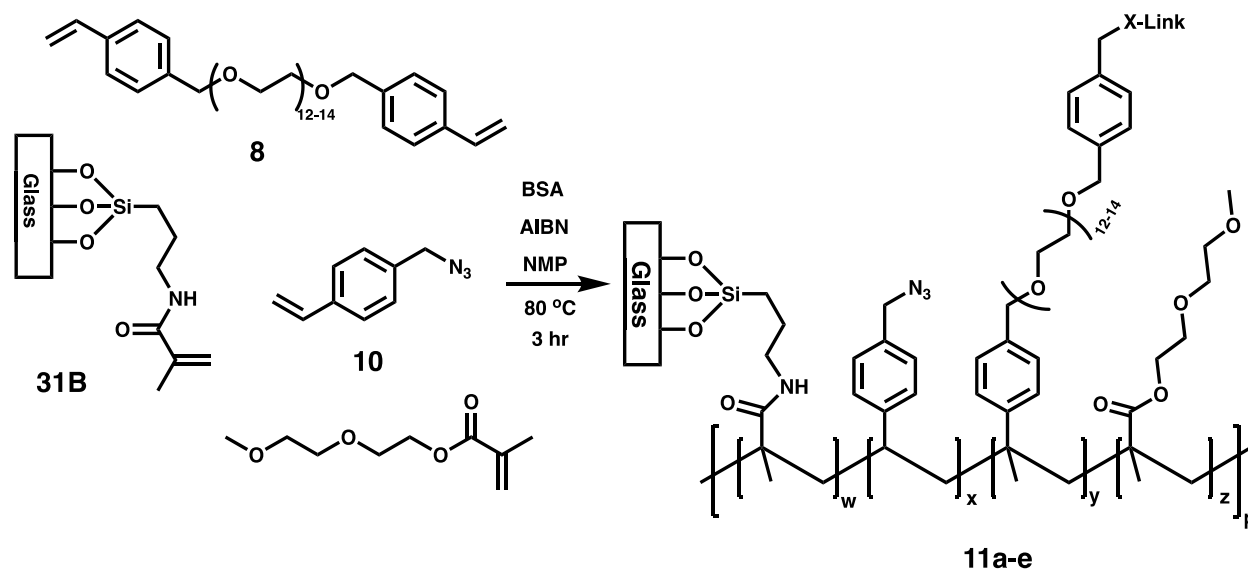


Figure 36: Hydrogel synthesis in the presence of BSA and with varying cross-link densities.

A series of polymerizations with cross-linker [8], monomer [10], and DEGMEMA, on glass were carried out to test a multitude of things. Firstly, that adding BSA would not interfere with the formation of a hydrogel, and secondly, that monomer [10], 4-vinylbenzyl azide (VBAZ), could be substituted for monomer [7] while keeping the hydrogel transparent and water compatible. Additionally, the ratio of cross-linker [8] to monomer [10] to DEGMEMA was varied in 5 different ways to investigate the effect of varying the percentage of cross-linker [8] while keeping the amount of monomer [10] and the overall number of vinyl groups constant. The amount of inhibitor present in DEGMEMA, VBAZ [10], and cross-linker [8] is 0.04%, ~0.5%, and ~1% (by mol) respectively. BSA was added at ~10% (by mol) vs the combined amount of DEGMEMA, [10], and [8], to insure it would be in large excess of the amount of polymerization

inhibitor present. The amount of AIBN was ~7% (by mol) vs the combined amount of DEGMEMA, [10], and [8]. The ratios of the monomers and cross-linker are shown in Table 1. [11b] is analogous to Fenske hydrogel [6A].

Table 1: Reagent ratios for the polymerization of hydrogels [11a-e].

Compound	VBAZ [10]	DEGMEMA	BVBPEG 850 [8]
Mol. Wt.	159.188	188.22	850
11a			
Ratio vs VBAZ [10]	1.00	1.35	0.17
mol %	40	53	7
% vinyl groups	37	50	13
mass %	28	45	26
11b			
Ratio vs VBAZ [10]	1.00	1.04	0.35
mol % polymer	42	43	15
% vinyl groups	36	38	26
mass %	24	30	46
11c			
Ratio vs VBAZ [10]	1.00	0.69	0.56
mol % polymer	45	31	25
% vinyl groups	36	25	20
mass %	21	17	62
11d			
Ratio vs VBAZ [10]	1.00	0.34	0.68
mol % polymer	49	17	34
% vinyl groups	37	13	50
mass %	20	8	72
11e			
Ratio vs VBAZ [10]	1.00	0	0.85
mol %	54	0	46
% vinyl groups	37	0	63
mass %	18	0	82

All 5 variants successfully polymerized, and the resulting hydrogels were very pale yellow and transparent. All 5 hydrogels being transparent was unexpected, as [11e] was 46% (by mol) cross-linker [8], and it was thought that the greatly increased cross-link density would result in a cloudy translucent hydrogel. The transparency is most likely due to the cross-linker length. PEG 600 is similar in length to ~20 polymerized vinyl units; so even with the cross-linker accounting for 63% of the polymer backbone, the average hydrogel pore size was probably still large enough to allow for transparency when swollen.

Though all 5 variants formed, some of the hydrogel dots delaminated from the glass slides. Part of this experiment was to test changes in swelling vs. delamination. Swelling is partially controlled by cross-link density, which was varied from 7% to 46%. The fact that all 5 variants had at least 30% of the gels delaminate regardless of the cross-link density shows that changes in swelling are not the definitive cause of delamination issues.

The initial NMP solvent for the gels was swapped to water mixtures via putting the gels through a series of different solvents. (NMP – NMP/EtOH – EtOH – EtOH/H₂O – H₂O). All the hydrogels remained transparent in the different solvents, and the solvent within the gels also seemed to be successfully changed.

The hydrogels being transparent and compatible with water indicate that 4-vinylbenzyl azide [10] is a viable monomer option. The water compatibility of the gels despite the vinylbenzyl group being hydrophobic, is most likely due to the high amount of cross-linker [8]. The cross-linker mainly consists of poly(ethylene glycol), and each gel had ~ 4 times (range of 3.7 - 4.1) more glycol units (OCH₂CH₂) than benzyl groups. Having more glycol units, which are

hydrophilic and can absorb multiple times their weight in water (hydroscopic), allows the polymer to swell and maintain its water compatibility.

These results also suggest that BSA does not interfere significantly with polymerization. Specifics require further experimentation, as a hydrogel is an insoluble solid structure and solid-state NMR is one method of characterization that was not available to us to further observe the effects of BSA.

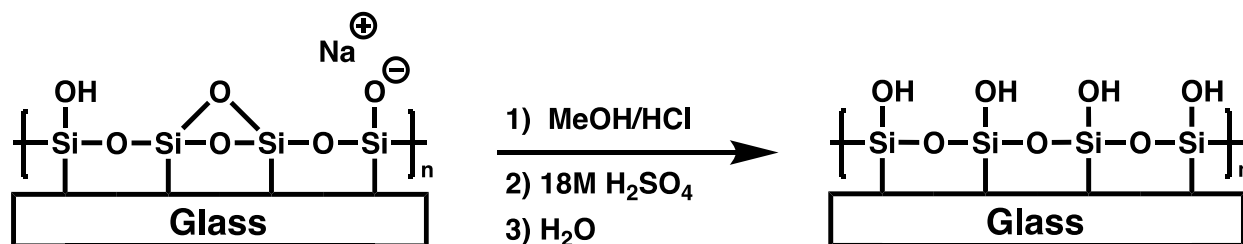
As the metal ion sensor project progressed, it became increasingly apparent that the current hydrogel sensor iteration had consistency and replication issues that were significantly affecting the project. The variances were small, but significant enough to impede our collaborator's efforts to develop an algorithm that would consistently take the absorbance reading and accurately display the concentration of heavy metal ions.

Every completed batch of sensors (hydrogel on glass with dye and other groups attached) varied from batch to batch and from gel to gel within a batch. Some of the sources of variation, (ex: amount of sensor dye in each gel) were caused from the dye loading process due to small differences between batches. Also, according to NMR spectra from Katryna Williams²⁰, some of this is due to the rate of dye degradation. Dye degradation is measured by UV and NMR compared over multiple days. Other issues are affiliated with the polymerization process. Trying to pinpoint where in the process the variances were coming from, and what exactly was causing them, was extremely difficult, as there was no concrete method of characterization between the monomer and the evaluation of the final gel.

The hydrogel polymers varied in the number of free amines, exact ratios of monomers and cross-linker, and degree of polymerization. The hydrogels also occasionally failed and delaminated for a then unknown reason.

2.1.8 Silanization of Glass

Several methods for the silanization of glass are known⁵⁴⁻⁵⁷. However, most of these are complex procedures to obtain very precise results. For the purposes of this project, specific amounts of silane coverage were not necessary. Tyler Fenske developed a method that would give a satisfactory range of results with enough coverage to allow for attachment of hydrogels but not so much as to sacrifice the glass transparency²².



29

Figure 37: Cleaning the surface of glass microscope slides.

The surface of the glass must be cleaned and the surface silanols exposed for silanization to take place⁵⁸. The glass slides were cleaned by soaking them in a solution of 50:50 (by volume) solution of methanol : 12M hydrochloric acid for at least 30 minutes, preferably overnight. After removal from the MeOH/HCl bath and rinsing with 18 MΩ water, the slides were placed in a bath of concentrated H₂SO₄ for a least an hour. The slides were kept in H₂SO₄ and rinsed and dried off prior to silanization.

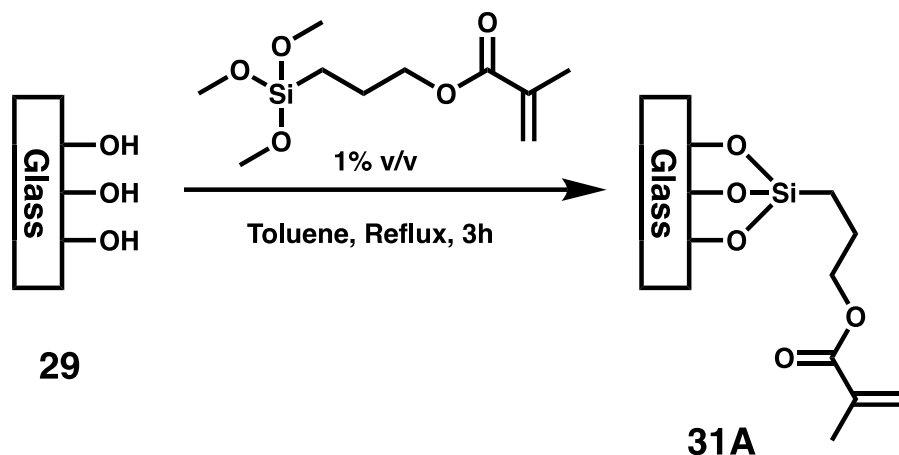


Figure 38: Glass silanization in solution with TMSPM.

The original glass silanization was a liquid phase procedure utilizing a solution of 3-(trimethoxysilyl)propyl methacrylate (TMSPM) in toluene. The solution phase procedure was inefficient, using a large excess of TMSPM. Also, the linkage to glass here is methacrylate based, which is less hydrolytically stable than methacrylamide. For these reasons, Fenske took procedures from literature that used gas phase deposition of APTMS^{54,59} and modified them until he had a simpler procedure that could be performed at atmospheric pressure.

It was originally hypothesized that the reason the hydrogels were delaminating was because of the stress caused by swelling, straining the connection between the gel and the glass slide to the breaking point. The radical polymerization is conducted in NMP as it is a polar aprotic and high boiling solvent. The gels are initially demolded in NMP before being transferred to a water/EtOH mixture. The swelling of hydrogels is partially solvent dependent. It was thought that the sudden change from NMP to water was essentially shocking the gels and causing delamination. A gradual change in solvents was executed, with the gels going from NMP to NMP/EtOH to EtOH to water/EtOH. Despite this, delamination was still observed. It was then hypothesized that the swelling of the gels in water, whether or not the solvent change was

sudden or gradual, was responsible for delamination. One of the other factors that affect swelling is cross-link density, as more cross-links both reduce the porosity of the gel and prevent the different backbone chains from moving as far away from each other and thus also reducing the amount the hydrogel swells. Part of the purpose of the hydrogel polymerization reactions in the previous section was to experiment with different cross-linking densities both lower and higher than the usual 15%. The goal was to investigate if there was a limit where the cross-link density would render the gels nontransparent, as well as observe the swelling and possible delamination of the resulting hydrogels. A small difference (qualitative) in swelling based on cross-link density was observed, and there was no effect on transparency. However, a portion of the gels on each slide still delaminated, despite one of the variations being composed of 46% cross-linker. This is the maximum amount of cross-linker that can be added without changing the amount of functional monomer. These results indicate that the cause of delamination is not due to the swelling of the hydrogel dots. This means that the reason for delamination occurs at an earlier point in the process. The actual radical polymerization of the gels was not at fault, as hydrogel formation must be successful for delamination to occur. This is additionally supported by the fact that free-floating gels not attached to glass had previously been synthesized by Tyler Fenske²². As delamination has something to do with the hydrogel glass interface, it was hypothesized that something in the glass silanization procedure was the problem.

At this point all silanization was being performed with vapor deposition of APTMS, first one slide at a time in a petri dish on a hot plate [31B], and then in batches of 5 using a crystallization dish in a vacuum oven [31D].

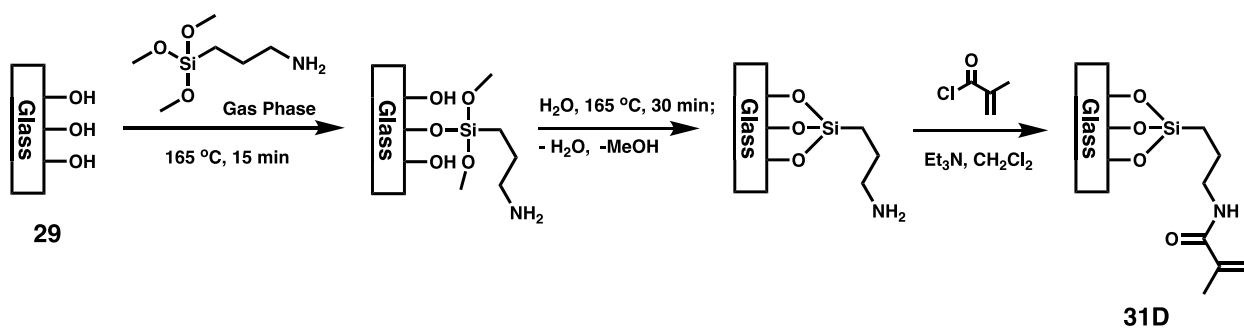


Figure 39: Gas phase silanization of glass with APTMS and subsequent reaction with methacryloyl chloride to obtain a polymerizable handle.

The silanization of the glass still had issues. Tyler Fenske could get it to work most of the time. However, the silanization could only be evaluated by water contact angle, or once the polymer gels were formed (and they either stayed on the glass or delaminated). After Tyler Fenske's graduation, the silanization procedure he developed proved to be inconsistently replicable. Hydrogels attached to the silanized slides delaminated, about 50% of the time, showing the silanization to be inadequate for bonding the polymer to glass. Out of 12 gels per slide in 5 slide batches, the gels that delaminated varied greatly, from 2-3 delaminating on each slide in one batch, to 7-8 per slide in the next batch. There were also a significant number of batches where 100% of the gels delaminated. This was concerning both because of the amount of effort and reagents wasted in the case of a failure (silanization and methacrylation took a full day and night, and polymerization took another day), and because some of the gels had tenuous connections to glass and delaminated during the dye loading process or a short time later in storage. Overall silanization success rate was <40% taking into account these later delaminations. The reason for the difference between my results and the results previously achieved by Tyler Fenske was not obvious. It was hypothesized that some key detail in the procedure that was routine for Fenske didn't get recorded. This is supported by the three

collaborative attempts by me and Katryna Williams to replicate the existing silanization, which all resulted in delamination.

This was resolved in repeated step by step testing of the silanization procedure to see which steps were necessary and which were superfluous, as well as trying to pinpoint which steps were variable enough to result in unexpected failure after polymerization. All variations were evaluated by using the slides in the synthesis of hydrogel [6A]. In the end, some superfluous solvent rinses were removed, and the reagent amounts were increased.

Most importantly, the problematic silanization step was found to be the preheating of the slides and crystallization dish before the addition of APTMS. Fenske's procedure called for the crystallization dish and lid (that were used to contain the APTMS), the glass slides, and the slide holder to be preheated at 165°C for 15 minutes. Then the dish was to be removed, APTMS was to be added, the lid placed back on the dish, and the whole setup placed back in the oven as fast as possible. This was problematic as well as dangerous. The time someone took to add the APTMS, put the lid on the dish and everything back into the oven varied, and since APTMS immediately started to vaporize upon contact with the hot dish, some of it was lost rather than contained and used in the reaction. Rushing through the procedure to avoid potential failure of the process while handling **165 °C glassware** also posed a safety hazard; increasing the chance of getting burned or making a mistake.

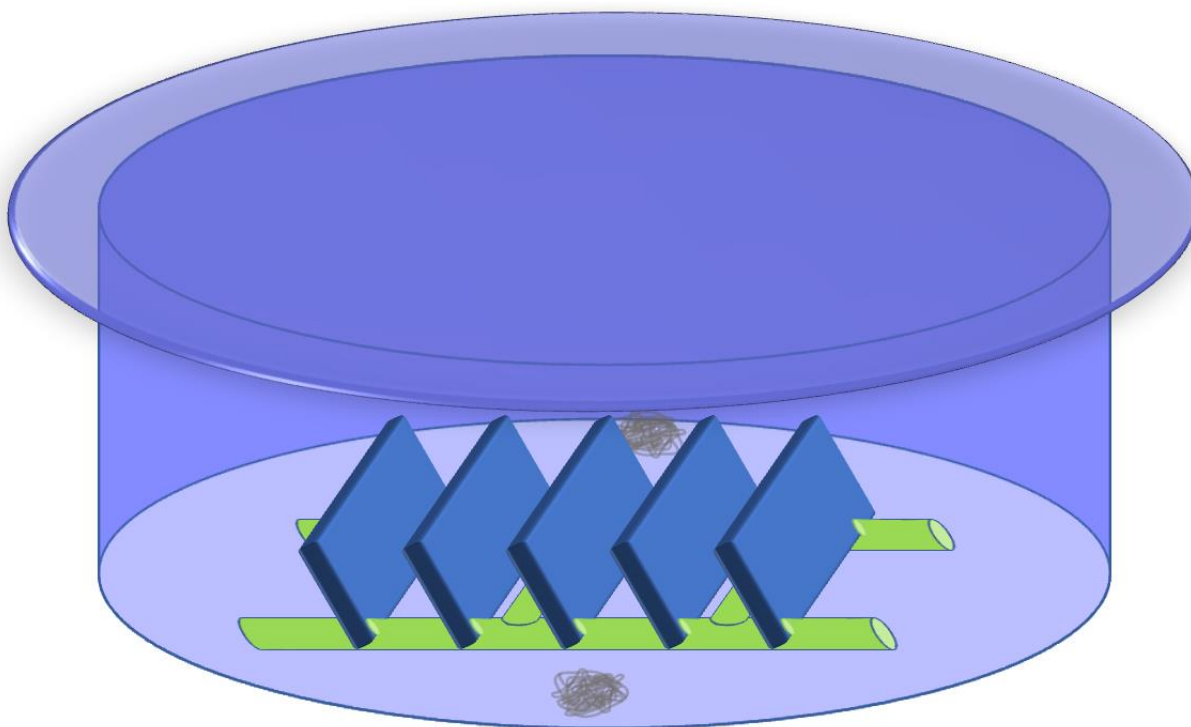


Figure 40: Large crystallization dish and lid with a rack of 5 glass slides inside.

Eliminating the preheat step and doubling the amount of APTMS used improved the results but didn't completely fix the delamination problem. It was hypothesized that since the original procedure called for a 15 min preheat and then 15 min of reaction time, that the reaction time was now shorter than necessary, since the glass had to warm up in the oven before the APTMS vaporized and any reaction occurred. A series of tests were carried out to determine the ideal reaction time. Silanization was tested with a 30, 45, or 60 min reaction time. 30 min resulted in delamination of a few of the gels on a slide. 45 min resulted in all of the hydrogel dots staying attached, but there were a few with minorly damaged edges. 60 min resulted in visible cloudy raised areas where the APTMS had built up too much. After further testing, 50-55 min was determined to be the optimal reaction time, with no observed delamination or damage to the gels, and no cloudy areas interfering with transparency.

With the delamination issue solved, focus was shifted to addressing the other sources of inconsistency in the polymers. The issue of physically removing the polymerization inhibitor causing small but uncontrollable changes to the reagent ratios had already been partially addressed (see previous section on hydrogels [11a-e]). However, a definite conclusion on the effects of BSA could not be drawn from that experiment, as there is the possibility that any polymerization inhibitor present was simply overwhelmed by the number of radicals. This would have resulted in the formation of a gel but with a slightly lower degree of polymerization. Unfortunately, the degree of polymerization was never evaluated. Unreacted monomers and cross-linker would have been washed out into NMP during demolding, so there wasn't any left in the final gel. It is technically possible to analyze the NMP solution, but since NMP is a high boiling solvent (b.p. 202°C), evaporating the relatively large volume of solution (~200 – 400 ml) down to obtain what is possibly a few milligrams of residue is impractical. Another way to approach this would be analyzing the polymer. However, analyzing and characterizing polymers while in the hydrogel solid-state is difficult. UWM doesn't have a solid-state NMR, DSC, TGA, SEM, or other suitable instruments for polymer characterization. Even destructive tests for polymers would have been informative.

While FTIR isn't normally a destructive test, attempting this on the hydrogels ended up crushing them due to the pressure needed to get a readable spectrum.

Synthesizing soluble polymer with the same ratios (sans cross-linker and glass), and similar conditions could serve as a model reaction that would allow for further evaluation of changes to the polymerization.

2.2 Soluble Polymers

2.2.1 – Azide Based Soluble Polymers

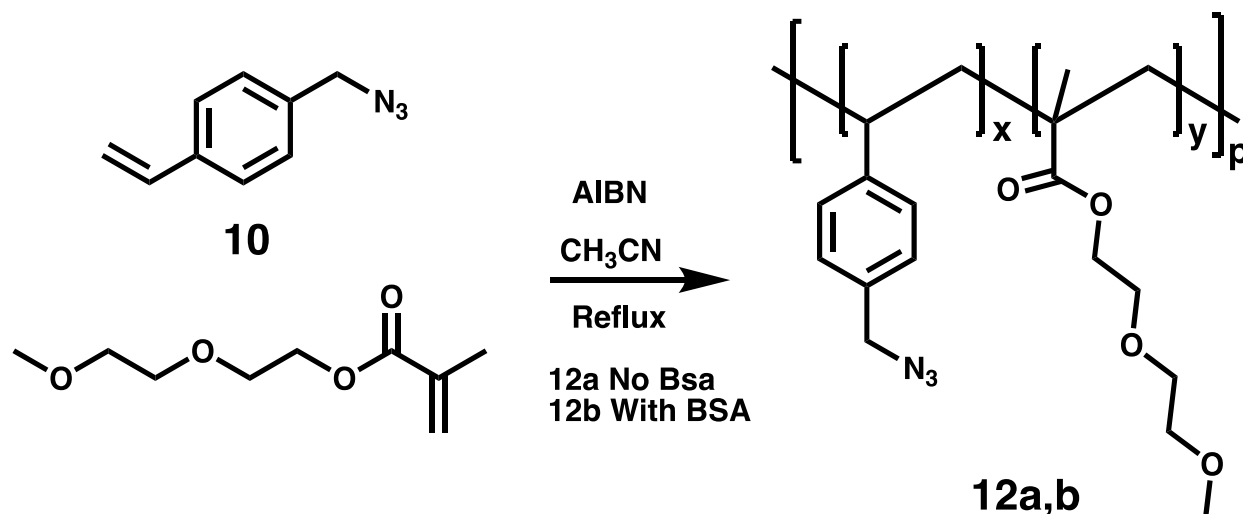


Figure 41: Co-polymerization of 4-vinylbenzyl azide [**10**] and DEGMEMA.

A set of soluble polymers with monomer ratios similar to hydrogel [**11b**] and Fenske hydrogel [**6A**] were synthesized to more closely evaluate the effects of BSA. These soluble polymers were co-polymers of VBAZ [**10**] and DEGMEMA. Polymer [**12a**] was synthesized in the absence of BSA, and polymer [**12b**] was synthesized in the presence of BSA. Neither experiment had any of the polymerization inhibitors removed from the monomers beforehand. Both polymerizations were carried out in refluxing acetonitrile under N₂. Acetonitrile was chosen as the solvent because its boiling point of 80 °C matches the usual polymerization temperature of the hydrogels. The inert N₂ atmosphere was meant to be roughly analogous to the enclosed mold used for the hydrogels. The polymerizations were run simultaneously. The reaction progress was tracked by NMR, with spectra being taken every 3 h.

The results of this experiment are interesting. The BSA did seem to make a difference but smaller than expected. The initial polymerization rate of both polymers was extremely similar; with both having ~ 85% (+/- 1%) monomer conversion at 3 h. After 6 h, the reaction without BSA [**12a**] had 92% monomer conversion, and the reaction with BSA [**12b**] had 97% conversion. After 9h, [**12a**] had 96% conversion, and [**12b**] had 99% conversion. After 12h, [**12a**] had 99% conversion ([**12b**] was stopped after 9h). (There is some experimental error here, as these reactions were forced to completion with the addition of more AIBN at the later points).

The amount of polymerization inhibitor in commercial monomer products is usually < 0.1%. DEGMEMMA contains 0.04% (by mol) inhibitor. A higher amount of inhibitor, but usually not more than 0.5%, was added to the synthesized monomers. The VBAZ [**10**] used in this case had 0.1%. The amount of BSA added to [**12b**] was 0.5% (by mol) vs the total amount of monomer. For both reactions, the initial amount of AIBN was 5% (by mol) relative to the total amount of monomer. The half-life of AIBN at 80°C is ~85 min, so 3h is a little more than 2 half-lives; 23% of the original AIBN amount remains after 3h, and 5% remains after 6h. The results of this experiment show that in the beginning and main part of the polymerization, BSA had a negligible effect on the reaction rate. This indicates that the number of radicals generated by AIBN were more than sufficient to negate the effect of the polymerization inhibitor, and that as such the effect BSA had on the polymerization inhibitor did not make a significant difference in the outcome of the polymerization reaction.

An interesting side observation gained from the NMR spectra, was that the 2 monomers are not incorporated into the polymer at the same rate, despite the initial ratio being 1:1. After

3 h, 15% monomer was remaining, consisting of 5% VBAZ [**10**] and 10% DEGMEMA. This ratio was the same for both reactions.

The homopolymer of VBAZ [**10**] was synthesized to further investigate the polymerization.

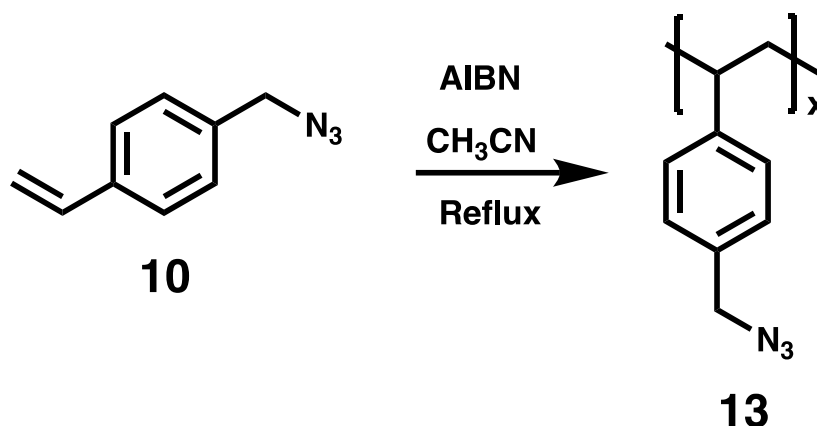


Figure 42: Homo-polymerization of 4-vinylbenzyl azide [**10**].

Free radical polymerization of 4-vinylbenzyl azide [**10**] was performed using a catalytic amount of AIBN at 80°C. This produced poly(4-vinylbenzyl) azide [**13**] as a viscous orange oil. The chain length of this polymer is unknown. The average molecular weight and chain length of a linear polymer is usually determined using gel permeation chromatography (GPC). As UWM does not have access to a GPC instrument, this analysis was unable to be performed. Using the correlation between polymer molecular weight and viscosity is a possible way to obtain an estimation. However, this was not done as the only viscometers available were glass ones that required sample sizes several times larger than the scale of the polymerization reaction. The lack of a suitable standard was also an issue.

The polymerization had a 46% mass efficiency. Most of the lost mass was due to an orange solid that also formed. The solid was presumably the same solid produced when the

monomer was not stored properly. The two solids had similar properties, as both were insoluble in most organic solvents. Covering the reaction set up with aluminum foil to reduce light exposure didn't improve the mass efficiency. As heat appears to be the main issue, a low temperature radical initiator might give a better result. However, as no such radical initiator was readily available to the research group, focus was shifted to other soluble polymers.

There were several attempts to reduce poly(4-vinylbenzyl azide) [**13**] to an amine. Any reduction method that used a metal catalyst (not attached to a substrate) was taken out of consideration due to the chance of metal ion traces ending up in the final polymer.

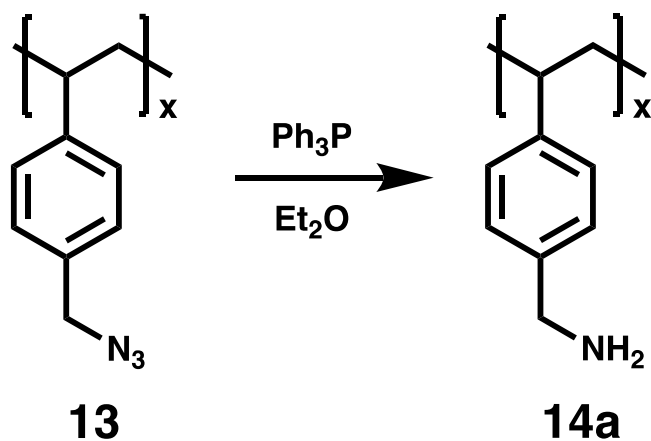


Figure 43: Reaction of poly(4-vinylbenzyl azide) [**13**] with triphenylphosphine.

The first reduction attempt was a Staudinger reaction using triphenylphosphine in ether, but isolation of the desired product [**14a**] was unsuccessful. The issue here wasn't the reaction itself but the workup. The reaction seemed to proceed normally (tracked by TLC), and everything stayed soluble in diethyl ether. The presence of amines was confirmed by a qualitative ninhydrin test. The workup was the same as in the synthesis of [**3**] and [**7**]. However, as soon as the sodium hydroxide solution was added, the polymer separated from both the organic and aqueous layers and floated on top of the solution clumped together around the

triphenylphosphine oxide as a very viscous substance (texture of soft taffy). All attempts to redissolve the polymer/triphenylphosphine oxide mixture in a variety of solvents were unsuccessful. It is thought that due to its long length and high hydrophobic character, the polymer may have acted similar to a hydrophobic protein when exposed to base, folding up on itself and minimizing contact with water. Some of the triphenylphosphine oxide was swept up because it contains similar hydrophobic groups (aromatic rings) and precipitates from basic solution. Why the polymer was unable to be redissolved is debatable, but one likely reason is entanglement. Polymer chain entanglements are a form of physical crosslinking. If the polymer formed enough entanglements when it tightly clumped up, it would be a semi-solid and dissolving it wouldn't be feasible.

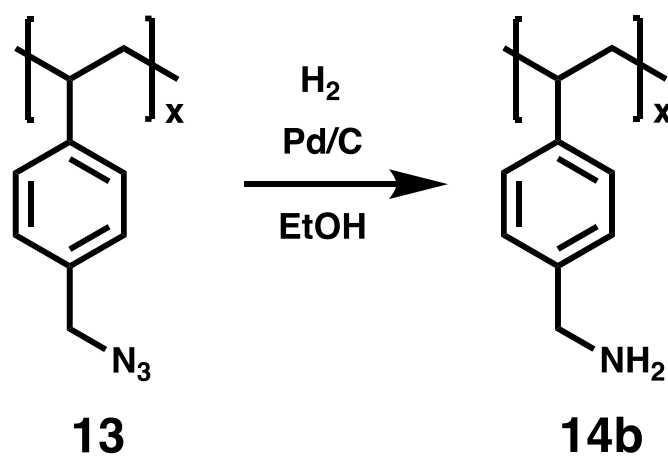


Figure 44: Hydrogenation of poly(4-vinylbenzyl azide) [**13**].

The second attempt to reduce poly(4-vinylbenzyl azide) [**13**] was via hydrogenation, which can be used on soluble polymer but not a hydrogel, as the palladium on carbon would get caught in the pores. This reaction works but it is exceedingly slow, with little progress after a week. After 2 weeks with the hydrogenation still nowhere near completion, it was deemed not worth pursuing further.

2.2.2 4-Vinylbenzyl Phthalimide and Soluble Polymers

It was hypothesized that the Gabriel synthesis might be an easier route to an amine monomer.

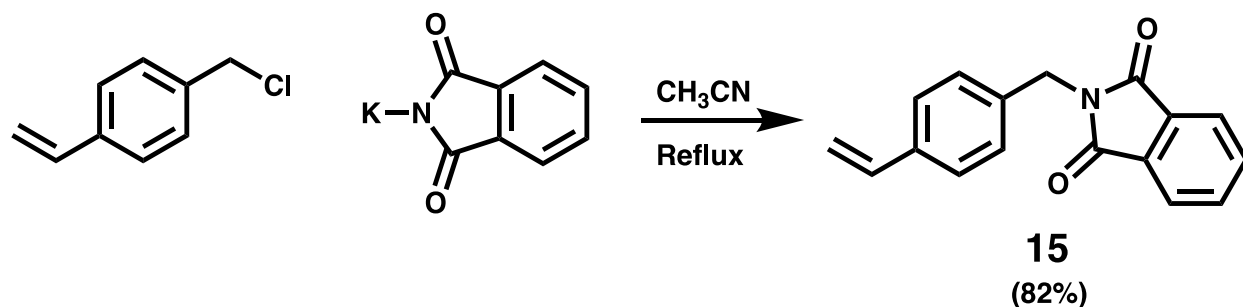


Figure 45: Synthesis of 4-vinylbenzyl phthalimide [**15**] via S_N2 reaction.

4-vinylbenzyl phthalimide [**15**] was synthesized via a S_N2 reaction with 4-vinylbenzyl chloride and potassium phthalimide in acetonitrile. The reaction took several days, tracked by TLC. The crude compound [**15**] was obtained by removing the reaction solvent under reduced pressure. Excess potassium phthalimide was removed by washing the crude with water. Compound [**15**] was then isolated and purified through multiple hot filtrations and recrystallizations in ethanol. The first recrystallization yielded ~ 50% of the product an off-white crystalline solid. Crystal size ranged from small needles to crystals the size of powdery glitter. Concentrating and recrystallizing the mother liquor yielded slightly less than half the remaining product every time it was repeated (~50%, ~19, ~10% , ~4%); 83% yield overall. The crystallization is slow and these numbers were obtained with crystallization at room temperature overnight. When recrystallization was continued for several weeks, 72% recovery was obtained with large translucent crystals from a single recrystallization.

4-Vinylbenzyl phthalimide [**15**] should be stored cold and in the dark to prevent polymerization. A polymerization inhibitor cannot be added, as adding it before recrystallization

would be redundant and adding it after recrystallization would simply result in a mixture of 2 solids. 4-Vinylbenzyl phthalimide (VBP) [15] is more stable than 4-vinylbenzyl azide [10], even with no polymerization inhibitor present. It is bench stable at least short-term (at least 2 days) unlike 4-vinylbenzyl azide [10]. It is stable in the dark freezer for years. If any degradation does occur the monomer can simply be purified by recrystallization.

There are 2 routes to get to the desired amine polymer. The first is to polymerize the phthalimide monomer [15] and then cleave the molecule with hydrazine to yield the free amine polymer. Alternately, VBP [15] could be reacted with hydrazine first to obtain an amine monomer which could then be polymerized. Both routes were investigated.

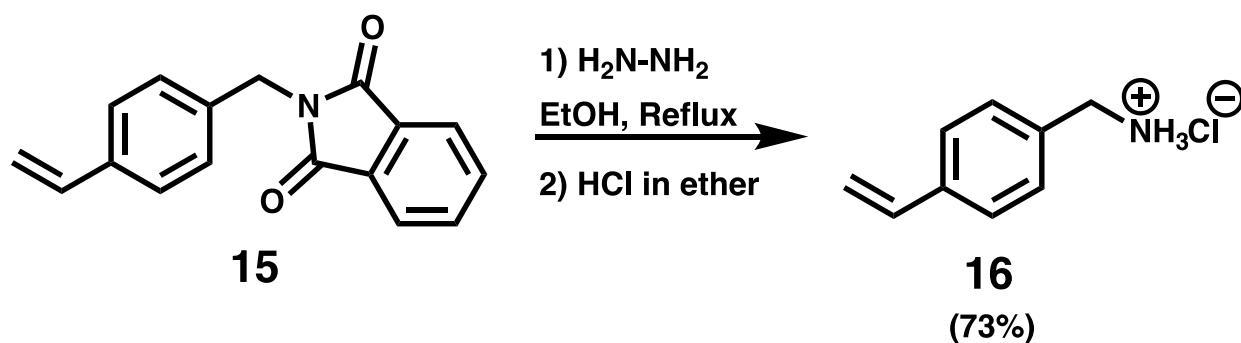


Figure 46: Synthesis of 4- vinylbenzyl amine HCl salt.

4-Vinylbenzyl phthalimide [15] was reacted with hydrazine hydrate in refluxing ethanol. This produced both 4-vinylbenzyl amine and phthalhydrazide, some of which precipitated out as a white solid. The two products were separated by making the reaction solution alkaline with sodium hydroxide until all solids were dissolved and then extracting the 4-vinylbenzyl amine out with diethyl ether. 4-Vinylbenzyl amine can be isolated as a pale yellow oil. However, 4-vinylbenzyl amine is very hydroscopic, so it was converted to its hydrochloride salt with an anhydrous HCl ether solution. The hydrochloride salt is stable and easier to isolate and handle

than the oil 4-vinylbenzyl amine. 4-Vinylbenzyl amine HCl [**16**] precipitated out of solution as a white solid and was cleanly isolated by vacuum filtration. However, [**16**] is somewhat hygroscopic and should be stored cold and the dark under nitrogen atmosphere.

With monomers VBP [**15**] and VBA HCl [**16**] being more stable and easier to handle than the previous azide [**7**], [**10**], and boc protected amine [**5**] monomers, it is feasible that almost every step of making the hydrogel polymers could be performed before cross-linking to form a solid gel. Attaching the dye and perturbation moieties to the soluble polymer would allow for characterization between every step. Taking NMR spectra of the soluble polymer after a dye is attached allows for more precise knowledge of the amount of dye that will end up in the final hydrogel. This also allows for further reaction to adjust those ratios if necessary. Cross-linking the soluble polymer after the main polymerization is completed also allows for further experimentation with cross-linker size and cross-link density without needing to account for monomer conversion percentage (as using purified soluble polymer makes it a constant).

To achieve this a new cross-linker is needed as the previous ones are only usable with radical polymerization. Instead of cross-linking between the polymer chain backbones these cross-links will be between the amine sidechains. Thus the cross-linker needs to have terminal groups that will readily react with amines. There are a multitude of methods for this⁶⁰. PEG could be oxidized to a dicarboxylic acid and then converted to a di(acid chloride). That option is a long synthesis from poly(ethylene glycol) and is also hazardous. Alternately, PEG could be oxidized to the diacid and then coupled to the amine polymer with HBTU. However, this is also a long synthesis compared to the previous cross-linker [**8**].

One of the most efficient methods is with carbonyldiimidazole (CDI). CDI reacts readily with both amines and alcohols and can couple them together. The soluble polymer, poly(ethylene glycol), and CDI can be mixed together at the same time. However, in the interest of characterization, poly(ethylene glycol) and CDI were mixed together first.

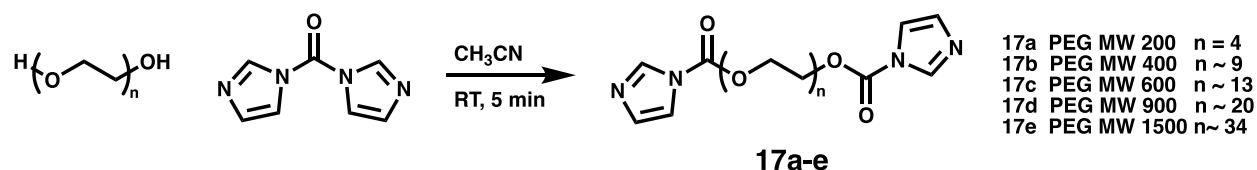


Figure 47: Five different lengths of poly(ethylene glycol) bis(carbonyl imidazole) [**17a-e**].

Five different lengths of PEG were reacted with CDI in acetonitrile to form cross-linkers [**17a-e**]. Cross-linker [**17c**] was isolated to confirm that the reaction was proceeding as expected. The NMR was clean and matched the expected spectrum. The reaction solutions can be used without the cross-linker [**17a-e**] being isolated. Acetonitrile is a suitable solvent for gel formation and the imidazole conveniently acts as a base during the amine coupling. However, the crosslinkers [**17a-e**] are sensitive to moisture and will react with the water in the air or a wet solvent, causing the reverse reaction. The experiments herein used non-anhydrous solvents, so crosslinker [**17a-e**] solutions were prepared fresh and used the same day. An anhydrous solvent and nitrogen atmosphere are needed to store the crosslinker longer.

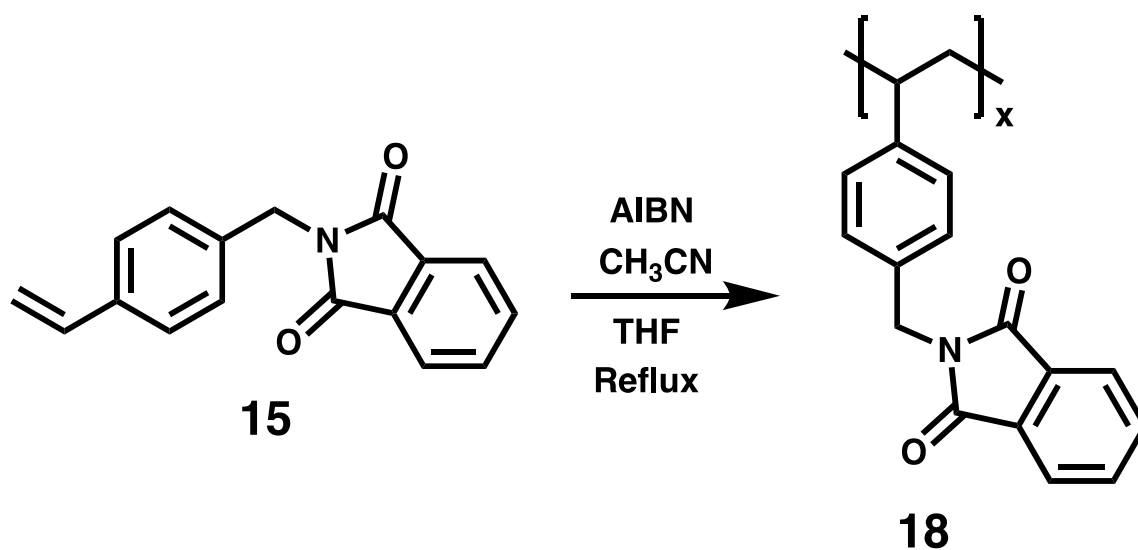


Figure 48: Homo-polymerization of 4-vinylbenzyl phthalimide [15].

4-Vinylbenzyl phthalimide [**15**] can be polymerized in refluxing THF or acetonitrile. However, the poly(4-vinylbenzyl phthalimide) [**18**] is not very soluble and will start precipitating out of the solution part-way through the polymerization. This is problematic as ideally the polymer chain length should be long and have a low distribution. Polymer chains precipitating out once they are a certain size limits the length of the polymer chains and produces smaller chains as the polymerization continues. Performing the polymerization in DMF succeeded in keeping everything in solution but complicated the reaction and work up. The temperature is more difficult to maintain at 80 °C and the polymerization must be carried out under nitrogen to prevent side reactions. DMF also proved to be extraordinarily difficult to remove from the product polymer [**18**], to the point where it was easier to leave it there during the subsequent reaction and then remove it during that purification. Polymerization in benzene was carried out at 80 °C and allowed clean isolation of polymer [**18**] as a white power by precipitating it out of the reaction mixture with ether. However, benzene is a known carcinogen, and other solvent options should be considered before determining benzene to be the most optimal solvent.

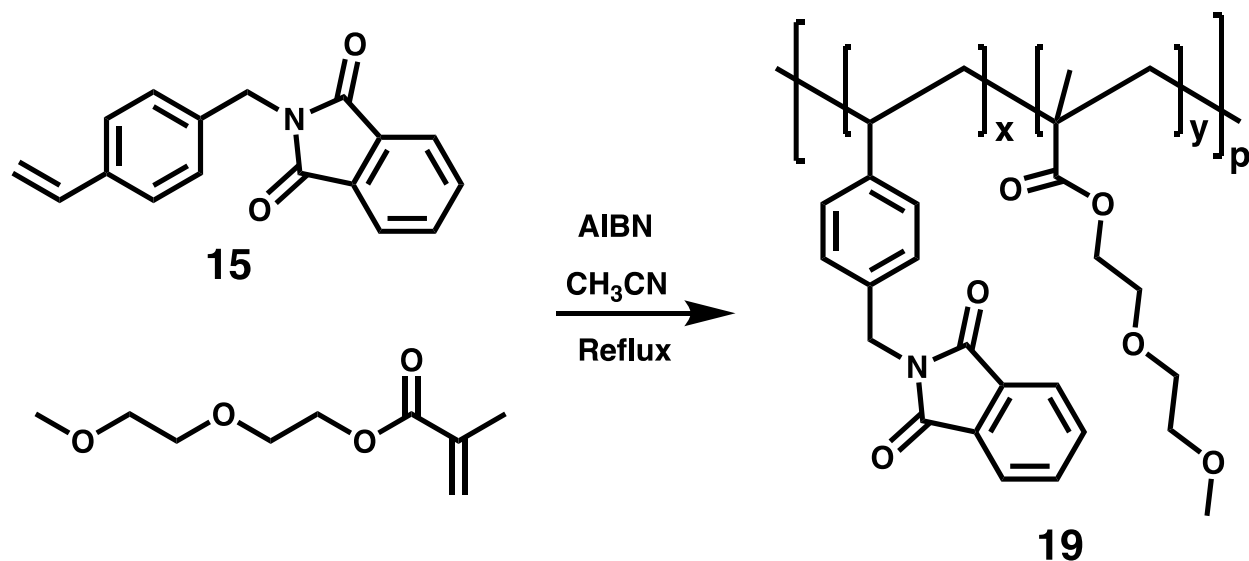


Figure 49: Co-polymerization of 4-vinylbenzyl phthalimide and DEGMEMA.

Co-polymerization of VBP [15] with DEGMEMA proceeded readily in acetonitrile without issue. The addition of the DEGMEMA co-monomer greatly increases the solubility of the polymer. Poly{(4-vinylbenzyl phthalimide)-co-[di(ethylene glycol) methyl ether methacrylate]} [19] was isolated by precipitation from THF with hexanes. The precipitation was carried out carefully to obtain polymer [19] as a powder.

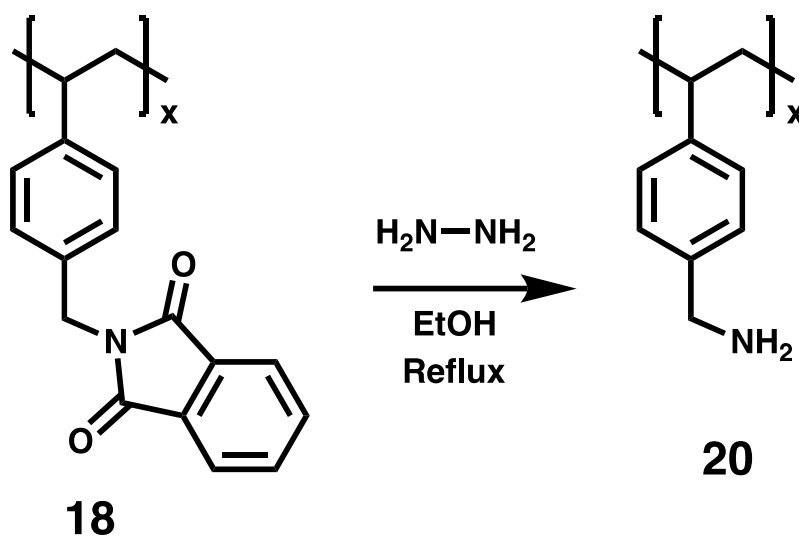


Figure 50: Synthesis of poly(4-vinylbenzyl amine) [20] from poly(4-vinylbenzyl phthalimide) [18].

Poly(4-vinylbenzyl phthalimide) [18] was deprotected using hydrazine hydrate in ethanol to form poly(4-vinylbenzyl amine) [20]. Polymer [18] was not soluble in ethanol, and only dissolved when hydrazine was added. A clear solution was observed for a brief moment before white solid (presumably phthalhydrazide) started to precipitate. Most of the phthalhydrazide was removed via hot filtration. The amine polymer [20] was soluble in boiling ethanol but not very soluble at room temperature. Polymer [20] could initially be precipitated from hot ethanol with diethyl ether. Any remaining hydrazine could be removed by dissolving polymer [20] in methanol and precipitating it with slightly basic water (pH 7.5 to 8). It was difficult to remove the last traces of phthalhydrazide. Therefore, polymer [20] was dissolved in THF and the phthalhydrazide slowly precipitated on standing and was removed by filtration. It is not recommended to attempt to use aqueous acid to dissolve polymer [20] for purification. Once amine polymer [20] was protonated and dissolved in water it was almost impossible to re-isolate it.

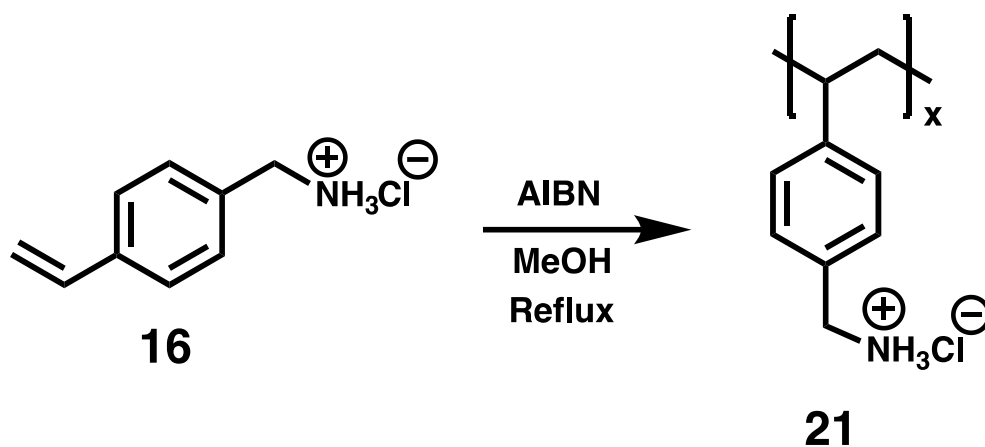


Figure 51: 4-Vinylbenzyl amine HCl [16] polymerization to poly(4-vinylbenzyl amine HCl) [21].

The issue of removing phthalhydrazide from the polymer could be completely avoided by polymerizing 4-vinylbenzyl amine HCl [**16**]. The polymerization proceeded somewhat slowly in refluxing methanol due to methanol's boiling point of 65 °C being lower than the optimal temperature for AIBN. The half-life of AIBN is 10 h at 65 °C vs ~85 min at 80 °C. Accordingly, polymerization at 65 °C takes several times as long as at 80 °C. A radical initiator that operates at lower temperatures would greatly improve this reaction but was unfortunately not available. Poly(4-vinylbenzyl amine HCl) [**21**] was isolated by precipitating it from methanol with acetone.

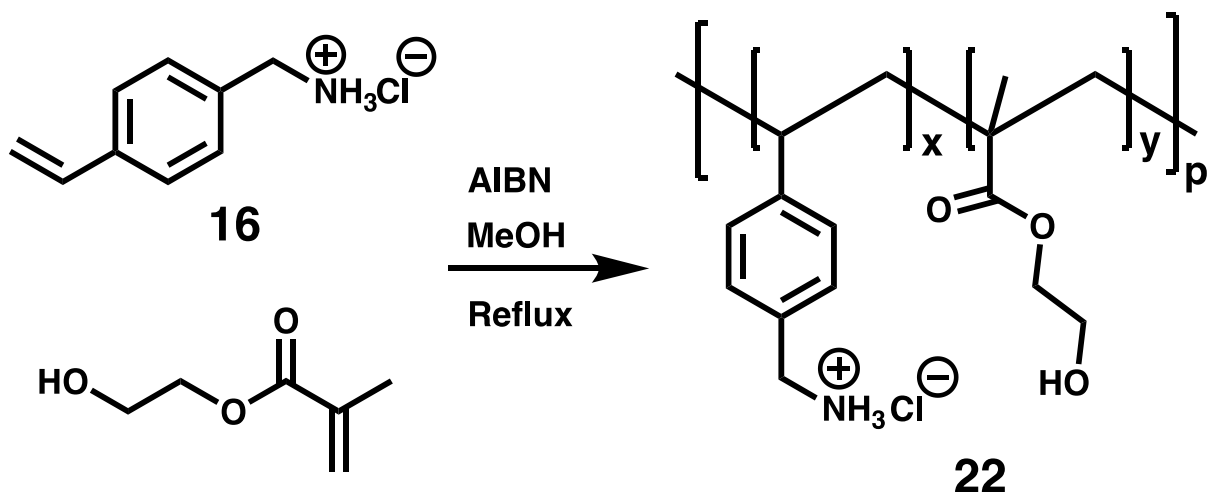


Figure 52: Co-polymerization of 4-vinylbenzyl amine HCl [**16**] and HEMA.

The co-polymerization of 4-vinylbenzyl amine HCl [**16**] and HEMA was carried out in refluxing methanol. Similarly, to the homo-polymerization of 4-vinylbenzyl amine HCl [**16**], the rate of polymerization was rather slow and took 2 days. Polymer [**22**] can be precipitated from methanol with either THF or diethyl ether. However, it is very hydroscopic and while it was being collected via filtration the majority of it went from a nice powder to a very viscous sticky substance. The high humidity in the lab that day also influenced this.

2.3 Hydrogels From Soluble Polymer

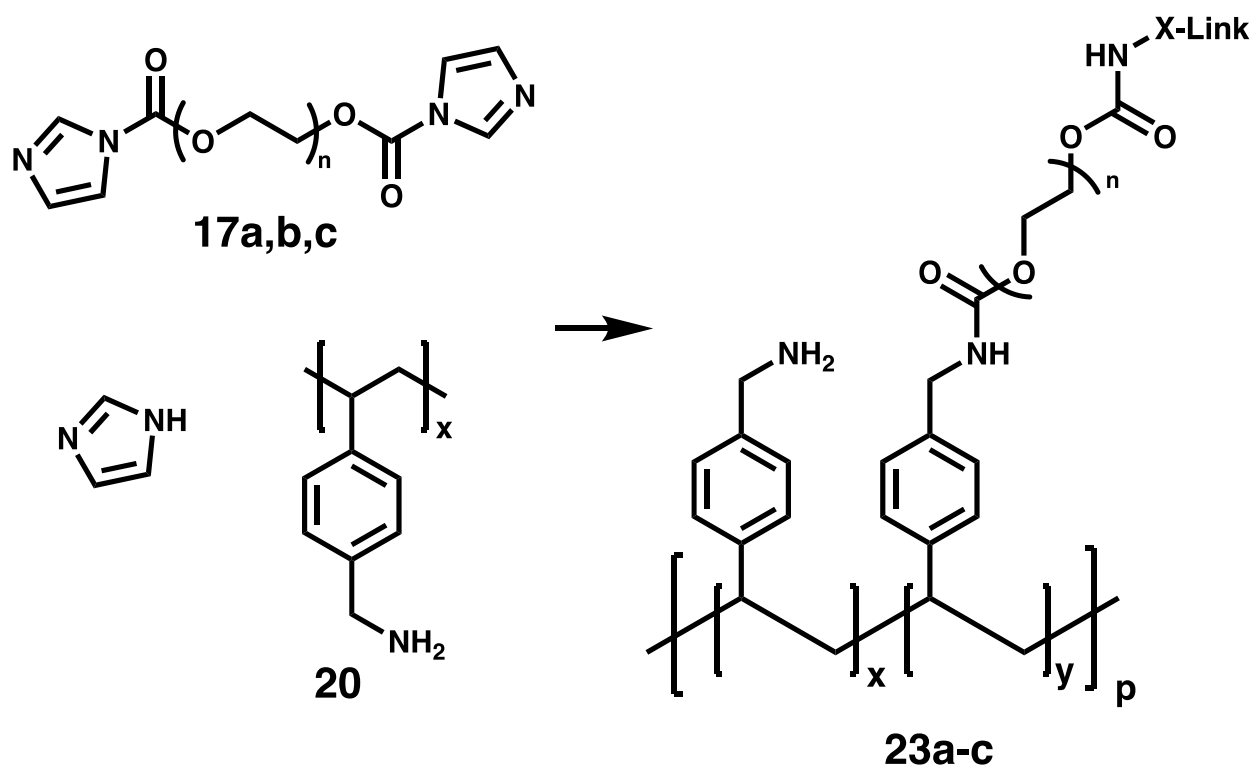


Figure 53: Minimum crosslinker length; Qualitative gel tests with poly(4-vinylbenzyl amine) and poly(ethylene glycol) bis(carbonyl imidazole) [**17a-e**].

A series of qualitative test reactions were carried out to see if CDI cross-linker [**17a-c**] and polymer [**20**] would react to form a hydrogel. None of the crosslinkers used were isolated. The first few tests did not produce a gel because the concentration was too low. The concentration was increased and poly 4-vinylbenzyl amine [**20**] reacted with cross-linker [**17a**] (PEG MW 200), however the resulting hydrogel was cloudy and pale yellow in color. Cross-linker [**17b**] (PEG MW 400) successfully formed a gel, but that turned out to also be cloudy and translucent. Cross-linker [**17c**] (PEG MW 600) resulted in a transparent gel, that was still very slightly yellow in color. Cross-linker [**17c**] is roughly the same length as the previous cross-

linkers, bis(4-vinylbenzyl) poly(ethylene glycol) (average MW 850) [8] and poly(ethylene glycol) dimethacrylate (av. MW 750) since the PEG core is the same length in each. A few tests failed to form gels when using a crosslinker solution more than 2 days old. The crosslinkers are sensitive to moisture and will react with the water in the air or a wet solvent. Gel tests [see 23a-c] using crosslinker [17c] a day after it was made were successful but slower due to some [17c] having been converted back into PEG, lowering the amount of cross-linker in the solution.

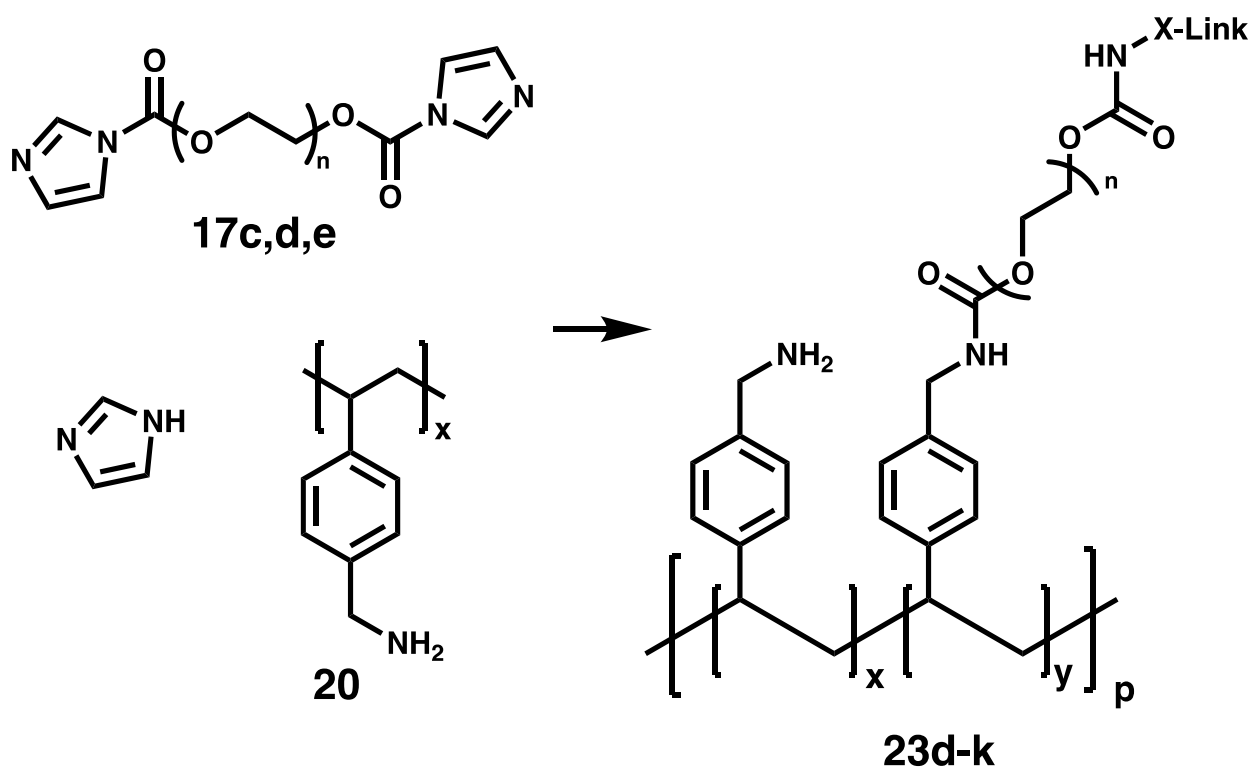


Figure 54: Timed gel tests with poly(4-vinylbenzyl amine) and poly(ethylene glycol) bis(carboxyl imidazole) [17c-e].

Table 2: Hydrogel formations tests with free amine polymer [20]

Rxn	X-linker	Solvent(s)	Polymer mmol amine	X-linker mmol	X-linker equiv %	Total g sol	Mmol polymer/ g sol	Gel time (min)
23d	17c	NMP/DMF	0.0522	0.00678	13	0.0507	1.03	<10
23e	17c	NMP/DMF	0.0957	0.00766	8	0.0767	1.25	3
23f	17c	NMP/DMF	0.0869	0.00678	7.8	0.0888	0.98	<10
23g	17d	NMP/DMF	0.0898	0.00744	8.3	0.1011	0.89	5
23h	17d	NMP/DMF	0.0440	0.0090	20	0.0913	0.48	15
23i	17d	NMP/DMF	0.1205	0.01143	10	0.1412	0.85	3
23j	17e	NMP/DMF	0.1152	0.00825	7.2	0.1596	0.72	3
23k	17d	NMP/DMF	0.07669	0.00635	8.3	0.1507	0.51	<5

Timed gel tests were carried out with poly(4-vinylbenzyl amine) [20] and CDI-PEG-CDI cross-linkers [17c-e], varying the percent cross-linker and the total concentration. There were no trends observed between gel time and cross-linker percentage or overall concentration. The trend was that all gel times were very fast, 5 minutes on average. This is not enough time to get the polymer solution into the mold and get the bubbles out before the gel starts to set. There was an attempt to do so that resulted in bubbly semi-set polymer gel half filling the mold.

It was hypothesized that forming a hydrogel using poly(4-vinylbenzyl amine HCl), rather than the free amine polymer, might be slower. This is because the amines need to be de-protonated to go through the substitution reaction with cross-linker [17a-e].

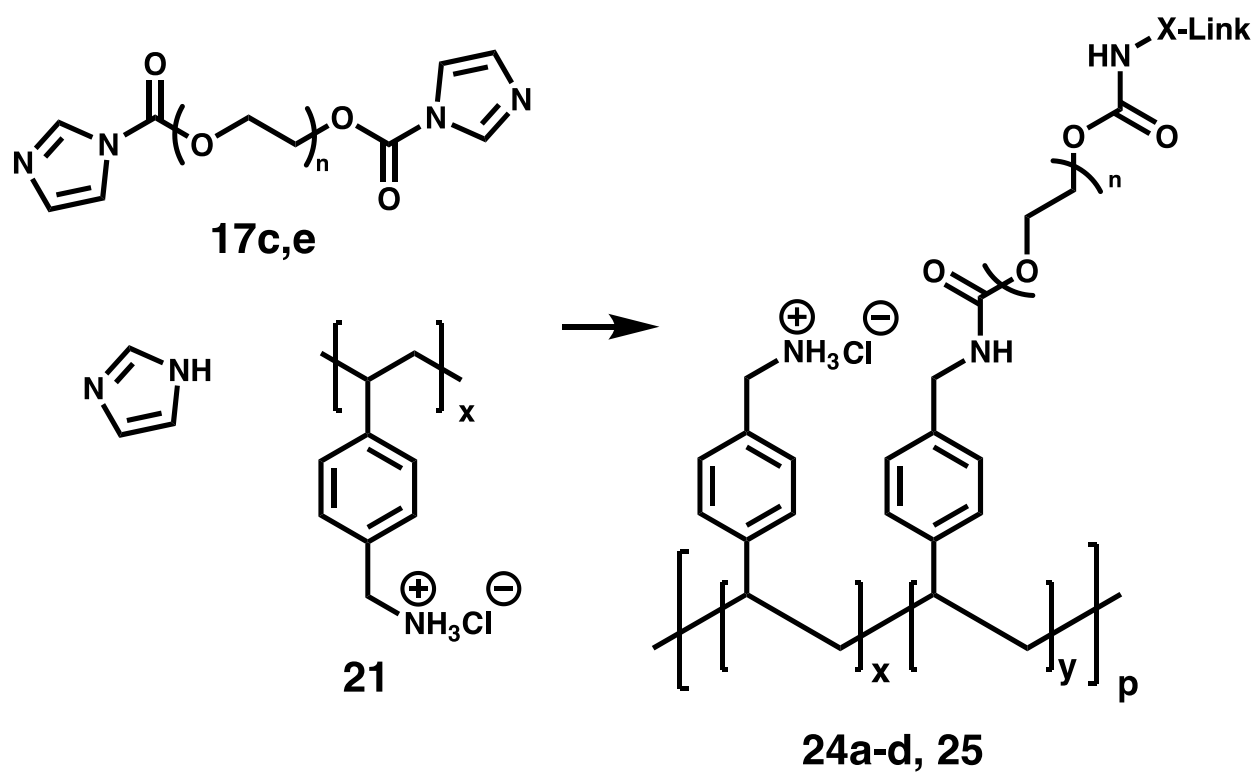


Figure 55: Timed gel tests with poly(4-vinylbenzyl amine HCl) and poly(ethylene glycol) bis(carbonyl imidazole) [17c,e].

Table 3: Hydrogel formations tests with amine HCl polymer [21]

Rxn	X-linker	Solvent (s) used	Polymer mmol amine	X-linker mmol	X-linker equiv %	Total mass solution	Mmol polymer/g sol	Gel time
24a	17e	H ₂ O/ DMF	0.126	0.00712	5.5	0.1545	0.81	~30 min
24b	17e	H ₂ O/ CH ₃ CN	0.0407	0.00489	12	0.0805	0.50	30+ min
24c (25)	17e	H ₂ O/ CH ₃ CN	0.214	0.0137	6	0.2682	0.80	25+ min
24d (26)	17c	H ₂ O/ CH ₃ CN	0.570	0.0725	12.7	0.4042	1.41	~20 min

Gel tests with the hydrochloride salt of polymer [21] and cross-linker [17e] (PEG MW 1500) gave preliminary results [24a] indicating a gel time of ~20-30 minutes. The gel tests were repeated twice more with new solutions and the gel time remained in the ~20-30 min window. This gave enough time to ensure the polymer solution is homogeneous and cast gels.

The reaction solution from gel [24c] was used to make free-floating gels. Free-floating gels were made by using one hydrophobic C-18 slide [30] and one unmodified slide so that the hydrogel polymer wouldn't adhere to the glass. The gels [25] swelled to approximately 5 times their original size. This is thought to be due to the reduced cross-linking (6% vs 15% for radical rxn gels), the longer cross-linker [17e] (1200 MW PEG vs 600 MW), and the lower concentration of the solution (it's ~1/3rd as concentrated). This result was interesting but undesired for the sensor gels since the hydrogel polymer needed to remain attached to glass and can't be allowed to swell too much. This also indicated that increasing the length of the cross-linker would probably not be helpful, and cross-linker [17c] (PEG600CDI) was the best choice.

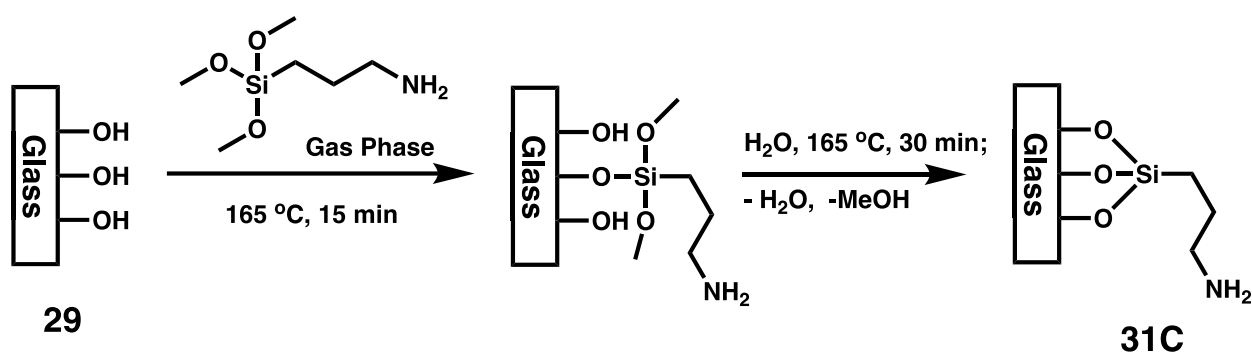


Figure 56: Amine terminated silanized glass slides [31C].

Modifying the silanization procedure to produce glass slides suitable for forming hydrogels from soluble polymer was relatively simple. The majority of the existing silanization procedure [31C] was followed, omitting the methacrylation step with methacryloyl chloride.

This produced silanized glass slides with free amines on the surface [**31C**] rather than methacrylamides [**31D**].

In addition to acting as the cross-linker, poly(ethylene glycol) bis(carbonyl imidazole) [**17c**] can connect the polymer chains to the glass surface [**31C**] by linking the amine groups of the poly(4-vinylbenzyl amine HCl) [**21**] side chains and the APTMS chains on the glass. This does alter the cross-linking density mildly because the amount of amino propyl chains on the glass surface are not known.

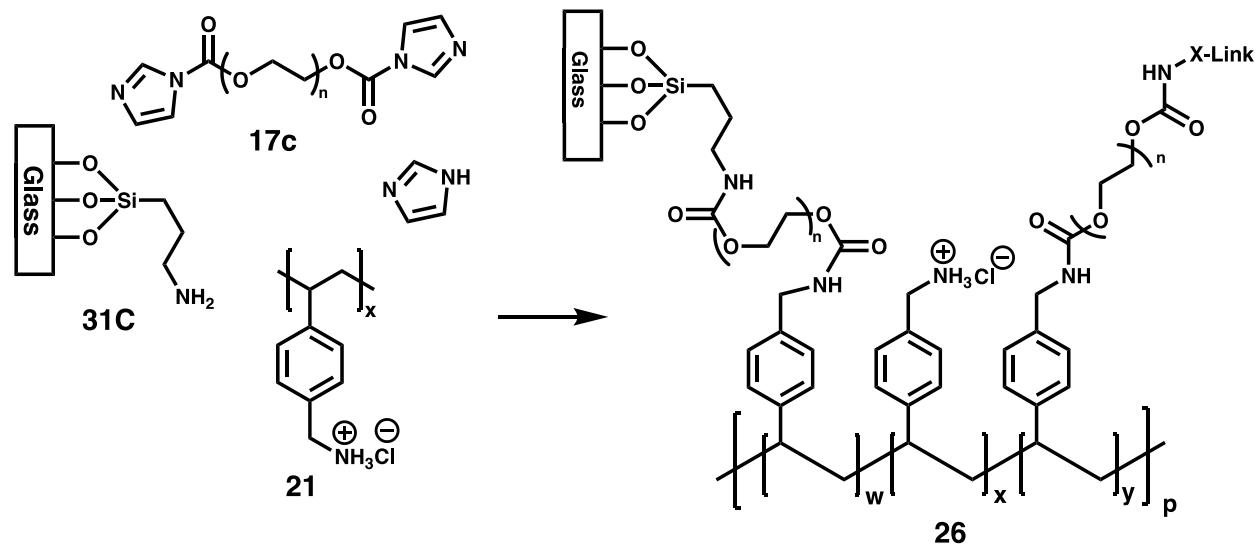


Figure 57: Hydrogel dots attached to glass; from soluble polymer [**21**] and cross-linker [**17c**].

Poly(4-vinylbenzyl amine HCl) [**21**] and cross-linker [**17c**] were mixed and the solution was applied to the polymer dot mold. The hydrogels were let set at room temperature. Some of the reaction solution was reserved, and started to set after 20 min. See the entry for [**26/ (24d)**] in Table 3. The hydrogels [**26**] are clear, transparent, water compatible, and have been stable on glass in 18M Ω water for over a year.

2.4 RAFT reactions

Having made hydrogels attached to glass from soluble polymer, the next step in improving the polymers is making the soluble polymer more consistent. It was hypothesized that a controlled radical polymerization (CRP) method, specifically RAFT, would result in more uniform and replicable polymerizations for the soluble polymers.

Before any RAFT reactions could take place, a chain transfer agent (CTA) was needed. There are 3 main classes of CTAs for RAFT, 2 of which are applicable to styrenes, methacrylamides and methacrylates: dithiobenzoates and trithiocarbonates. Of the 2, dithiobenzoates are easier to synthesize.

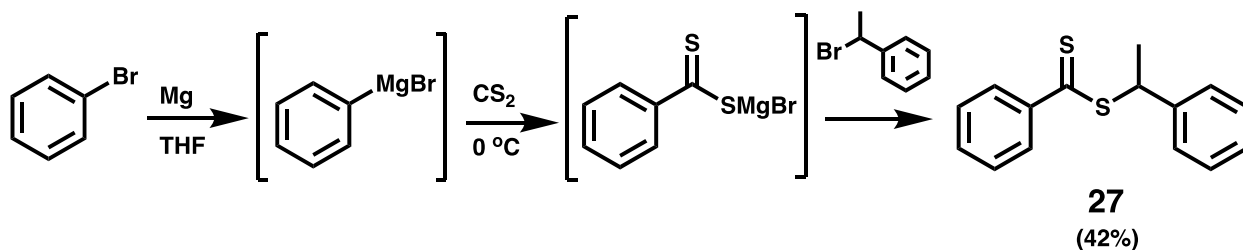


Figure 58: Grignard reaction to synthesize 1-phenylethyl dithiobenzoate [27].

1-Phenylethyl dithiobenzoate [27] was made via a Grignard reaction with phenylmagnesium bromide, carbon disulfide, and (1-bromoethyl)benzene. [27] was purified with flash column chromatography (10:1, hexanes /EtOAc). 1-Phenylethyl dithiobenzoate [27] is a bright red oil that must be kept in the freezer and under N₂ atmosphere.

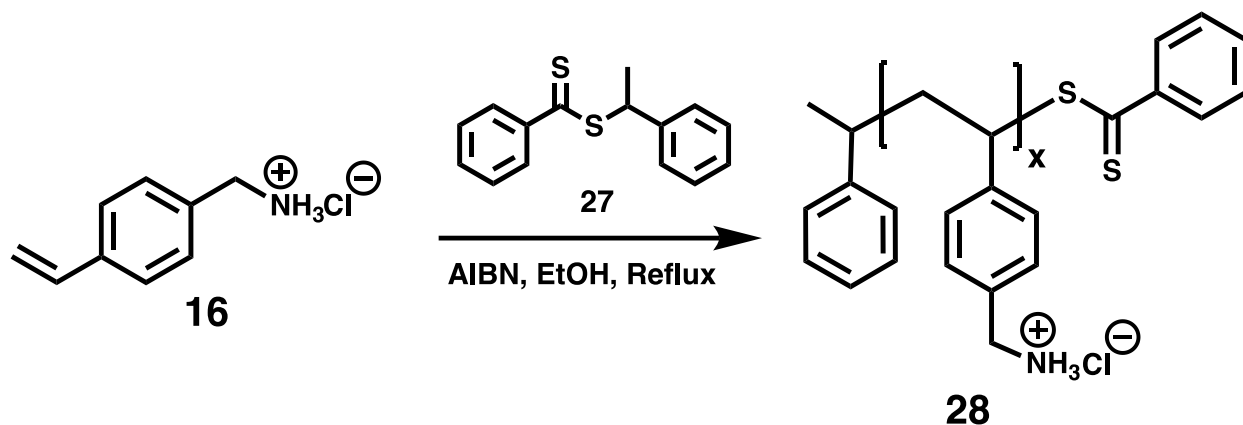


Figure 59: RAFT polymerization of 4-vinylbenzyl amine HCl [**16**].

1-Phenylethyl dithiobenzoate [**27**] was used as the CRT in the RAFT polymerization of 4-vinylbenzyl amine HCl [**16**]. The ratio of monomer [**16**]: CTA[**27**]: AIBN was 95:1:0.13.

Unfortunately, the reaction's progress stalled, remaining at < 10% after a week. It is suspected that the dithiobenzoate RAFT CTA [**27**] caused significant reaction retardation. Upon further investigation in the literature, I found several papers demonstrating that dithiobenzoates cause reaction retardation in styrene polymerizations if the conditions aren't quite right. Though they are easier to make than trithiocarbonates, dithiobenzoates in general are not the optimal chain transfer agent for styrene monomers. Switching to a trithiocarbonate CTA more suited to styrenes might provide a better result.

2.5 Conclusion

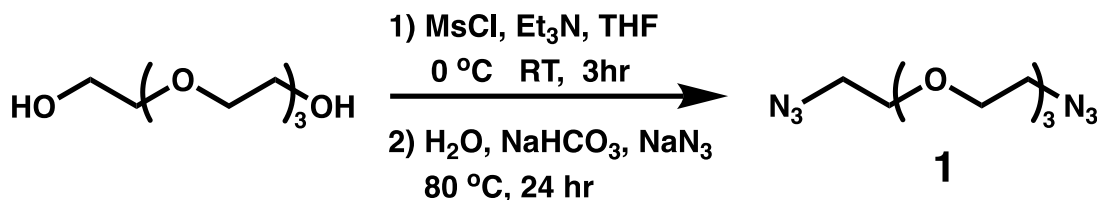
In the pursuit of making and improving hydrogel polymers attached to glass to become a solid support for metal ion chemosensors, many things have been achieved. The synthesis of the functional monomer has been shortened from a 4-step route with N-boc amine tetra(ethylene glycol) methacrylamide [5]; to 2 steps with azide tetra(ethylene glycol) methacrylamide [7]; to 1 step with 4-vinylbenzyl azide [10]. 4-Vinylbenzyl azide [10] was found to be unstable. A new route to an amine monomer was investigated by switching the protecting group to phthalimide rather than azide. 4-vinylbenzyl phthalimide [15] was found to be much more stable and easier to purify and is also a 1 step synthesis. [15] was also deprotected to give 4-vinylbenzyl amine HCl [16]. All 5 monomers were shown to be compatible with polymerization, and all but [15] were used to form a hydrogel attached to glass. A more hydrolytically stable crosslinker than poly(ethylene glycol) dimethacrylate (average MW 750) was needed, and so the terminal methacrylates were switched to 4-vinylbenzyl groups. The points weakest to hydrolysis in bis(4-vinylbenzyl) poly(ethylene glycol) (av. MW 850) [8] are the ethers within poly(ethylene glycol). As ethers are much more hydrolytically stable than methacrylates, and most of the hydrogel polymer is based on PEG, crosslinker [8] is as stable as it reasonably can be for this application. The variety of new monomers and the new cross-linker were used to form new hydrogels attached to glass, all of which proved to be transparent and compatible with water. A cross-linking variation experiment revealed that the hydrogel dots can contain 46% cross linker and still be transparent. Hydrophobic groups can be included in the hydrogel if there are sufficient hydrophilic groups present to keep the hydrogel majorly hydrophilic as a whole. The previously unknown cause of hydrogels delaminating from glass

was found to originate from the silanization procedure. Changes made to improve the silanization procedure were successful and did not result in delamination in subsequent reactions. A variety of soluble polymers were made to offer a further degree of control over the composition and properties of the polymers, as well as provide insight into the polymerization reactions. It was found that the polymerization inhibitors present in the monomers did not need to be removed; their effect negligible compared to the amount of AIBN added during polymerization. The monomer with the shortest synthesis, 4-vinylbenzyl azide [10], was successfully polymerized but was unfortunately unstable to air, heat, and light, and tends to form an undesirable degradation side product. The monomer 4-vinylbenzyl phthalimide [15] was found to be much more stable and easier to purify. A variety of homo-polymer and copolymers with different properties were successfully synthesized. Amine terminated soluble polymers were successfully made via two different routes: de-protecting poly(4-vinylbenzyl phthalimide) [18] and polymerizing 4-vinylbenzyl amine hydrochloride [16]. A compound based on poly(ethylene glycol) and carbonyldiimidazole was devised as the new cross linker which functions by coupling to 2 amine groups, connecting them. Of the 5 different lengths of cross-linker [17a-e], poly(ethylene glycol) bis(carbonyl imidazole) (ave, MW 800) [17c] was found to be the most optimal for the hydrogel dots, limiting swelling while maintaining transparency. Poly(ethylene glycol) bis(carbonyl imidazole) (ave, MW 800) [17c] can also connect amine terminated soluble polymer to the glass surface. Clear, transparent, stable, and water compatible hydrogels covalently attached to glass were successfully made from cross-linker [17c] and poly(4-vinylbenzyl amine hydrochloride) [21].

Chapter 3. Experimental

1: Tetra(ethylene glycol) diazide -or- O,O'-bis(2-azidoethyl)diethylene glycol -or-

1,11-Diazido-3,6,9-trioxaundecane -or- 1-azido-2-(2-(2-(2-azidoethoxy)ethoxy)ethoxy)ethane



This material was synthesized by Tyler Fenske.

Procedure followed from Schwabacher et al. J Org. Chem. 1998, 63, 1727-1729.⁵³

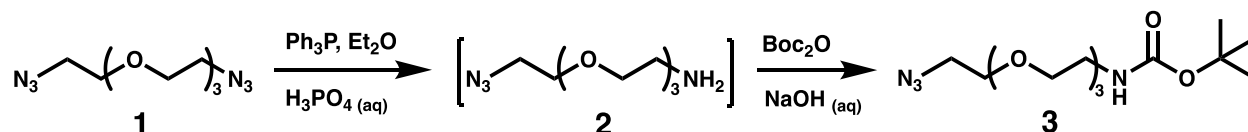
From paper: (compound number changed [1])

1,11-Diazido-3,6,9-trioxaundecane, [1]. To tetra(ethylene glycol) (50.78 g, 0.26 mol), dried by addition and rotary evaporation of 25 mL of toluene, in 200 mL of THF under N₂ was added CH₃SO₂Cl (45 mL, 0.58 mol) by syringe. The solution was stirred on an ice bath as Et₃N (81 mL, 0.58 mol) in 50 mL of THF was added dropwise over 27 min, forming a yellow-white precipitate. After 1 h the ice bath was removed, and the mixture was left to stir for 3.5 h with occasional swirling. Addition of H₂O (122 mL) dissolved the solid, forming two liquid phases, which were chilled on a cold-water bath, NaHCO₃ (12 g, to pH 8) was added followed by NaN₃ (34.88 g, 0.54 mol), and stirring was started. **WARNING:** If azide is added to acid, toxic and explosive HN₃ will form. Distillation of THF to a solution temperature of 80 °C was followed by reflux for 24 h. The aqueous layer was extracted five times with 100-mL aliquots of Et₂O, and each Et₂O layer was backwashed with the same 50-mL aliquot of saturated NaCl. The Et₂O layers were combined, dried over sodium sulfate, filtered, and concentrated by rotary evaporation, and traces of

solvent were removed by evacuation to yield 43.7g of [1] as an oil (67%). TLC (silica gel 1:1 EtOAc: hexanes, KMnO_4 , $R_f = 0.61$) showed a single component. At smaller scale (≤ 20 g of tetra(ethylene glycol)) azide substitution carried out at 75-80 °C in H_2O solvent after removal of all THF by rotary evaporation gave diazide [1] in 85% yield,

^1H NMR: δ 3.68 (m, 12H), 3.40 (t, $J = 5.1$ Hz, 4H). IR (neat): 2915, 2109 cm^{-1} . MS (EI) $M + H$ calcd 245.1, found 245.1. Anal. Calcd for $\text{C}_8\text{H}_{16}\text{N}_6\text{O}_3$: C, 39.34; H, 6.60; N, 34.41. Found: C, 39.33; H, 6.61; N, 34.10

3: N-Boc-amine tetra(ethylene glycol) azide -or- N-boc-amine-TEG-azide
-or- tert-butyl (2-(2-(2-(2-azidoethoxy)ethoxy)ethoxy)ethyl)carbamate



Tetra(ethylene glycol) diazide [1] (4.51g, 18.48 mmol) was combined with aq. H_3PO_4 (40 mL, 0.65M). A solution of Ph_3P (4.26g, 16.17 mmol) in ether (30 mL) was added dropwise over 20 minutes under nitrogen. The biphasic solution was stirred rapidly for 24 hours. Reaction progress was monitored by TLC, looking for the disappearance of Ph_3P .

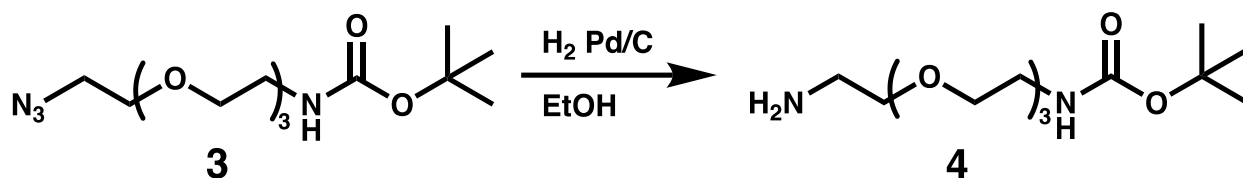
The reaction mixture was then phase separated and the aqueous layer was washed 3 times with 50 mL portions of diethyl ether. NaOH (9.02 g, 225.47 mmol) was gradually added to the aqueous layer. The solution was allowed to warm via the exothermic heat of dissolution and

any remaining ether was allowed to evaporate. The solution was then sealed and chilled overnight at $\sim 5^{\circ}\text{C}$ (fridge temperature) in order to crystallize out triphenyl phosphine oxide. The aqueous solution of intermediate **[2]** was filtered' rinsing with 100 ml of deionized water. Boc anhydride (di-tert-butyl dicarbonate) (5.06 g, 23.19 mmol) was added, and the solution was boiled for 1 hour, letting some of the water evaporate, then stirred for an additional 2 hours without heating. The resulting solution was then extracted 3 times with 40 mL portions of ethyl acetate. The organic portions were combined, dried over sodium sulfate, and concentrated on the rotary evaporator. The residue was then dried on the Schlenk line (vacuum) overnight. Compound **3** was isolated as a pale-yellow oil. Yield = 3.61g (70%).

^1H NMR (500 MHz, CDCl_3) δ 5.00 (br-S, 1H), 3.68 (m, 10H), 3.54 (t, $J = 5$ Hz, 2H), 3.39 (t, $J = 5$ Hz, 2H), 3.31 (br-S, 1H), 1.45 (s, 9H). ^{13}C NMR (126 MHz, CDCl_3) δ 155.99, 79.17, 70.73, 70.67, 70.64, 70.26, 70.23, 70.08, 50.69, 40.37, 28.43. ESI-MS Calcd for $\text{C}_{13}\text{H}_{26}\text{N}_4\text{O}_5$ ($\text{M}+\text{H}^+$) 319.37, found 319.15.

4: N-Boc tetra(ethylene glycol) diamine

-or- tert-butyl (2-(2-(2-(2-aminoethoxy)ethoxy)ethoxy)ethyl)carbamate



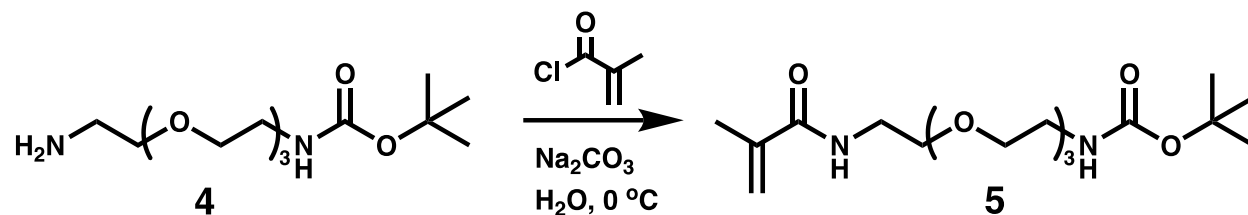
Compound [**3**] (3.61g, 11.34 mmol) was dissolved in 20 mL of ethanol and 5% Pd/C (62 mg) was added. The reaction flask was sealed, and the system was flushed with hydrogen gas and capped with a balloon filled with hydrogen. The balloon was replaced whenever it was observed to be deflated. The reaction was stirred for 48 hours. The reaction mixture was filtered through celite, rinsing with 20 mL of hot ethanol. The solution was concentrated under reduced pressure and a sample was taken for NMR in CDCl₃. The NMR spectrum indicated that the reaction was incomplete. The previous residue was redissolved in ethanol and 5% Pd/C (62 mg) was added. The reaction was once again placed under hydrogen gas and stirred for an additional 48 hours.

The reaction mixture was filtered through celite, rinsed with hot ethanol, and concentrated under reduced pressure. This yielded 2.95 g (89%) of a pale-yellow oil.

¹H NMR (500 MHz, CDCl₃) δ 5.42 (br-S, 1H), 3.65 (m, 10H), 3.54 (t, J = 5 Hz, 2H), 3.31 (br-S, 2H), 2.81 (t, J = 5 Hz, 2H), 1.44 (s, 9H). ¹³C NMR (126 MHz, CDCl₃) δ 156.41, 70.56, 70.38, 70.32, 70.28, 70.12, 70.06, 40.93, 28.46. ESI-MS Calcd for C₁₃H₂₈N₃O₅ (M+H⁺) 293.97, found 293.25.

5: Boc-amine tetra(ethylene glycol) methacrylamide

-or- tert-butyl (14-methyl-13-oxo-3,6,9-trioxa-12-azapentadec-14-en-1-yl)carbamate

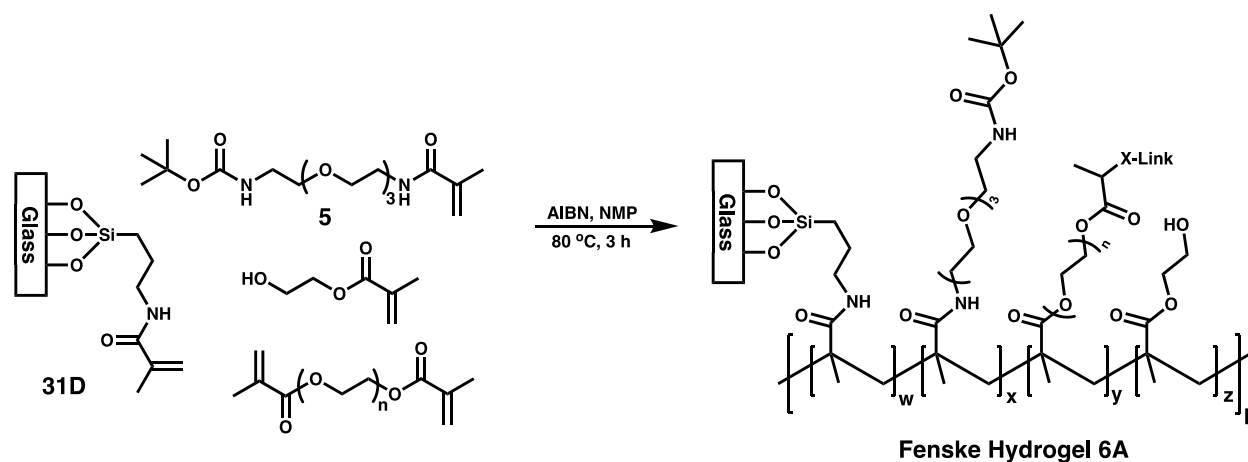


Compound [**4**] (2.95g, 10.09 mmol) was combined with 4-methoxyphenol (20 mg, polymerization inhibitor), sodium carbonate (2.87g, 27.07 mmol) and 15 mL of deionized water. The mixture was cooled to 0°C and methacryloyl chloride (1.15 ml, 11.77 mmol) was added drop wise while stirring. The reaction was stirred for 18 hours and allowed to come to room temperature. The resulting mixture was phase separated, extracting 4 times with 10 mL portions of dichloromethane. The organic portions were combined, dried over sodium sulfate, and concentrated under reduced pressure. The product was a pale-yellow oil. Yield = 3.31g (91%)

¹H NMR (500 MHz, CDCl₃) δ 6.38 (br-s, 1H), 5.70 (s, 1H), 5.33 (s, 1H), 5.00 (br-s, 1H), 3.63 (m, 10H), 3.54 (t, J = 5 Hz, 4H), 3.30 (t, J = 5 Hz, 2H), 1.97 (s, 3H), 1.45 (s, 9H). ¹³C NMR (500 MHz, CDCl₃) δ 168.46, 155.97, 140.11, 119.41, 70.51, 70.24, 69.80, 39.38, 28.42, 18.65.

6A - Fenske Hydrogel

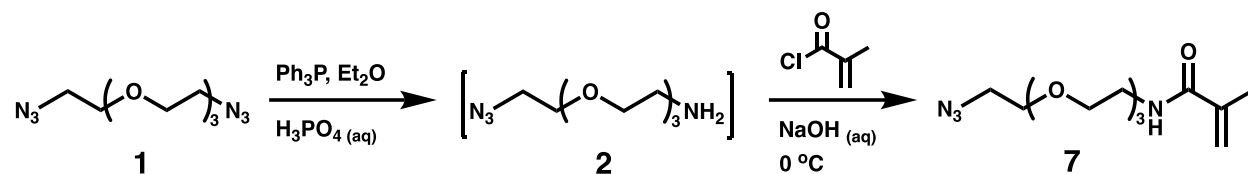
Glass-brush-[3-(trimethoxysilyl)propyl methacrylamide]-graft-*{net-poly[N-boc amine tetra(ethylene glycol) methacrylamide]-co-(2-hydroxyethyl methacrylate)-v-[poly(ethylene glycol) dimethacrylate (750)]}*



N-Boc-amine tetra(ethylene glycol) methacrylamide [5] (0.993 g, 2.76 mmol) was combined with 2-hydroxyethyl methacrylate (HEMA) (0.368 g, 2.83 mmol) and PEGDMA 750 (0.764 g, 1.01 mmol) and dissolved in toluene. The solution was passed through an inhibitor removal column to remove any MEHQ and BHT. The toluene was removed under reduced pressure. AIBN (125.2mg, 0.076 mmol) was added, the mixture was dissolved in NMP (3 ml), and the resulting solution was degassed under vacuum for 30 seconds. The polymerization solution was then immediately used to make 5 slides of polymer (see general hydrogel polymerization procedure [32]). Any remaining solution was stored in the freezer.

7: Azido tetra(ethylene glycol) methacrylamide

-or- N-(2-(2-(2-(2-azidoethoxy)ethoxy)ethoxy)ethyl)methacrylamide



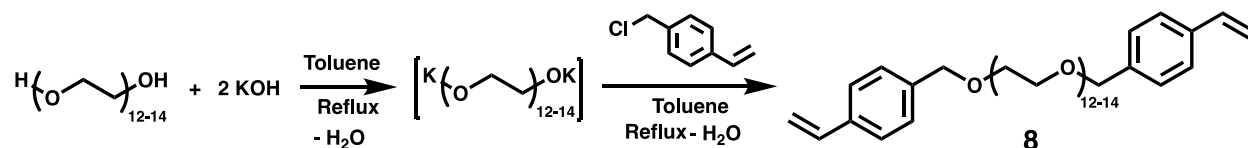
Tetra(ethylene glycol) diazide [1] (206.5 mg, 0.85 mmol) was combined with 2ml of 0.65 M phosphoric acid. Triphenylphosphine (195.7 mg, 0.75 mmol) was dissolved in 2 ml of diethyl ether and added dropwise. An additional 1ml of ether was used to ensure complete transfer. The reaction was left to stir under nitrogen and tracked by TLC.

After 24 hours, the aqueous and organic layers of the reaction were separated, and the aqueous layer was washed twice with 2 ml portions of ether. Sodium hydroxide (1.02 g) was added slowly to the aqueous layer. Any remaining ether was allowed to evaporate, and the flask was placed in the fridge to chill overnight. Precipitated triphenyl phosphine oxide was removed by vacuum filtration, rinsing with 20 ml of water. An additional 1.03 g of sodium hydroxide was added to the solution, which was then chilled in the fridge for several days. The solution was then filtered again, rinsing with 20 ml of water. Methacryloyl chloride (0.08 ml, 0.82 mmol) was added at 0°C , and the reaction was left to stir, and tracked by TLC. After 50 min, 10 ml of dichloromethane was added, and the mixture was stirred vigorously for 10 min. The layers were allowed to settle, and the organic layer was removed, dried over sodium sulfate, and concentrated by rotary evaporation. A sample of the product was taken for proton NMR which showed the reaction to be ~80% complete.

The crude product was recombined with the original water layer and 0.1 ml (1.02 mmol) of methacryloyl chloride and left to stir overnight. TLC shows no free amine remaining by acidic ninhydrin stain. 15 ml of brine was added to the reaction solution, which was then extracted with 15 ml of dichloromethane. The organic layer was washed with 15 ml of brine. The aqueous layer was extracted twice with 10 ml portions of dichloromethane and then twice more with 5 ml portions. The organic portions were combined, dried over sodium sulfate, and concentrated by rotary evaporation. The product is a pale-yellow oil. Yield: 156 mg (73%).

$^1\text{H NMR}$ (500 MHz, CDCl_3): δ 1.96 (3H, s), 3.39 (t, $J = 6.4$ Hz, 2H), 3.52 (t, $J = 6.4$ Hz, 2H), 3.59-3.70 (m, 10H), 5.32 (1H, d, $J = 4.1$ Hz), 5.70 (1H, d, $J = 4.1$ Hz)

8: Bis(4-vinylbenzyl) poly(ethylene glycol) (av. MW 850) (BVBPEG 850)



Poly(ethylene glycol) (av. MW 600) (10.08 g, 16.35 mmol) was dissolved in 100 ml of toluene and combined with potassium hydroxide (3.51 g, 62.47 mmol). The solution was diluted to 500 ml with toluene and set to reflux under nitrogen with a dean stark trap. After 5 hours, no more water was removed. The solution was cooled, and 4-vinylbenzyl chloride (6.41 g, 41.97 mmol) was added. The reaction was then left to reflux overnight.

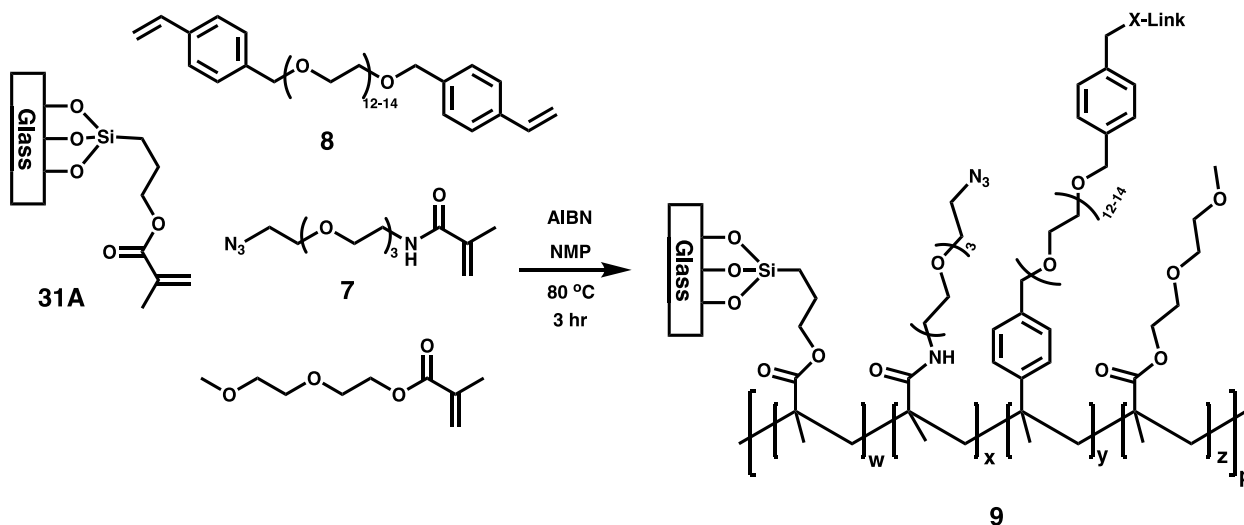
The reaction was let cool slightly and a 0.25 ml sample of the solution was taken and concentrated. A few drops each of acetic anhydride and pyridine were added along with 1 ml CDCl₃. The mixture was let stand for 30 min and then taken for proton NMR. Peaks that would indicate acetylated poly(ethylene glycol) were not visible.

The reaction solution was cooled to ~60 °C and a small amount of 4-methoxyphenol (MEHQ) was added to inhibit polymerization. The reaction solution was then filtered warm through a celite plug, rinsing with hot toluene. The filtered solution was concentrated by rotary evaporation.

The crude product was washed with hexanes a total of nine times. Four times with 75 ml portions and five times with 50 ml portions. The product was dried under vacuum to obtain a pale-yellow oil. Yield: 12.56 g (90%)

¹H NMR (500 MHz, CDCl₃): δ 3.64 (~60H, m), 4.55 (4H, s), 5.23 (2H, dd, J = 11.0, 1.1 Hz), 5.73 (2H, dd, J = 18.2, 1.1 Hz), 6.71 (2H, dd, J = 18.2, 11.0 Hz), 7.29-7.39 (8H, 7.30 (ddd, J = 8.1, 1.4, 0.5 Hz), 7.38 (ddd, J = 8.1, 1.8, 0.5 Hz)).

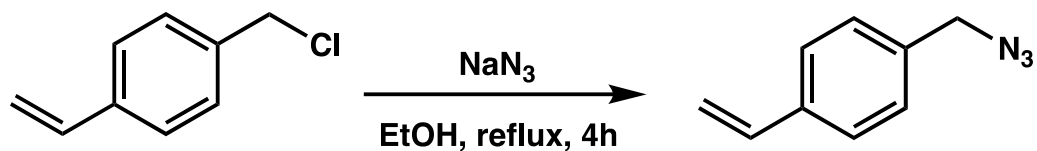
9: Glass-*comb*-[3-(trimethoxysilyl)propyl methacrylate]-*graft*-{*net*-poly[azide tetra(ethylene glycol) methacrylamide]-*co*-[di(ethylene glycol) methyl ether methacrylate]-*v*-[bis(4-vinylbenzyl) poly(ethylene glycol) (850)]}



Azide monomer [7] was dissolved in toluene, run through a small inhibitor removal column (Aldrich), and then reconcentrated under reduced pressure. Monomer [7] (0.0741g, 0.259 mmol) was combined with di(ethylene glycol) methyl ether methacrylate (DEGMEMA) (0.0646g, 0.343 mmol), cross-linker [8] (0.0682g, 0.080 mmol), NMP (0.244 ml), and AIBN (11.6 mg, 0.706 mmol). The solution was degassed under vacuum.

The solution was then used to make 2 slides of polymers (see general polymer prep procedure [32]). Silanization used was method [31A] - solution phase.

10: 4-Vinylbenzyl azide (VBAZ) -or- azidomethyl styrene -or- 1-(azidomethyl)-4-vinylbenzene

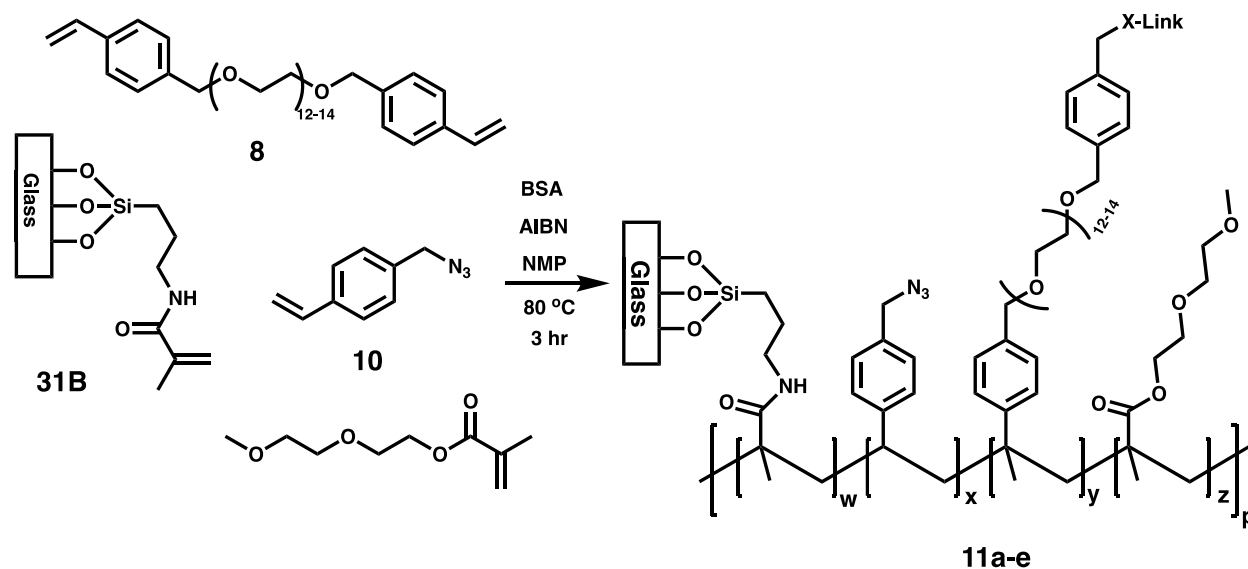


Sodium azide (0.967 g , 14.9 mmol) was combined with 4-vinylbenzyl chloride (1.3ml, 1.45 g, 9.5 mmol) and 10 ml of ethanol. The reaction was heated to reflux and tracked by TLC (hexanes).

After 4 hours, the reaction was cooled, and 40 ml of diethyl ether was added. The solution was extracted with twice with 10 ml portions of water, once with 15 ml of brine and then once more with 10 ml of water. The organic layer was dried over sodium sulfate and concentrated by rotary evaporation and dried under reduced pressure. The product is a yellow liquid. Yield = 1.3953g (92%). Store in the dark in the freezer. Unstable at room temperature.

$^1\text{H NMR}$ (500 MHz, CDCl_3): δ 4.32 (2H, s), 5.27 (1H, dd, $J = 11.0, 1.1$ Hz), 5.77 (1H, dd, $J = 18.2, 1.1$ Hz), 6.72 (1H, dd, $J = 18.2, 11.0$ Hz), 7.27-7.43 (4H, 7.28 (ddd, $J = 8.2, 1.9, 0.6$ Hz), 7.42 (ddd, $J = 8.2, 1.2, 0.6$ Hz))

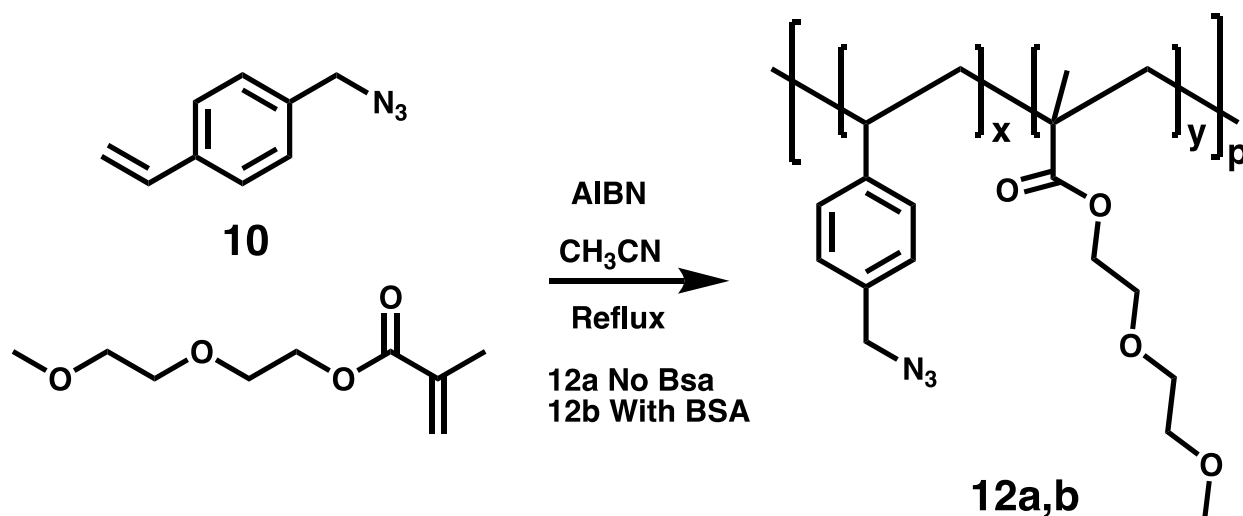
11 - {*Net*-poly[4-(vinylbenzyl) azide]-co-(2-hydroxyethyl methacrylate)-v-[bis(4-vinylbenzyl) poly(ethylene glycol) (850)]}-*block*-[3-(trimethoxysilyl)propyl methacrylamide]-*block*-glass



Monomer **[10]**, DEGMEMA, cross-linker **[8]**, NMP, AIBN, and BSA were combined in the following ratios (see table on page 83). The amount of **[10]** was held constant; the amount of cross-linker **[8]** was increased while the amount of DEGMEMA was proportionally decreased, keeping the vinyl group concentration constant. The 5 solutions were then used to make polymer dots using the general hydrogel polymer method **[32]** and silanized slide method **[31B]** - individual gas phase. All 5 variants successfully polymerized, and the resulting hydrogels were very pale yellow, transparent, and compatible with water. Each of the 5 slides had some of the hydrogel dots delaminate (3-4 per slide). Any difference in swelling was small enough to be barely observable. The difference from **[11a]** (7% cross-linker **[8]**) to **[11e]** (46 % cross-linker **[8]**) was a very small decrease in the height and width of the gels. The **[11a]** hydrogel dots had edges that were a little waffly and out of round, while the **[11e]** hydrogel dots were precisely the size of the polymer mold.

Compound	VBA (9)	DEGMEMA	BVBPEG 850	AIBN	BSA	NMP
Mol. Wt.	159.188	188.22	850	164.21	203.432	
Variation 11a						
mass	0.0370	0.0591	0.0344	0.0069	0.0100	0.2604
mmol	0.232	0.314	0.041	0.042	0.049	
equiv	1.00	1.35	0.17	0.18	0.21	
mol % polymer	40	53	7	7	8	
% vinyl groups	37	50	13			
mass %	28	45	26			
Variation 11b						
Mass (g)	0.0373	0.0457	0.0702	0.0065	0.0104	0.2553
mmol	0.234	0.243	0.083	0.040	0.051	
equiv	1.00	1.04	0.35	0.17	0.22	
mol % polymer	42	43	15	7	9	
% vinyl groups	36	38	26			
mass %	24	30	46			
Variation 11c						
mass	0.0376	0.0306	0.1114	0.0056	0.0139	0.2587
mmol	0.236	0.163	0.131	0.034	0.068	
equiv	1.00	0.69	0.56	0.14	0.28	
mol % polymer	45	31	25	6	13	
% vinyl groups	36	25	20			
mass %	21	17	62	3		
Variation 11d						
mass	0.0380	0.0154	0.1385	0.0071	0.0088	0.2662
mmol	0.239	0.082	0.163	0.043	0.043	
equiv	1.0000	0.3428	0.6842	0.1811	0.1812	
mol % polymer	49	17	34	9	9	
% vinyl groups	37	13	50			
mass %	20	8	72			
Variation 11e						
mass	0.0287	0	0.1305	0.0061	0.0091	0.1983
mmol	0.180	0	0.154	0.037	0.045	
equiv	1.0	0	0.9	0.2	0.2	
mol % polymer	54	0	46	11	13	
% vinyl groups	37	0	63			
mass %	18	0	82			

12: Poly{(4-vinylbenzyl azide)-*co*-[di(ethylene glycol) methyl ether methacrylate]}



Monomer conversion was evaluated by ¹H NMR, comparing the integration ratio of the vinyl peaks from 4.5 to 6.5 ppm vs. the peak at ~4.3 ppm [overlap of benzylic peak of [**10**] (δ 4.32) and the most downfield CH₂ peak of DEGMEMA (δ 4.31); monomers and polymer (δ 4.28)]

12a – No BSA:

4-Vinylbenzyl azide [**10**] (0.165g,), was combined with di(ethylene glycol) methyl ether methacrylate (0.189g), AIBN (0.0170g), and acetonitrile (1 ml).

The mixture was heated at 78°C under N₂. Samples were taken for NMR at 3 hours, 6 hours and 9 hours. Monomer conversion was 85% after 3h, 92% after 6h, and 96% after 9h. After the 9-hour sample, an additional 17.7 mg of AIBN was added and the polymerization was continued.

More NMR samples were taken at 12 hours and 15 hours. Monomer conversion was 99% after 12h and ~99.5% after 15h. There are in the NMR spectrum at 15h, and

At 15 hours the NMR spectrum showed very minor traces of DEGMEMA that were below the integration limit and no detectable peaks for VBAZ [**10**]. The reaction was not heated further.

12b – With BSA:

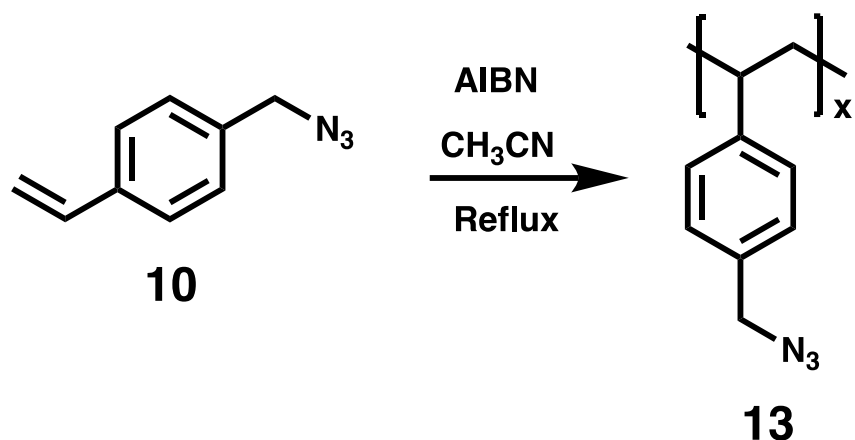
Monomer **9** (4-vinylbenzyl azide) (0.165g), was combined with di(ethylene glycol) methyl ether methacrylate (0.194g), AIBN (0.0170g), and acetonitrile (1 ml).

The mixture was heated at 78 °C under N₂. A sample was taken for NMR after 3 hours, showing 85% monomer conversion. An additional 18 mg of AIBN was added and the polymerization was continued. NMR samples were taken at 6 hours and 9 hours. Monomer conversion was 97% after 6h, and 99% after 9h.

Workup: Reaction [**12a**] was concentrated and dried overnight under reduced pressure. This yielded an extremely viscous yellow orange material with the consistency of taffy. Mass = 0.3461 g (92%). Note: NMR sample fractions were not recombined with the remaining reaction residue, which accounts for the lost mass.

¹H NMR (500 MHz, CDCl₃): δ 0.57-1.97 (4H, broad m)-[polymer backbone], 1.63 (3H, broad s), 3.40-3.76 (14H, broad m), 4.28 (4H, broad s), 7.13 (4H, broad d)

13: Poly(4-vinylbenzyl azide)

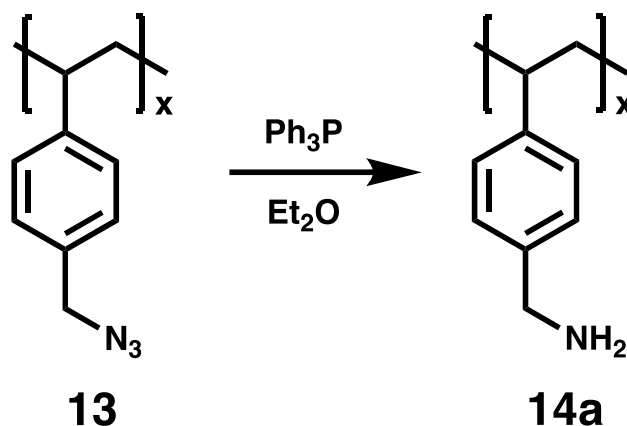


A 1: 0.9343 mixture of 4-vinylbenzyl azide: DMF (1.584 g VBAZ, 10 mmol) was combined with 15 ml of acetonitrile and 0.0835 g of azobisisobutyronitrile (AIBN). The reaction was heated at 80 °C for 5 hours. A sample of the solution was analyzed by NMR. The NMR spectrum showed the polymerization was 80% complete based on the ratios of monomer to the DMF internal standard (20% monomer remaining). The reaction was heated at 60 °C for a few hours. Proton NMR showed no change. Additional AIBN (0.0875 g) was added, and the reaction was heated for another 2 hours. ¹H NMR showed ~ 4% monomer remaining. The reaction solution was decanted to separate it from the insoluble side products. The solvent was then removed by rotary evaporation. The product was a viscous yellow oil. The product was washed by swirling with hexanes (10 ml) to remove the residual monomer. The hexanes wash was repeated twice more, then the product was dried under vacuum. The product was a glassy solid[1.175 g (74%)]. NMR: Reaction completion evaluated by lack of vinyl peaks from 4.5 to 6.5 ppm.

¹H NMR (500 MHz, DMSO-d₆): δ 0.82-1.93 (2H, broad m)-[polymer backbone], 4.38 (2H, broad s), 7.11 (4H, broad d)

14a: Poly(4-vinylbenzyl amine)

From reducing poly(4-vinylbenzyl azide) [13] with triphenyl phosphine.

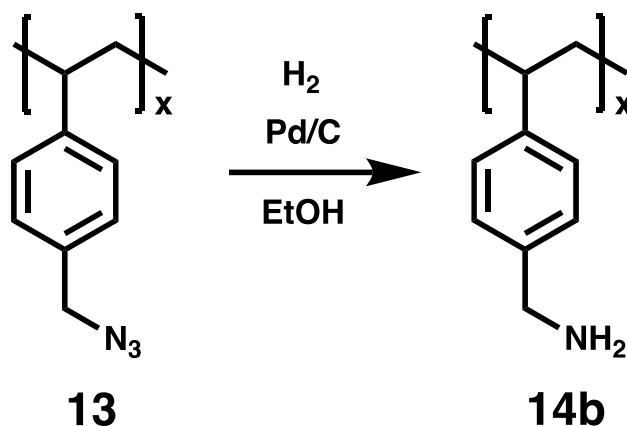


Poly(4-vinylbenzyl azide) [13] (0.137 g, 0.86 mmol [monomer basis]) was combined with 15 mL of ethanol and 15 mL of diethyl ether. Triphenyl phosphine (0.258 g, 0.98 mmol) was added and an additional 2 mL of ether was used to ensure complete transfer. The reaction mixture was let stir under nitrogen for 72 hours. An aliquot was qualitatively tested with ninhydrin, confirming the presence of free amines in the solution. The reaction solution was concentrated under reduced pressure. Water was added to the solution and the pH was brought to >10 by slow addition of sodium hydroxide. After the change in pH, the solution phase separated, with a thin orange layer on top of the aqueous layer. The solution was chilled overnight, and triphenylphosphine oxide crystallized out. The orange oil was observed to have aggregated, clinging to some of the triphenylphosphine oxide crystals. The mixture was semi-solid with the consistency of taffy. The orange semi-solid was separated from the aqueous layer and attempts were made to dissolve it. The orange mixture proved to be insoluble in most organic solvents and acidic water. [14a] was unable to be isolated.

14b: Poly(4-vinylbenzyl amine)

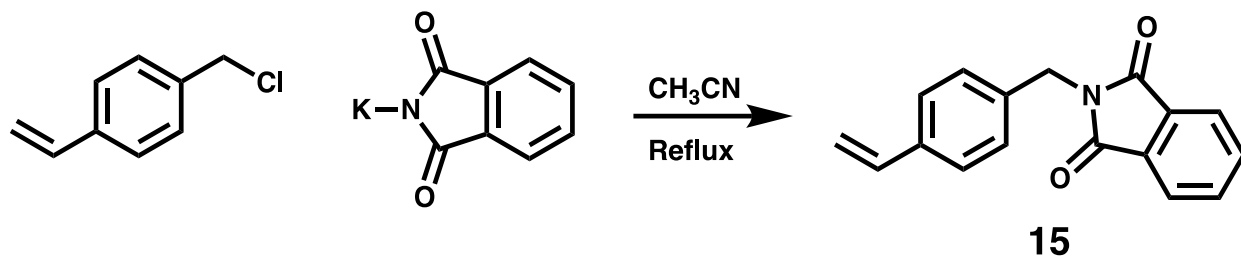
From reducing poly(4-vinylbenzyl azide) [**13**] with hydrogen and palladium on carbon.

H₂ Pd/C RAD-2-23, RAD-2-27



Poly(4-vinylbenzyl azide) [**13**] (0.200 g, 1.26 mmol [monomer basis]) was dissolved in 20 mL of THF and combined with 9.7 mg of 5% palladium on carbon. The reaction was placed under hydrogen and capped with hydrogen filled balloon. The balloon was replaced whenever it was observed to be deflated. The reaction mixture was stirred at room temperature, with reaction progress monitored periodically by NMR. The reaction was very slow and had not progressed much after a week. Determining the reaction completion percentage is difficult due to the benzylic peaks for the azide polymer [**13**] and the amine polymer [**14b**] overlapping, but it can be roughly estimated as 25%. After stirring for another week, the reaction was still under 50% complete. Polymer [**14b**] was not isolated.

15- 4-Vinylbenzyl phthalimide (VBP)



4-vinylbenzyl chloride (VBC) (8.43 g, 55 mmol) was combined with potassium phthalimide (13.8298 g, 75 mmol) and 100 ml of acetonitrile. The reaction was refluxed tracking by TLC in hexanes. After 5 days the reaction was stopped even though TLC still showed traces of VBC. The reaction solution was concentrated by rotary evaporation and the residue was mixed with water and filtered. Crude (damp) = 20.4043 g (140% yield). The crude solid was recrystallized from ethanol using hot filtration and isolated via vacuum filtration. The mother liquor was then concentrated and recrystallized. This was repeated 3 times. The product was isolated as an off-white crystalline solid.

1st crystallization crop = 7.4152 g (51% yield) Melting point = 104 -107 °C (Lit. 106 - 107°C)

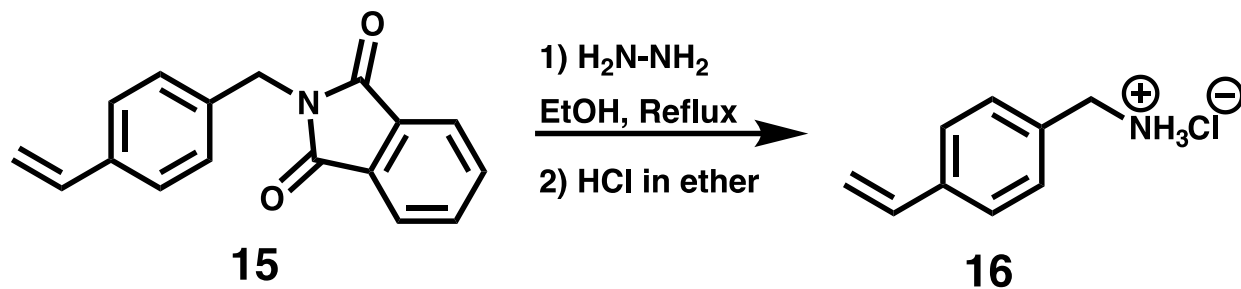
Product (crop 2) = 2.5917 g (18%) (69% overall) m.p. = 105-108 °C

Product (crop 3) = 1.3860 g (10%) (78% overall) m.p. = 104-107 °C

Product (crop 4) = 0.4864 g (3%) (82% overall) m.p. = 103.5-106 °C

¹H NMR (500 MHz, CDCl₃): δ 4.83 (2H, s), 5.21 (1H, dd, J = 11.0, 1.1 Hz), 5.70 (1H, dd, J = 18.2, 1.1 Hz), 6.69 (1H, dd, J = 18.2, 11.0 Hz), 7.34-7.41 (4H, 7.35 (ddd, J = 8.1, 1.6, 0.5 Hz), 7.39 (ddd, J = 8.1, 1.9, 0.5 Hz)), 7.68-7.85 (4H, 7.69 (ddd, J = 7.8, 7.6, 1.3 Hz), 7.83 (ddd, J = 7.8, 1.3, 0.5 Hz))

16- 4-Vinylbenzyl amine hydrochloride salt (VBA HCl)



4-(vinylbenzyl) phthalimide (VBP) [**15**] (8.9674 g, 1 equiv) was combined with 50 ml of ethanol; then hydrazine monohydrate (5.0 ml, 3 equiv) was added slowly to the solution. The reaction immediately started bubbling. The mixture was heated to reflux and the solid VBP dissolved. Once a solution was obtained a white solid quickly precipitated. 25 ml of ethanol was added, and the reaction was refluxed for 3 h, tracking by TLC (CH_2Cl_2).

The reaction was cooled and 100 ml of 15 wt. % NaOH (aq) was added. The mixture was stirred until most (90%) of the solid dissolved; then filtered and washed with 15 wt. % NaOH (aq). The aqueous solution was extracted with 4 portions of diethyl ether (2x200ml, 2x100ml), adding H_2O (150ml) when some NaOH precipitated. The ether layers were combined, concentrated to 300 ml, washed twice with 100 ml of 4 wt. % K_2CO_3 (aq), and dried over magnesium sulfate.

A solution of HCl in diethyl ether was prepared by generating HCl gas with sulfuric acid and NaCl and bubbling the gas through the ether for an hour and a half. The HCl in ether solution was dried over magnesium sulfate and then 200 ml was added slowly to the solution of product in ether. A white solid precipitated and was collected via vacuum filtration and dried under reduced pressure. Yield = 3.94 g (73%). A sample was taken for NMR in D_2O .

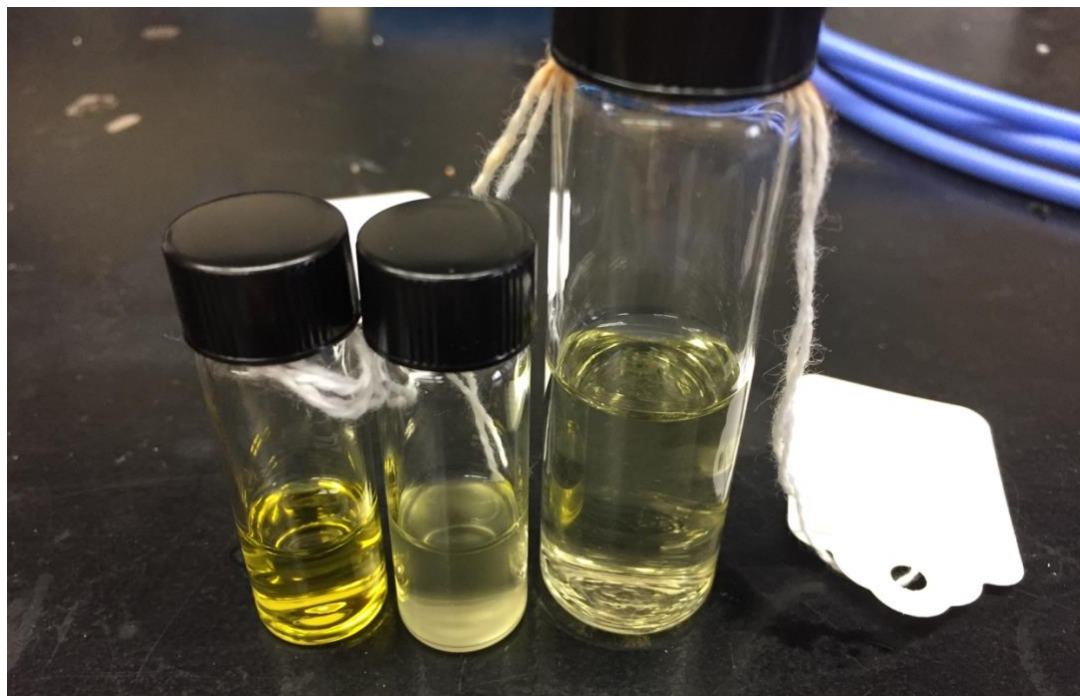
Hydrazine testing was done on both the aqueous layer and the product. Product [**16**] was negative for hydrazine and the aqueous layer tested positive for hydrazine.

^1H NMR (500 MHz, D_2O): δ 4.18 (2H, s), 5.37 (1H, dd, $J = 11.0, 1.1$ Hz), 5.90 (1H, dd, $J = 18.2, 1.1$ Hz), 6.82 (1H, dd, $J = 18.2, 11.0$ Hz), 7.44 (2H, ddd, $J = 8.0, 1.4, 0.5$ Hz), , 7.57 (2H, ddd, $J = 8.0, 1.8, 0.5$ Hz)

Hydrazine testing, General procedure:

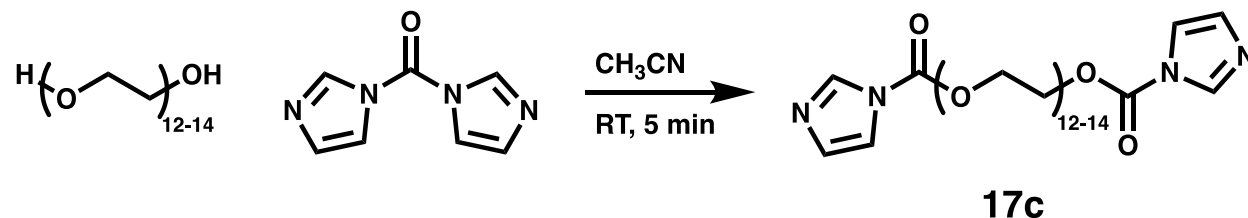
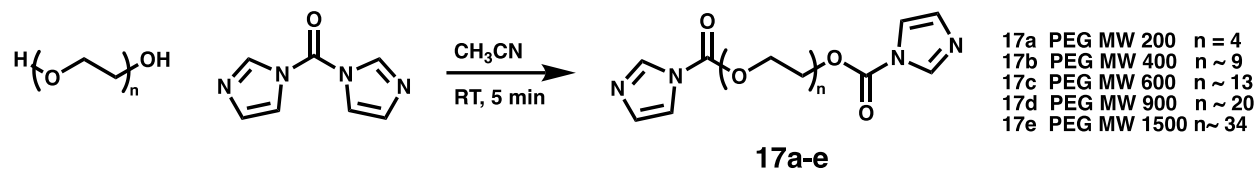
A solution of paradimethylaminobenzaldehyde was made in acidic (HCl) water and methanol (0.12 M). A solution of hydrazine hydrate in water was made (0.015 M). The test solution was acidified to mix with water. A few drops of the paradimethylaminobenzaldehyde solution were added to the solution being tested.

A sample testing positive for hydrazine will turn a darker yellow/orange.



From left to right: polymer [20] in THF before precipitation from water (positive result: hydrazine present), polymer [20] after precipitation from water (negative result), paradimethylaminobenzaldehyde solution (control color).

17- Bis(carbonyl imidazole) poly(ethylene glycol) (800) (CDI-PEG-CDI)

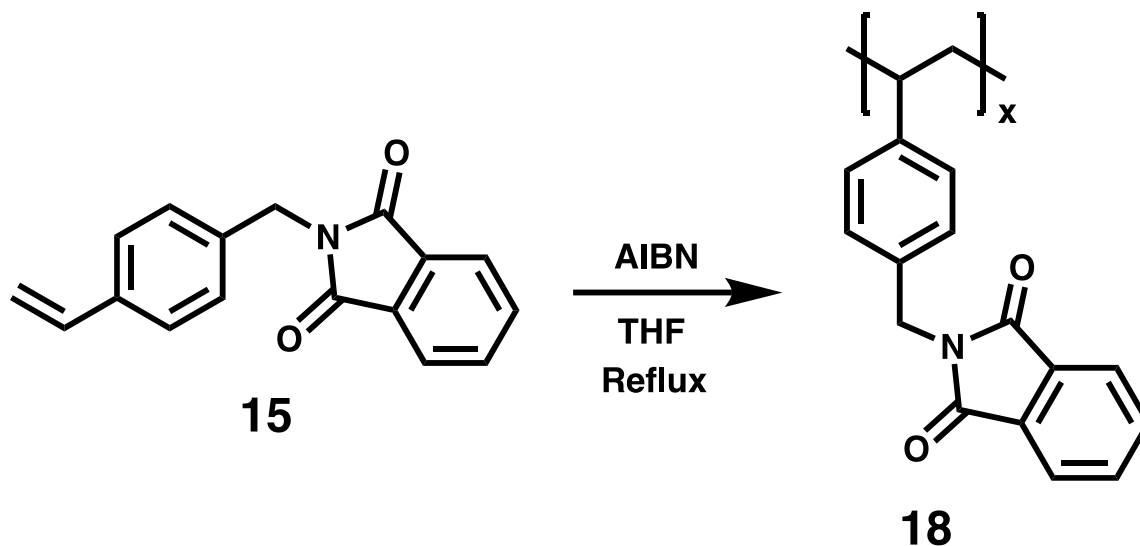


Poly(ethylene glycol) (av. MW 600) (0.9931 g, 1.61 mmol) was combined with carbonyl diimidazole (0.7071 g, 4.36 mmol) and 25 ml of acetonitrile. The solution was stirred under nitrogen at room temperature for 6.5 hours. A small sample of the reaction mixture was concentrated and taken for NMR analysis to assess reaction completion.

To reaction was added 20 ml of toluene and 10 ml of water were added. The layers were separated, and the aqueous layer was extracted 4 times with 20 ml portions of toluene. The organic portions were combined and concentrated by rotary evaporation. Yield: 0.6331 g (50%)
The product is a pale-yellow oil.

¹H NMR: δ 3.48-3.70 (48H,m), 4.47 (4H, t, *J* = 7.3 Hz), 7.06 (2H, dd, *J* = 4.8, 1.9 Hz), 7.26 (2H, dd, *J* = 4.8, 2.5 Hz), 8.09 (2H, dd, *J* = 2.5, 1.9 Hz)

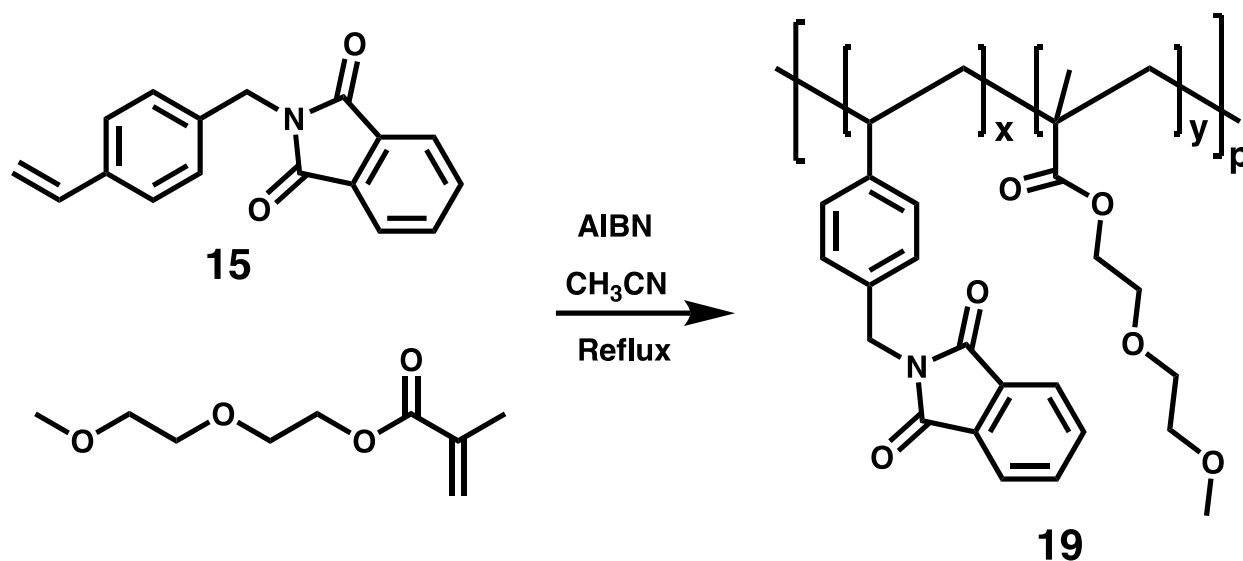
18 - Poly 4-vinylbenzyl phthalimide



4-Vinylbenzylphthalimide (VBP) (3.56 g, 13.5 mmol) was combined with AIBN (0.05 equiv) and dissolved in 15 ml of THF (with some heating). The reaction was refluxed for 6 hours under nitrogen. The reaction solution was transferred to an Erlenmeyer flask and 15 ml of acetonitrile was added. Polymer [18] was precipitated from the solution by slow addition of methanol (50 ml) while stirring. The precipitate was collected via vacuum filtration, washing with methanol. A small amount of polymer was dissolved in THF, and the purity was assessed by TLC using dichloromethane as eluent vs a VBP standard. The spot indicating VBP in the polymer sample triggered repeated precipitations using 10 ml each of THF and acetonitrile and 50 ml of methanol. TLC showed the absence of VBP after the second precipitation. The polymer was a white solid, which was dried under reduced pressure. Mass = 2.69 g (75%)

^1H NMR (500 MHz, CDCl_3): δ 0.71-1.95 (2H, broad m)-[polymer backbone], 4.68 (2H, broad s), 6.32 (2H, broad d), 6.98 (2H, broad d), 7.66 (4H, broad d)

19 - Poly {(4-vinylbenzyl phthalimide) -co- [di(ethylene glycol) methyl ether methacrylate]}



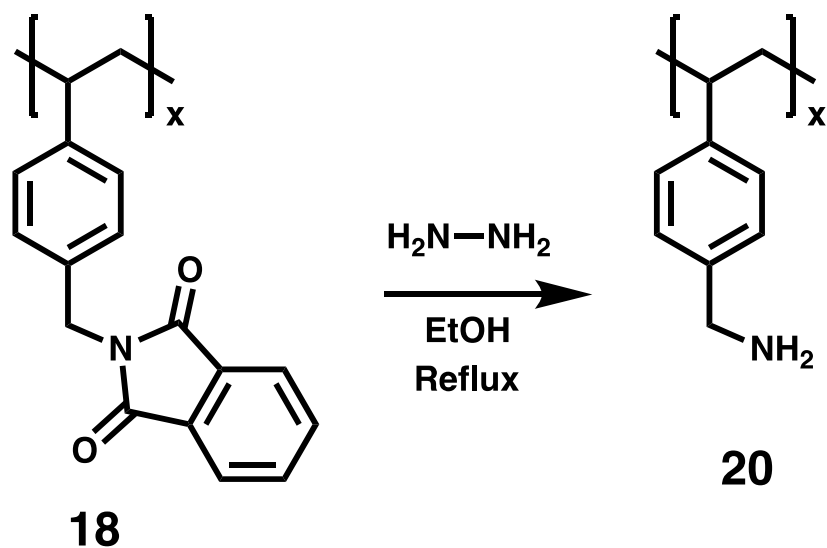
4-(Vinylbenzyl) phthalimide (VBP) [**15**] (1.0802 g, 0.41 mmol, 1 equiv) was combined with di(ethylene glycol) methyl ether methacrylate (DEGMEMA) (0.7714 g, 0.41 mmol, 1 equiv) and AIBN (0.0756 g, 0.046 mmol, 0.056 equiv). The mixture was dissolved in 20 mL of acetonitrile and refluxed overnight. After cooling the reaction, an aliquot was analyzed by NMR, showing 70% completion [\sim 30% monomer remaining (22% DEGMEMA, 8% VBP)]. The reaction solution was concentrated under reduced pressure. Crude [**19**] = 1.9726 g (107 %)

A sample of the crude (0.193 g) was dissolved in acetonitrile (0.67 ml). Methanol was added (1.3 ml) and the solution turned cloudy. Upon standing, polymer [**19**] appeared to have oiled out rather than precipitating. The addition of acetonitrile (0.67 ml) produced more viscous oil. Another sample of crude (0.142 g) was dissolved in THF (1.15 ml); hexanes (1.55 ml) was added, and the solution turned cloudy white. The solution was allowed to settle and again polymer [**19**] appeared to have oiled out. As the polymer was sticking to the sides of the vial, the solution was decanted off and the polymer was rinsed 2x with hexanes (\sim 0.5 ml). The remaining

solvent was removed under reduced pressure. The residue was analyzed by ^1H NMR, showing ~3% monomer remaining. Multiple precipitations are needed.

^1H NMR (500 MHz, CDCl_3): δ 0.40-2.07 (4H, broad m)-[polymer backbone], 1.72 (3H, broad s), 3.33-3.74 (14H, broad m), 4.71 (4H, broad s), 6.56-7.20 (4H, broad d)

20 - poly 4-vinylbenzyl amine



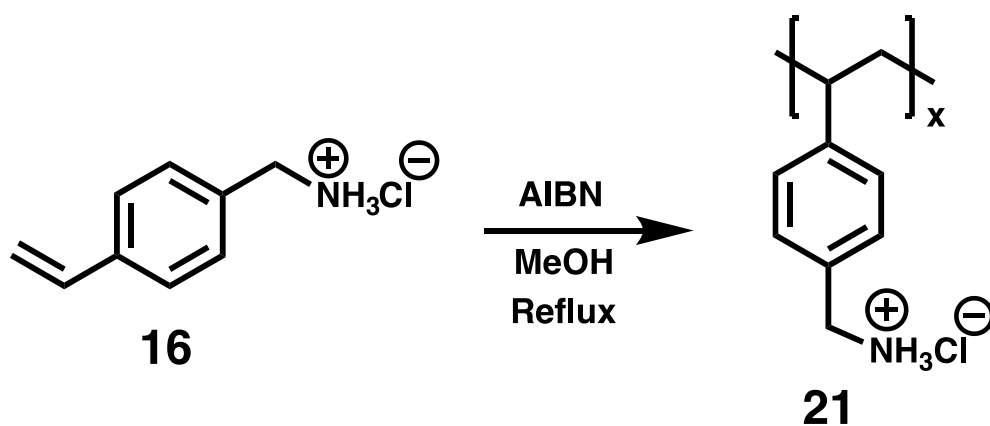
Poly-4(vinylbenzyl) phthalimide (2.66g, 10 mmol (monomer basis)) was combined with 20 ml of ethanol and hydrazine hydrate (1.6 ml, 33 mmol). The reaction was refluxed for 16 hours. A white precipitate formed. The reaction mixture was hot filtered in ethanol. The ethanol filtrate was concentrated to 10 ml and the polymer was precipitated from the solution by addition of diethyl ether (50 ml) with stirring while the solution was still warm.

The solution was allowed to cool, and an additional 20 ml of ether was added. The precipitated polymer was collected via vacuum filtration, rinsing with ether. Product was a white solid, yield = 1.14g (85%)

Both a sample of the collected polymer and the filtrate were tested for hydrazine using para-dimethylaminobenzaldehyde in acidic solution (aqueous HCl). A yellow color indicates the presence of hydrazine. The absence of phthalhydrazide can be confirmed by IR spectroscopy.

^1H NMR (500 MHz, D_2O): δ 0.81-2.03 (2H, broad m)-[polymer backbone], 3.65 (2H, broad s), 6.50-7.01 (4H, broad d)

21 - Poly 4-vinylbenzyl amine HCl



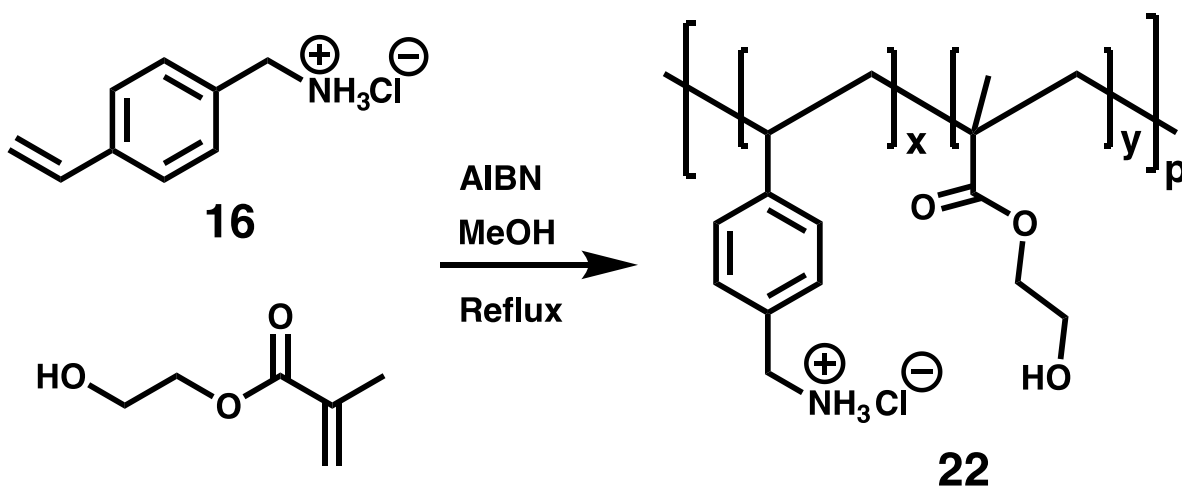
4-vinylbenzyl amine hydrochloride (.9574 g, 5.64 mmol) was combined with AIBN (.0610g, 0.37 mmol, 0.066 equiv) and dissolved in 25 ml of MeOH. The solution was refluxed. After 8 hours, an aliquot was evaporated giving a white/semi-clear solid (0.0135g), that was dissolved in D_2O

and analyzed by $^1\text{H-NMR}$. (reaction $\sim 62\%$ complete) The reaction was refluxed for another day and a half and then redissolved in MeOH (solvent had evaporated). A sample of the crude product was analyzed by $^1\text{H-NMR}$ in D₂O (reaction 98% complete). The reaction solution (~ 25 ml) was transferred to an Erlenmeyer flask and the polymer was precipitated by slow addition of acetone (50 ml) while stirring.

The precipitated polymer was collected via vacuum filtration, rinsing with acetone. The product was dried under reduced pressure. Mass = 0.7279 g (76% yield). A sample was taken for NMR in D₂O. (any trace of monomer is below the integration accuracy limit).

$^1\text{H NMR}$ (500 MHz, DMSO- d_6): δ 0.60-2.24 (2H, broad m)-[polymer backbone], 4.02 (2H, broad s), 6.55-7.15 (4H, broad d)

22 – poly 4-vinylbenzyl amine -*co*- 2-hydroxyethyl methacrylate



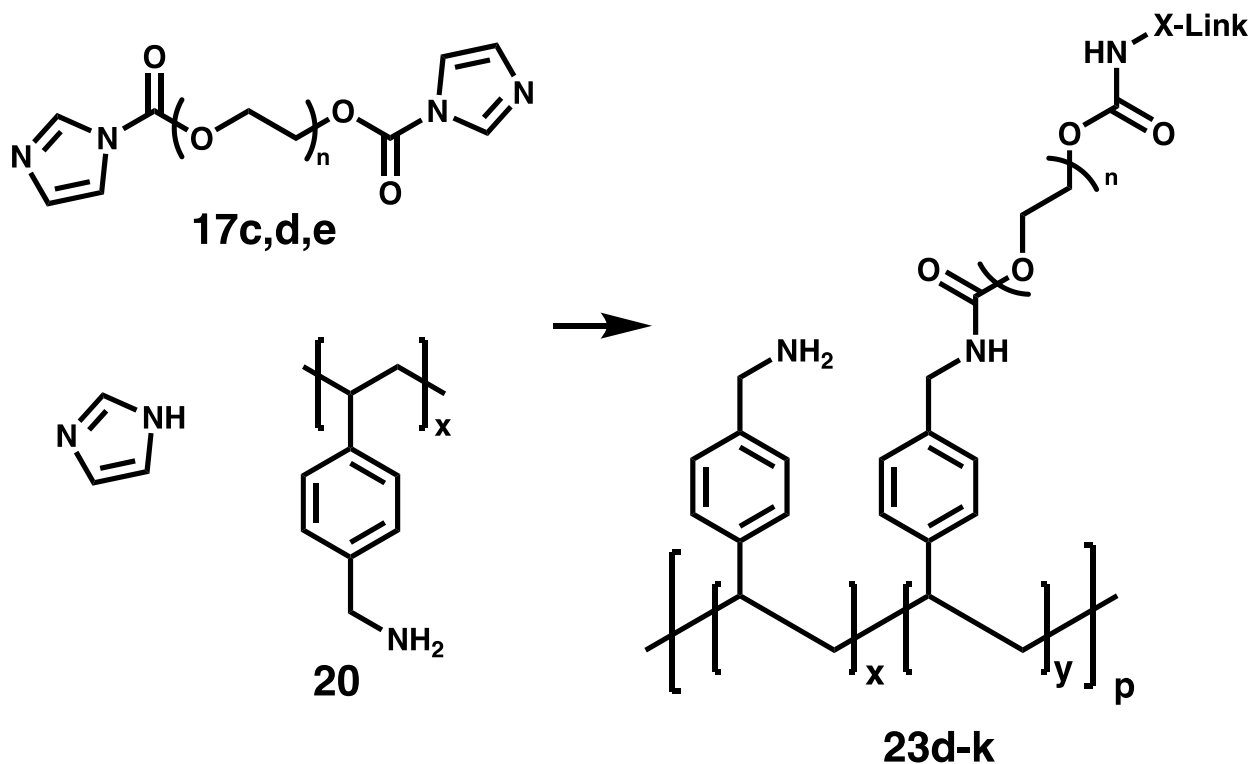
4-Vinylbenzyl amine hydrochloride (0.955 g, 5.63 mmol, 1 equiv) was combined with hydroxyethyl methacrylate (0.739 g, 5.68 mmol, 1.01 equiv), AIBN (0.0962 g, 0.586 mmol, 0.051 equiv overall), and 25 ml of methanol. The mixture was refluxed for 2 days. The solvent was removed by rotary evaporation and a sample was analyzed by NMR.

A portion was used to test precipitation conditions. Crude **[22]** (0.1406 g) was dissolved in 2 ml of MeOH and precipitated by adding THF dropwise (8 ml total, 1:4 ratio). The precipitate was collected via vacuum filtration and analyzed by NMR. Product = 0.0906 g (64% recovery).

The same method was applied to the rest of the crude product, and it seemed to precipitate at first, but then clumped/oiled out of solution. The solvent was removed, and the precipitation was reattempted with methanol and diethyl ether (1:4 ratio). The polymer precipitated when ether was added quickly to a rapidly stirred solution. However, during collection via vacuum, the solid clumped up and lost its form (powder to taffy consistency) and rinsing with ether didn't return it to a powder.

^1H NMR (500 MHz, D_2O): δ 0.30-2.36 (4H, broad m)-[polymer backbone], 1.73 (3H, broad s), 3.03-3.74 (4H, broad m), 4.03 (4H, broad s), 6.81-7.23 (4H, broad d)

23d to 23k : *Net*-poly{[4-(vinylbenzyl) amine]-*v*-[bis(carbonyl imidazole) poly(ethylene glycol) (850)]}-*block*-[(3-aminopropyl) trimethoxysilane]-*block*-glass



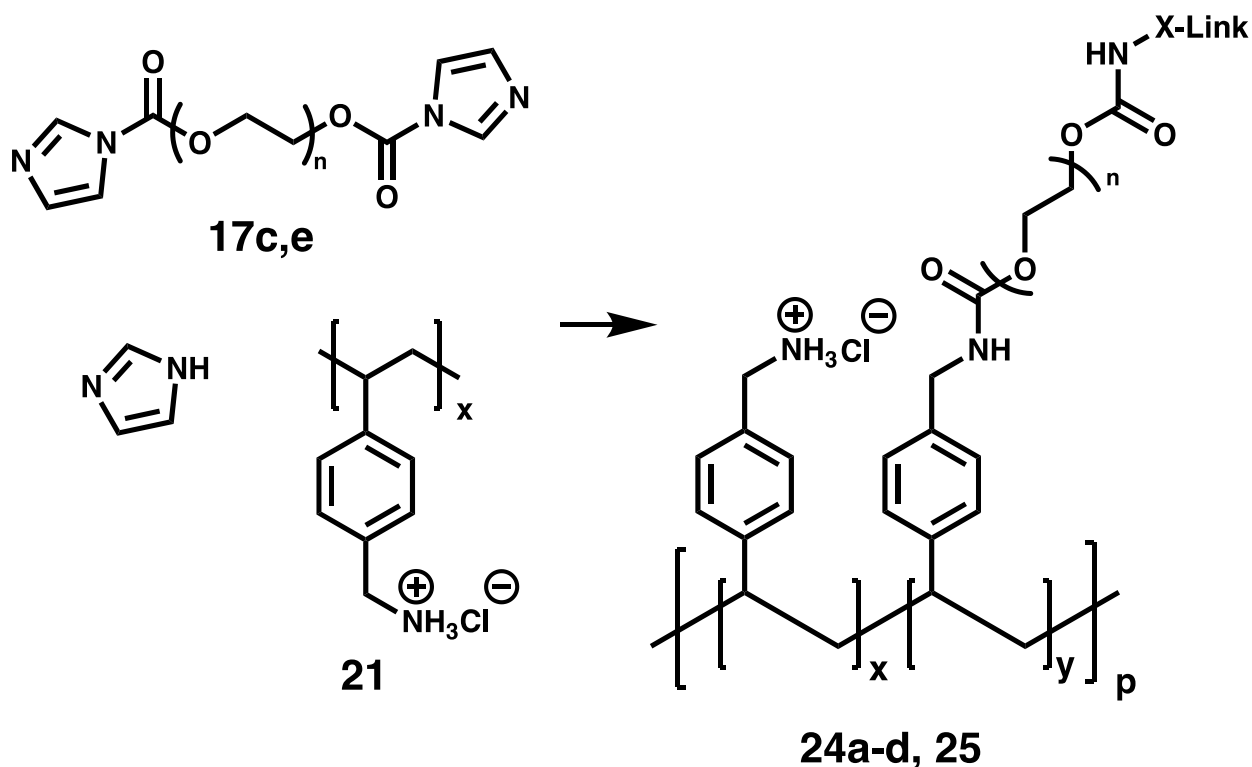
Rxn	X-linker	Solvent(s)	Polymer mmol amine	X-linker mmol	X-linker equiv %	Styrene: glycol ratio ¹	Total g sol	Mmol amine / g sol	Gel time (min)
23d	17c	NMP/DMF	0.0522	0.00678	13		0.0507	1.03	<10
23e	17c	NMP/DMF	0.0957	0.00766	8		0.0767	1.25	3
23f	17c	NMP/DMF	0.0869	0.00678	7.8		0.0888	0.98	<10
23g	17d	NMP/DMF	0.0898	0.00744	8.3	1:1.7	0.1011	0.89	5
23h	17d	NMP/DMF	0.0440	0.0090	20	1:4	0.0913	0.48	15
23i	17d	NMP/DMF	0.1205	0.01143	10	1:2	0.1412	0.85	3
23j	17e	NMP/DMF	0.1152	0.00825	7.2	1:2.4	0.1596	0.72	3
23k	17d	NMP/DMF	0.0767	0.00635	8.3	1:1.7	0.1507	0.51	<5

¹Aromatic ring to glycol (CH₂CH₂O) ratio. Approximate, using [17c] ~ 13, [17d] ~ 20, and [17e] ~ 34 glycol units.

A solution of carbonyl diimidazole (CDI) was made by dissolving CDI in DMF (or acetonitrile). Poly(ethylene glycol) (200-1500 av. MW) was added, and the mixture was vortexed. Poly(4-vinylbenzyl amine) [20] was dissolved in NMP (or DMF) (with heating) with the aid of methanol (polymer dissolved in NMP/MeOH mixture and then MeOH is evaporated off). A portion of the cross-linker solution was placed in a vial, water was added and the mixture was vortexed. Polymer [20] solution was added, and the mixture was vortexed again. The vial was checked every few min for gel formation. The table on pg. 99 contains only the reactions that formed a hydrogel.

24a-d - Poly {(4-vinylbenzyl amine HCl)-v-[bis(carbonyl imidazole) poly(ethylene glycol)]}

-or- CDI-PEG-CDI



A solution of carbonyl diimidazole (CDI) was made by dissolving CDI in DMF (or acetonitrile). CDI-PEG-CDI solutions were made by combining poly(ethylene glycol) (200-1500 av. mol MW) and the CDI solution. The mixture was vortexed for 5 min. Poly(4-vinylbenzyl amine hydrochloride) was dissolved in water (with heating) with the aid of methanol. The polymer dissolved in a mixture of water and MeOH followed by evaporation of MeOH.

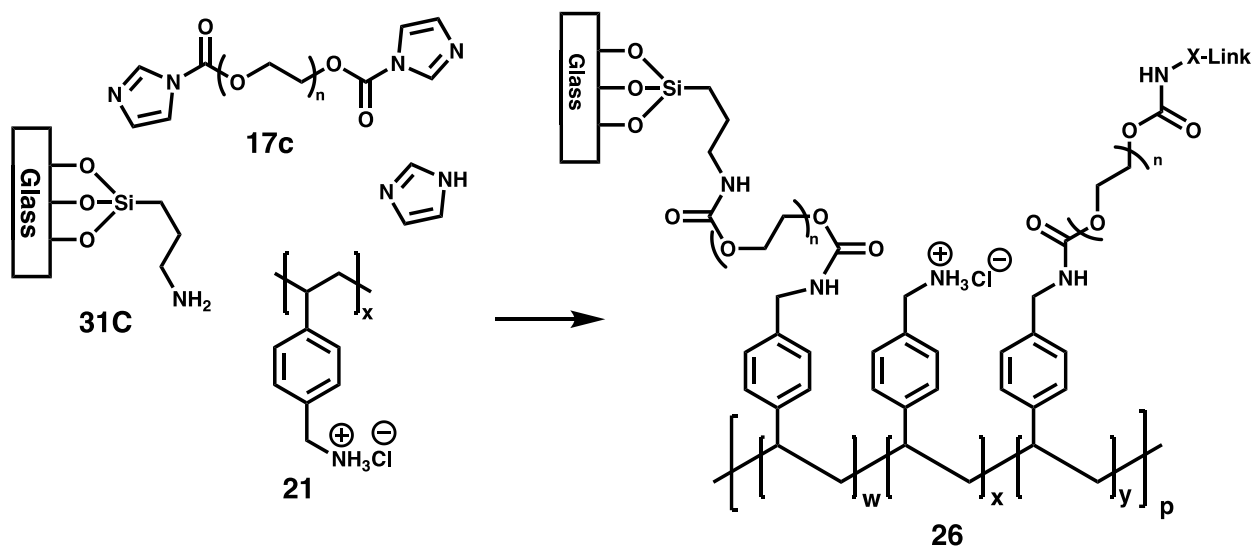
Rxn	X-linker	Solvent (s) used	Polymer mmol amine HCL	X-linker mmol	X-linker equiv %	Styrene : glycol ratio ¹	Total mass sol (g)	Mmol amine HCL/ g sol	Gel time
24a	17e	H2O/ DMF	0.126	0.00712	5.5	1:2	0.1545	0.81	~30 min
24b	17e	H2O/ CH ₃ CN	0.0407	0.00489	12	1:4	0.0805	0.50	30+ min
24c (25)	17e	H2O/ CH ₃ CN	0.214	0.0137	6	1:2	0.2682	0.80	25+ min
24d (26)	17c	H2O/ CH ₃ CN	0.570	0.0725	12.7	1:1.7	0.4042	1.41	~20 min

¹Aromatic ring to glycol (CH₂CH₂O) ratio. Approximate, using [17c] ~ 13, and [17e] ~ 34 glycol units.

25 – *Net*-poly[4-vinylbenzyl amine hydrochloride] -v-[bis(carbonyldiimidazole) poly(ethylene glycol) (850)]

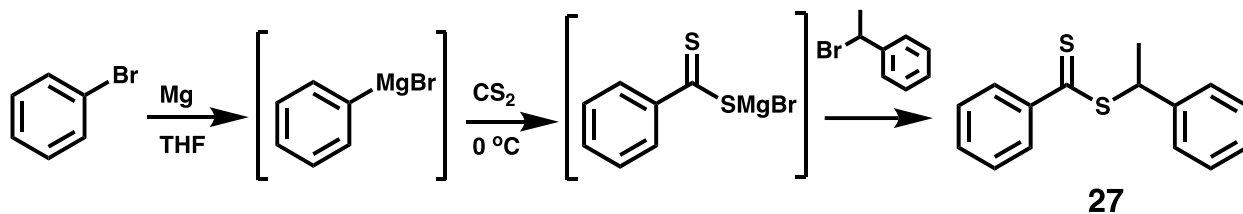
A gel test was done using a C18 slide [30] and a plain glass slide. Reagent ratios are shown in line [24c]/[25] of the table above. A C18 slide [30] was checked for hydrophobicity. A tape mold was applied to the C18 slide [30]. The polymerization solution was applied to the polymer mold [30] and a plain slide was placed on top. The slides are clamped with 2 blank slides on either side. The polymer was let set at room temperature overnight. The resulting gels were clear and transparent. The gels swelled to approximately 5 times their original size after demolding.

26 - *Net*-poly [4-(vinylbenzyl) amine] -*v*-[bis(carbonyl imidazole) poly(ethylene glycol) (850)]}-
block-[(3-aminopropyl) trimethoxysilane]-*block*-glass



Aminopropylated slides were made using 150 μ l of aminopropyltrimethoxysilane and heating for 1 hour 163 °C. Part of the solution RAD-3-097 (need Table) was used in the typical mold and the slides were clamped and heated at 70 °C for 3 hours. The slides were separated while soaking in water the next day. The gels seemed more swollen than usual maybe due to the hydrochloride salt of polymer being used. It was transparent and adhered to glass. The polymer gels were still intact on glass after storage in 18M Ω water after a year.

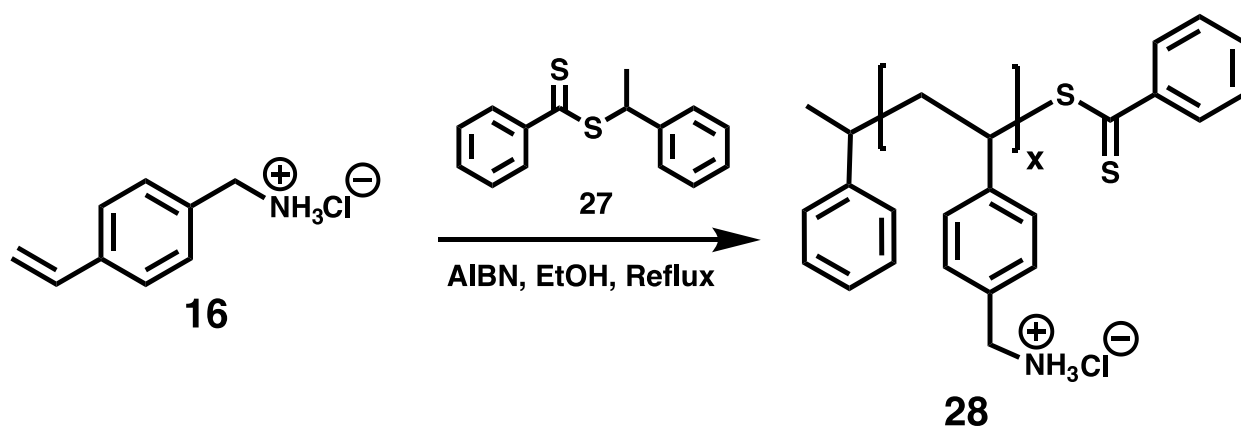
27 - 1-phenylethyl dithiobenzoate



Bromobenzene (1.5102 g, 9.6 mmol, 1 equiv) was combined with magnesium (0.2811g, 11.5 mmol, 1.2 equiv) in dry THF (8 ml). A speck of iodine was added, and the solution heated to 40 °C followed by reflux for 1 hour. After the Grignard reagent was formed, the reaction was cooled to 0°C, and carbon disulfide (0.7 ml, 11.6 mmol, 1.2 equiv) was added over a 30 minute period. The solution turned red-purple. The reaction was stirred for 1.5 hours and then let warm to room temperature. 1-bromoethyl benzene (1.6 ml, 1.2 equiv) was added dropwise. The reaction solution turned bright red. The reaction was stirred for 2 days, followed by TLC. The spot for dithiobenzoate never completely disappeared. 8 ml of water was added to the reaction mixture. The solvent was removed under reduced pressure. The aqueous solution was extracted 9 times with 25 ml portions of ethyl acetate. The organic portions were combined, dried over magnesium sulfate and concentrated. The product was dried under vacuum overnight and a red-pink oil was obtained. The product was purified by passing it through a silica gel (60) column with hexanes. Column fractions were collected until the pink color was extremely pale (almost clear) and no spot was observed on TLC. A brown band remained in column and was collected with ethyl acetate after all product fractions were collected. The pure fractions were combined and concentrated, yielding 1.0427 g (42%) of a red oil.

^1H NMR (500 MHz, CDCl_3): δ 1.81 (3H, d, $J = 7.4$ Hz), 5.25 (1H, q, $J = 7.4$ Hz), 7.28 (1H, tt, $J = 7.7$, 1.3 Hz), 7.35 (4H, m), 7.44 (2H dtd, $J = 7.9$, 1.3, 0.5 Hz), 7.50 (tt, $J = 7.2$, 1.5 Hz), 7.95 (2H, dtd, $J = 8.2$, 1.5, 0.4 Hz)

28 - Poly {(4-vinylbenzyl amine HCl)}

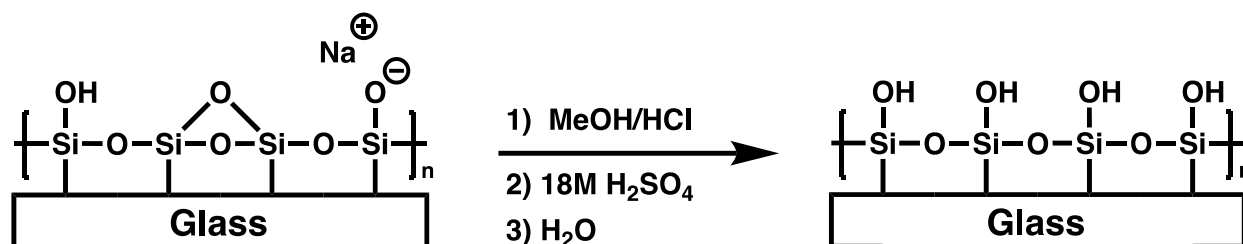


1-Phenylethyl dithiobenzoate [**27**] (0.0148 g, 0.057 mmol) was combined with 4-vinylbenzyl amine HCl [**16**] (0.927 g, 5.46 mmol) and AIBN (1.2 mg, 0.0073 mmol) in 25 ml of ethanol. The ratio of monomer [**16**]: CTA[**27**]: AIBN was 95:1:0.13. The reaction was refluxed under nitrogen. After 2 days, NMR showed $\sim 15\%$ monomer conversion.

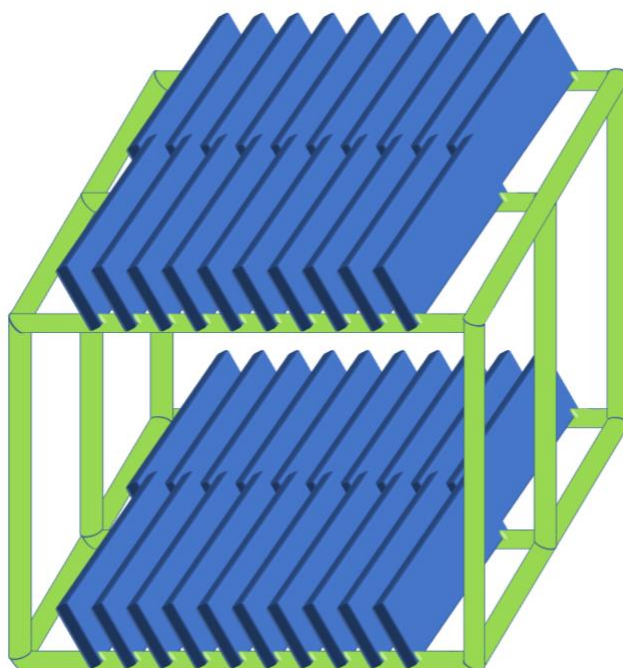
Minimal polymerization - No isolatable product

MAKING THE HYDROGELS

29 -Silanized slides – glass slide prep (cleaning off surface crud and freeing hydroxyls)



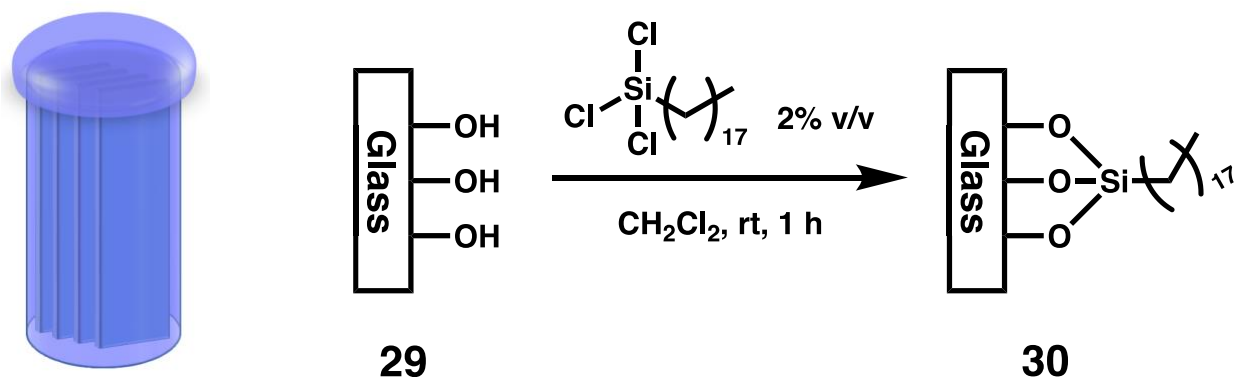
29



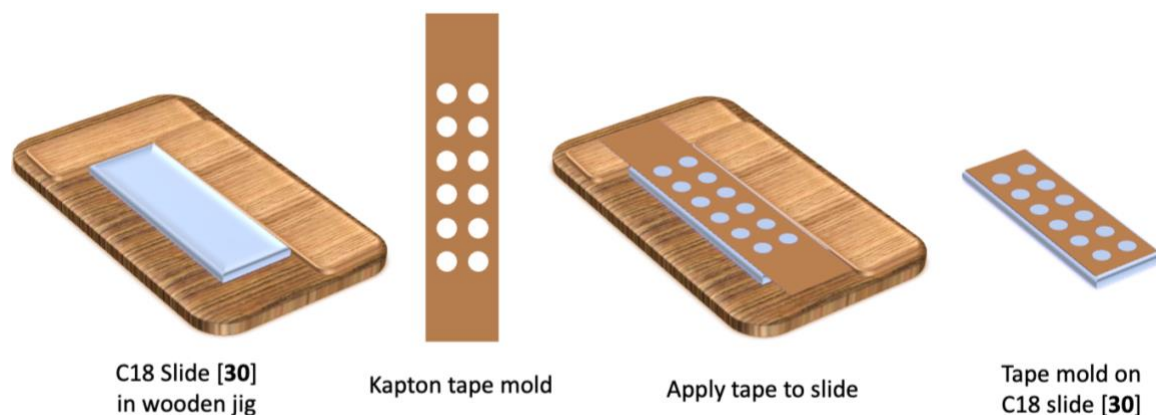
Microscope slides were placed into a custom glass rack.

A 50:50 (by volume) solution of methanol : 12M hydrochloric acid was prepared. Glass microscope slides were placed in the bath of MeOH:HCl and let sit for at least 30 minutes, preferably overnight. The slides were then taken out of the MeOH:HCl bath, rinsed with 18 Ω water, dried, and placed in a bath of concentrated H₂SO₄. The slides were stored in the sulfuric acid bath until needed.

30 - C18 Silanized slides — (octadecyltrichlorosilane)



A solution of 2% (v/v) octadecyltrichlorosilane (C18) in dichloromethane was prepared. 5 microscope slides were taken out of the sulfuric acid bath, rinsed well with 18 Ω water, methanol, and dichloromethane. The slides were then placed in the C18 solution for at least an hour (anywhere from 1-4 h, but not overnight). The slides were then removed from the solution, rinsed with dichloromethane and let dry. Excess C18 was wiped off the slides with a Kimwipe until the slides were transparent. The slides were then checked qualitatively for hydrophobicity (water should slide right off and not cling) and then dried again.



Kapton tape (1 Mil) with 12 holes in it was applied to the slides using the alignment template (custom). The tape was pressed down with a plastic spreader, taking care not to trap bubbles or dust and excess tap was cut off the ends. The taped slides were clamped (binder clips)

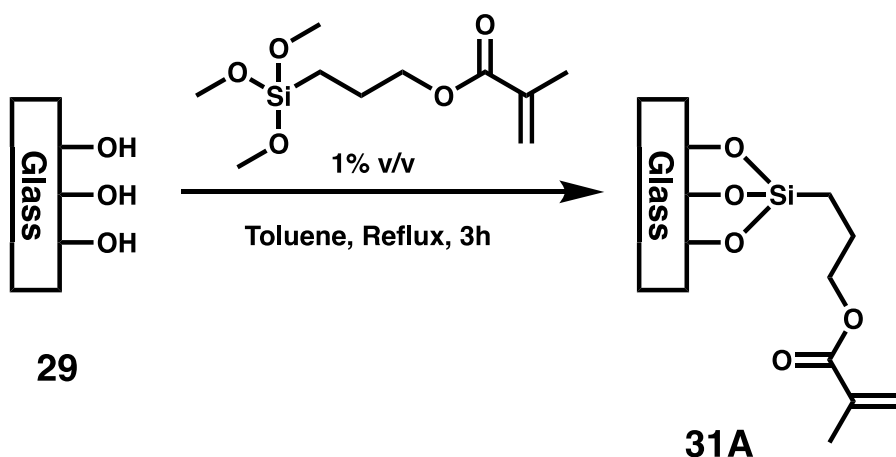
between 8 other slides, 4 on each side, for at least 1 hour (each C18 slide must be clamped separately). Then the slides were unclamped, and stored until they were used to make polymers.

Notes on Tape mold – manual punch – mention my improvement vs original.

A wide label was removed from the nonstick side of the backing and stuck to the rough paper side. A piece of Kapton tape (length of microscope slide plus 4 cm) was cut and applied to the nonstick side. Thus layered, the material is placed in a custom hole punch jig, with the top and bottom of the body made of Teflon, and the punches of steel. Once the material sheet was secured in the jig, a rubber hammer was used to hit the steel punches, creating 12 round holes in the Kapton tape. (Note: This replaced the original method of using a single manual hole punch, in order to make the holes consistently and evenly spaced)

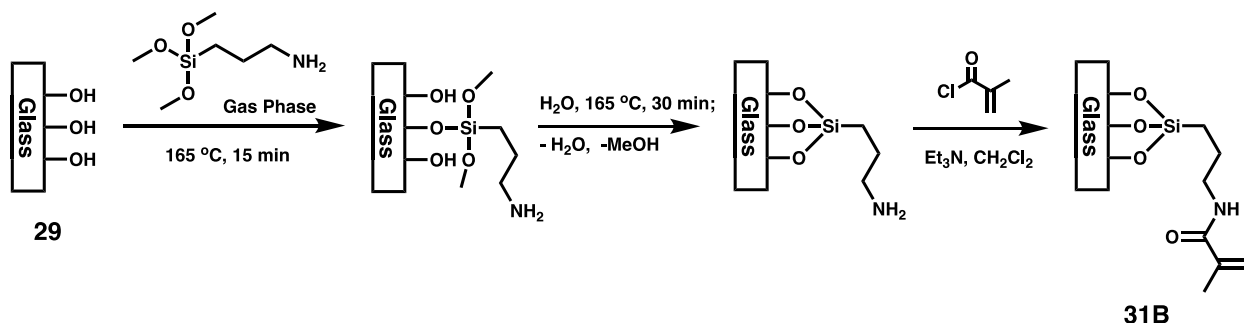
Later, a custom roll of precut pieces of Kapton tape with pre-punched holes was purchased by the Schwabacher group. This replaced the above procedure.

31A -Silanized slides – Solution phase



Five microscope slides were taken out of the sulfuric acid bath, rinsed with 18 Ω water, and dried. The slides were then placed in a vessel, held upright by Tygon tubing with slits in it. A 1% v/v solution of 3-(trimethoxysilyl)propyl methacrylate in toluene was added until the slides were completely submerged (~300 ml). Note: this is a large excess of TPM. The reaction was refluxed for 3 hours. The slides were then removed, rinsed with methanol, let dry, and then stored in NMP with a small amount of 4-methoxyphenol (MEHQ) until used. Water was used to evaluate the silanization by determining the water contact angle.

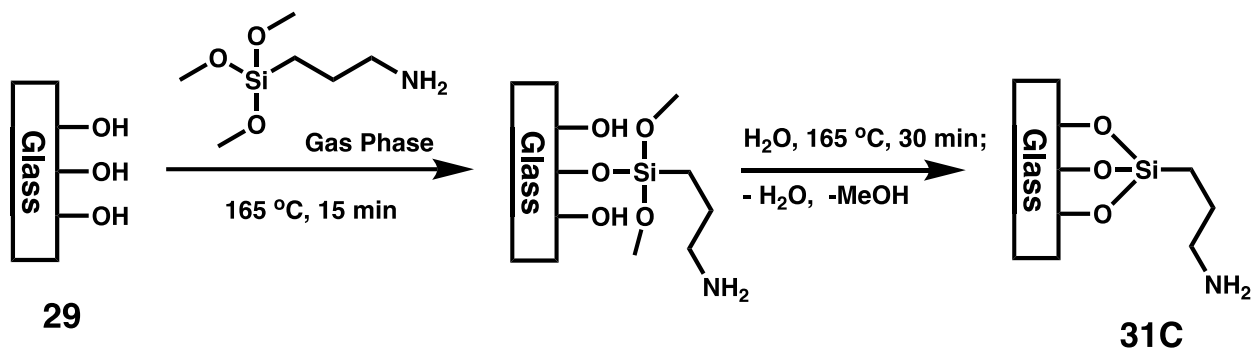
31B - Methacrylamidopropyl silanized glass slides – Gas phase



A microscope slide was taken out of the sulfuric acid bath, rinsed with 18 Ω water, and dried with a Kimwipe. An aluminum block was preheated to 170 °C, with a petri dish placed on top of it. Two capillary tubes were placed inside the petri dish, and the glass slide was placed on top of them and allowed to warm up for one minute. 20 μ L of (3-aminopropyl)trimethoxysilane was added to each side of the petri dish (to the empty surface on either side of the long edge of the slide), and the setup was covered with a watch glass. The system was heated for 20 minutes.

Then the watch glass was taken off the top and the petri dish was removed from the aluminum block and allowed to cool. This was repeated until 5 slides were obtained. All 5 slides were placed in a custom glass stand inside a crystallizing dish. The crystallizing dish was placed on the aluminum block and 200 μ L of 18 Ω water was added. The dish was covered and heated for 20 minutes, then uncovered and left to heat overnight. The silanized slides were then removed, cooled, and placed in a solution of methacryloyl chloride in dichloromethane overnight. The slides were then rinsed with dichloromethane and stored in NMP with a small amount of MEHQ.

31C - Aminopropyl silanized glass slides – used for soluble polymers

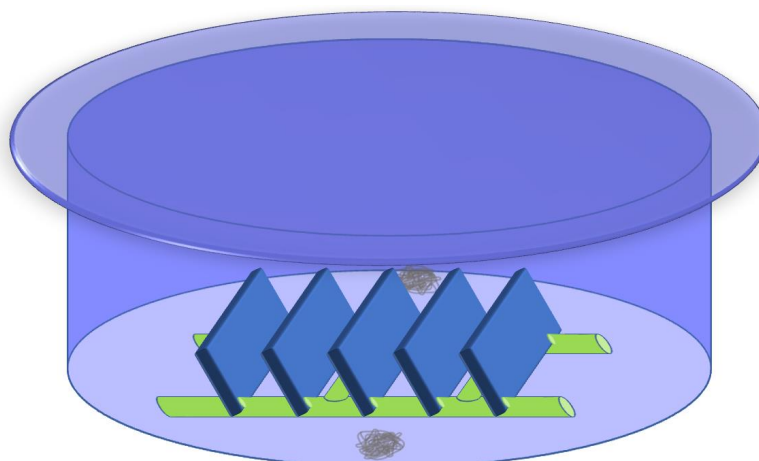
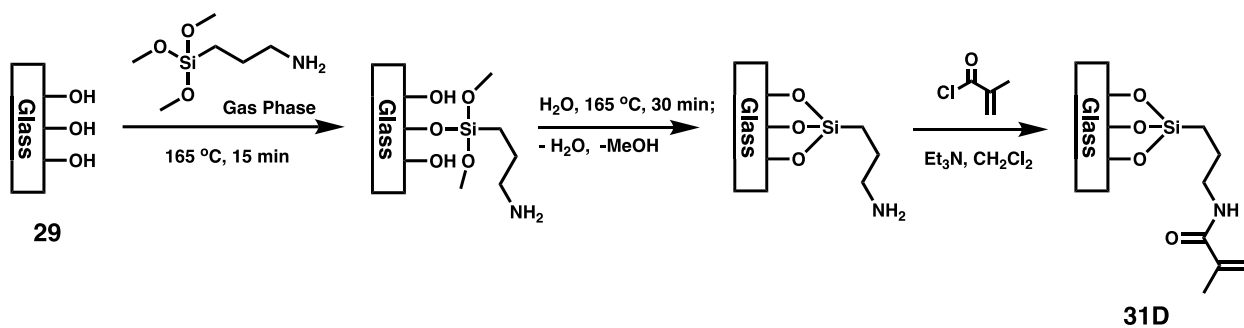


A vacuum oven was heated to 165°C.

Acid treated slides (x5) were rinsed well with 18 Ω water, then with methanol, and dried with a stream of nitrogen. A glass rack (custom) was placed in a large crystallization dish, and the slides were set upright in the rack. Two pieces of clean glass wool were each soaked with ~70 μ m (~140 μ m total) of 3-aminopropyltrimethoxysilane and placed inside the dish (at each end of the slides). The dish was covered and placed in the oven. The slides were heated at 165 °C

for 50 minutes and let cooled. The glass wool was removed, and 500 μl of water was distributed around the slides along the edges of the dish. The slides were heated while covered for 30 minutes. Then the dish was uncovered and heated for at least an hour under reduced pressure. The slides were then removed from the oven, let cool, rinsed with toluene and stored in toluene until use.

31D- Methacrylamidopropyl silanized glass slides – Gas phase – Batch of 5

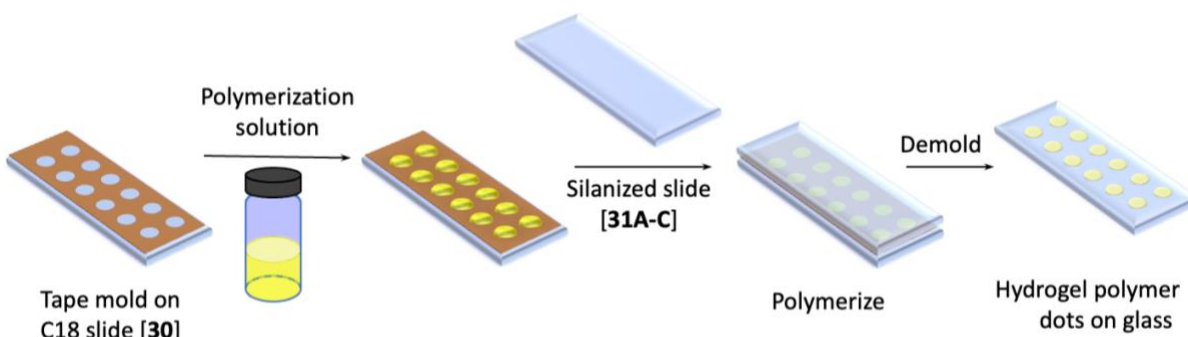


The vacuum oven was heated to 165°C.

Acid treated slides (x5) were rinsed well with 18 Ω water and then with methanol and dried with a stream of nitrogen. A glass rack (custom) was placed in a large crystallization dish, and the slides were set upright in the rack. Two pieces of clean glass wool were each soaked with ~70 μm (~140 μm total) of 3-aminopropyltrimethoxysilane and placed inside the dish (at each end of the slides). The dish was covered and placed in the oven. The slides were heated at 165 °C for 50 minutes, then removed from the oven and let cool. The glass wool was removed, and 500 μl of water was distributed around the slides along the edges of the dish. The slides were heated while covered for 30 minutes. Then the dish was uncovered and heated for at least an hour under reduced pressure.

A bath of 2% methacryloyl chloride and 2% triethylamine in dichloromethane was prepared. After heating, the slides were removed from the oven, cooled, washed with toluene and dichloromethane and placed in the methacryloyl chloride solution. After 12 hours the slides were removed from the solution, rinsed with dichloromethane and let air dry. The slides were stored in NMP with a few mg of MEHQ as stabilizer. Slides were stable stored this way and were usable even after a year.

32 - General hydrogel polymer on glass formation



General polymer prep. A silanized slide is taken out of storage in NMP, and rinsed with 18 Ω water, then methanol, and let air dry completely.

A C18 slide (#) with tape was taken and placed on a small stage (2 inches up) so it could be handled by the edges. Polymerization solution is deposited into each hole of the mold. The APTMS silanized slide is placed on top and carefully slid back and forth to push out any bubbles and excess polymerization solution. Once there were no bubbles visible, the slides were lined up and 5 regular slides were placed on each side of the polymer slide pair. The stack is then firmly clamped with 4 binder clips. This is repeated for the desired number of polymer slides. The stacks were placed in the oven at 80°C and heated for 3 hours and cooled. The slides were then unclamped, and the polymer slide pairs were placed in NMP and left to soak overnight. The two slides were then slowly and carefully pried apart, so as to not damage any of the polymer dots. The polymer dots slides were washed with a series of solvent mixtures until it is in the desired solvent. (This reduces the risk that a drastic change in swelling will shear the polymer dots from the glass) Store in centrifuge tubes (50ml).

Bibliography/Works Cited/References

- (1) Tchounwou, P. B.; Yedjou, C. G.; Patlolla, A. K.; Sutton, D. J. Heavy Metal Toxicity and the Environment. *EXS* **2012**, *101*, 133–164. https://doi.org/10.1007/978-3-7643-8340-4_6/COVER.
- (2) Jaishankar, M.; Tseten, T.; Anbalagan, N.; Mathew, B. B.; Beeregowda, K. N. Toxicity, Mechanism and Health Effects of Some Heavy Metals. *Interdisciplinary Toxicology* **2014**, *7* (2), 60–72. <https://doi.org/10.2478/INTOX-2014-0009>.
- (3) Engwa, G. A.; Ferdinand, P. U.; Nwalo, F. N.; Unachukwu, M. N.; Engwa, G. A.; Ferdinand, P. U.; Nwalo, F. N.; Unachukwu, M. N. Mechanism and Health Effects of Heavy Metal Toxicity in Humans. *Poisoning in the Modern World - New Tricks for an Old Dog?* **2019**. <https://doi.org/10.5772/INTECHOPEN.82511>.
- (4) Rabin, R. The Lead Industry and Lead Water Pipes “A Modest Campaign.” *American Journal of Public Health* **2008**, *98* (9), 1584–1592. <https://doi.org/10.2105/AJPH.2007.113555>.
- (5) Wani, A. L.; Ara, A.; Usmani, J. A. Lead Toxicity: A Review. *Interdisciplinary Toxicology* **2015**, *8* (2), 55–64. <https://doi.org/10.1515/intox-2015-0009>.
- (6) Renu; Agarwal, M.; Singh, K. Heavy Metal Removal from Wastewater Using Various Adsorbents: A Review. *Journal of Water Reuse and Desalination* **2016**, *7* (4), 387–419. <https://doi.org/10.2166/wrd.2016.104>.
- (7) Fu, F.; Wang, Q. Removal of Heavy Metal Ions from Wastewaters: A Review. *Journal of Environmental Management* **2011**, *92* (3), 407–418. <https://doi.org/10.1016/j.jenvman.2010.11.011>.
- (8) Baysal, A.; Ozbek, N.; Akman, S.; Baysal, A.; Ozbek, N.; Akman, S. *Determination of Trace Metals in Waste Water and Their Removal Processes*; IntechOpen, 2013. <https://doi.org/10.5772/52025>.
- (9) Liss, T. A.; Baer, D. R. Metal Complexes of Azo Dyes. I. Quadridentate Complexes from Bidentate Azo Compounds and Alkanediamines or Ethanolamine. *Inorganic Chemistry* **1969**, *8* (6), 1328–1336. https://doi.org/10.1021/IC50076A026/ASSET/IC50076A026.FP.PNG_V03.
- (10) Jezorek, J. R.; Freiser, H. 4-(Pyridylazo)Resorcinol-Based Continuous Detection System for Trace Levels of Metal Ions. *Analytical Chemistry* **1979**, *51* (3), 373–376. https://doi.org/10.1021/AC50039A012/ASSET/AC50039A012.FP.PNG_V03.
- (11) Benkhaya, S.; M'rabet, S.; El Harfi, A. Classifications, Properties, Recent Synthesis and Applications of Azo Dyes. *Heliyon* **2020**, *6* (1), e03271–e03271. <https://doi.org/10.1016/J.HELIYON.2020.E03271>.
- (12) Gürses, A.; Açıkyıldız, M.; Güneş, K.; Gürses, M. S. Classification of Dye and Pigments. In *Dyes and Pigments*; Gürses, A., Açıkyıldız, M., Güneş, K., Gürses, M. S., Eds.; SpringerBriefs in Molecular Science; Springer International Publishing: Cham, 2016; pp 31–45. https://doi.org/10.1007/978-3-319-33892-7_3.
- (13) Bafana, A.; Devi, S. S.; Chakrabarti, T. Azo Dyes: Past, Present and the Future. *Environ. Rev.* **2011**, *19* (NA), 350–371. <https://doi.org/10.1139/a11-018>.
- (14) Barros, V. P.; Assis, M. D. Iron Porphyrins as Biomimetical Models for Disperse Azo Dye Oxidation. *Journal of the Brazilian Chemical Society* **2013**, *24* (5), 830–836. <https://doi.org/10.5935/0103-5053.20130110>.

- (15) Grudpan, K.; Taylor, C. G. Some Azo-Dye Reagents for the Spectrophotometric Determination of Cadmium. *Talanta* **1989**, *36* (10), 1005–1009. [https://doi.org/10.1016/0039-9140\(89\)80183-3](https://doi.org/10.1016/0039-9140(89)80183-3).
- (16) Wang, M.; Funabiki, K.; Matsui, M. Synthesis and Properties of Bis(Hetaryl)Azo Dyes. *Dyes and Pigments* **2003**, *57* (1), 77–86. [https://doi.org/10.1016/S0143-7208\(03\)00011-1](https://doi.org/10.1016/S0143-7208(03)00011-1).
- (17) Hansen, M. J.; Lerch, M. M.; Szymanski, W.; Feringa, B. L. Direct and Versatile Synthesis of Red-Shifted Azobenzenes. *Angewandte Chemie International Edition* **2016**, *55* (43), 13514–13518. <https://doi.org/10.1002/anie.201607529>.
- (18) Hagemann, T. M. Guest Host Chemistry Part I: The Synthesis of Metal Selective Sensors Part II: The Synthesis of Antibiotic Precursors and Intermediates. PhD. Disertation, University of Wisconsin-Milwaukee, Milwaukee, WI, 2022. <https://dc.uwm.edu/etd/2894>.
- (19) Labeots, J. A Real-Time Approach to Process Monitoring of Heavy Metals: Spectrophotometric Characterization and Application of Novel Azo. PhD. Disertation, University of Wisconsin-Milwaukee, Milwaukee, WI, 2019. <https://dc.uwm.edu/etd/2089>.
- (20) Williams, K. Part I: Synthesis of Quinolones for Inhibition of the B-Barrel Assembly Machine in Gram Negative Bacteria; Part II: Synthesis of Azo Dye Sensors for Detection of Metal Ions in Aqueous Environments. PhD. Disertation, University of Wisconsin-Milwaukee, Milwaukee, WI, 2022. <https://dc.uwm.edu/etd/2962>.
- (21) Oehm, S. A. Studies in Molecular Recognition: Non-Proteogenic Amino Acids for Antibiotic Studies and Chemosensors for Recognition and Reporting of Metal-Ions. PhD. Disertation, University of Wisconsin-Milwaukee, Milwaukee, WI, 2018. <https://dc.uwm.edu/etd/1889>.
- (22) Fenske, T. G. A Study in Molecular Recognition: Synthesis of a B-Sheet Mimic & Quantitation of Metal Ions in Aqueous Solutions Through Solid Supported Semi-Selective Chemosensors. PhD. Disertation, University of Wisconsin-Milwaukee, Milwaukee, WI, 2019. <https://dc.uwm.edu/etd/2182/> (accessed 2023-04-24).
- (23) Matyjaszewski, K. Polymer Chemistry: Current Status and Perspective. *Chemistry International* **2017**, *39* (4), 7–11. <https://doi.org/10.1515/ci-2017-0404>.
- (24) Ghadban, A.; Albertin, L. Synthesis of Glycopolymer Architectures by Reversible-Deactivation Radical Polymerization. *Polymers* **2013**, *5* (2), 431–526. <https://doi.org/10.3390/polym5020431>.
- (25) University, C. M. *Objectives - Controlled Radical Polymerization Consortium - Department of Chemistry - Carnegie Mellon University*. <https://www.cmu.edu/chemistry/crp/objectives/index.html> (accessed 2023-04-25).
- (26) Jenkins, A. D.; Jones, R. G.; Moad, G. Terminology for reversible-deactivation radical polymerization previously called “controlled” radical or “living” radical polymerization (IUPAC Recommendations 2010). *Pure and Applied Chemistry* **2009**, *82* (2), 483–491. <https://doi.org/10.1351/PAC-REP-08-04-03>.
- (27) Akhtar, M. F.; Hanif, M.; Ranjha, N. M. Methods of Synthesis of Hydrogels ... A Review. *Saudi Pharmaceutical Journal* **2016**, *24* (5), 554–559. <https://doi.org/10.1016/j.jsps.2015.03.022>.
- (28) Bashir, S.; Hina, M.; Iqbal, J.; Rajpar, A. H.; Mujtaba, M. A.; Alghamdi, N. A.; Wageh, S.; Ramesh, K.; Ramesh, S. Fundamental Concepts of Hydrogels: Synthesis, Properties, and Their Applications. *Polymers* **2020**, *12* (11), 2702. <https://doi.org/10.3390/polym12112702>.
- (29) Farasati Far, B.; Naimi-Jamal, M. R.; Safaei, M.; Zarei, K.; Moradi, M.; Yazdani Nezhad, H. A Review on Biomedical Application of Polysaccharide-Based Hydrogels with a Focus

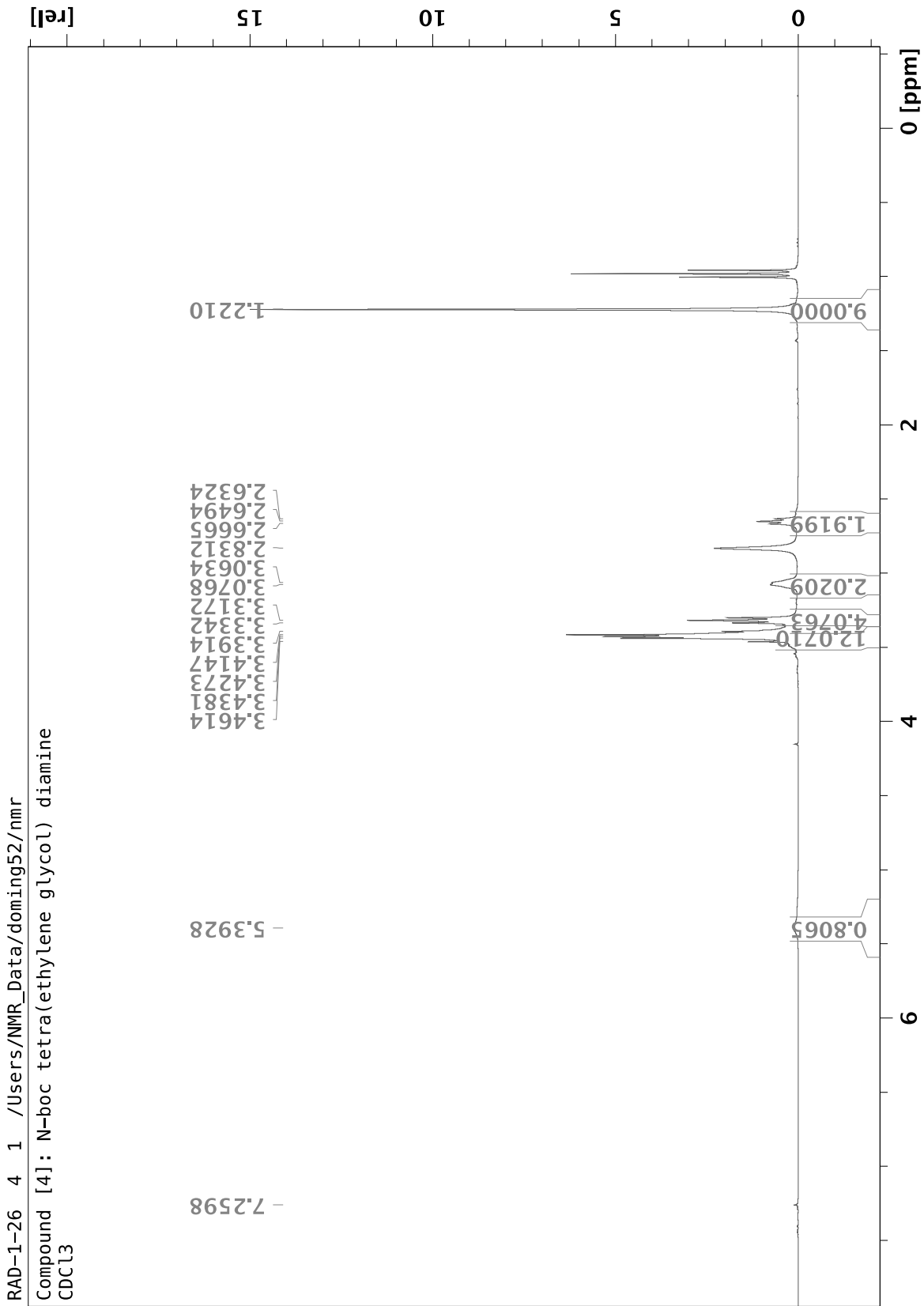
- on Drug Delivery Systems. *Polymers* **2022**, *14* (24), 5432.
<https://doi.org/10.3390/polym14245432>.
- (30) Wichterle, O.; Lím, D. Hydrophilic Gels for Biological Use. *Nature* **1960**, *185* (4706), 117–118. <https://doi.org/10.1038/185117a0>.
- (31) Ferreira, N. N.; Ferreira, L. M. B.; Cardoso, V. M. O.; Boni, F. I.; Souza, A. L. R.; Gremião, M. P. D. Recent Advances in Smart Hydrogels for Biomedical Applications: From Self-Assembly to Functional Approaches. *European Polymer Journal* **2018**, *99*, 117–133. <https://doi.org/10.1016/j.eurpolymj.2017.12.004>.
- (32) Holback, H.; Yeo, Y.; Park, K. 1 - Hydrogel Swelling Behavior and Its Biomedical Applications. In *Biomedical Hydrogels*; Rimmer, S., Ed.; Woodhead Publishing Series in Biomaterials; Woodhead Publishing, 2011; pp 3–24.
<https://doi.org/10.1533/9780857091383.1.3>.
- (33) Chamkouri, H.; Chamkouri, M. A Review of Hydrogels, Their Properties and Applications in Medicine. *AJBSR* **2021**, *11* (5), 485.
- (34) Kopecek, J. Hydrogels: From Soft Contact Lenses and Implants to Self-Assembled Nanomaterials. *Journal of Polymer Science Part A: Polymer Chemistry* **2009**, *47* (22), 5929–5946. <https://doi.org/10.1002/pola.23607>.
- (35) Khan, F.; Atif, M.; Haseen, M.; Kamal, S.; Khan, M. S.; Shahid, S.; Nami, S. A. A. Synthesis, Classification and Properties of Hydrogels: Their Applications in Drug Delivery and Agriculture. *J. Mater. Chem. B* **2022**, *10* (2), 170–203.
<https://doi.org/10.1039/D1TB01345A>.
- (36) Wang, W.; Xiang, L.; Diaz-Dussan, D.; Zhang, J.; Yang, W.; Gong, L.; Chen, J.; Narain, R.; Zeng, H. Dynamic Flexible Hydrogel Network with Biological Tissue-like Self-Protective Functions. *Chem. Mater.* **2020**, *32* (24), 10545–10555.
<https://doi.org/10.1021/acs.chemmater.0c03526>.
- (37) Ma, J.; Li, X.; Bao, Y. Advances in Cellulose-Based Superabsorbent Hydrogels. *RSC Adv.* **2015**, *5* (73), 59745–59757. <https://doi.org/10.1039/C5RA08522E>.
- (38) Huang, Y.; Zhong, M.; Shi, F.; Liu, X.; Tang, Z.; Wang, Y.; Huang, Y.; Hou, H.; Xie, X.; Zhi, C. An Intrinsically Stretchable and Compressible Supercapacitor Containing a Polyacrylamide Hydrogel Electrolyte. *Angewandte Chemie International Edition* **2017**, *56* (31), 9141–9145. <https://doi.org/10.1002/anie.201705212>.
- (39) Wang, X.; Hu, H.; Yang, Z.; He, L.; Kong, Y.; Fei, B.; Xin, J. H. Smart Hydrogel-Functionalized Textile System with Moisture Management Property for Skin Application. *Smart Mater. Struct.* **2014**, *23* (12), 125027. <https://doi.org/10.1088/0964-1726/23/12/125027>.
- (40) Ionov, L. Hydrogel-Based Actuators: Possibilities and Limitations. *Materials Today* **2014**, *17* (10), 494–503. <https://doi.org/10.1016/j.mattod.2014.07.002>.
- (41) Adamo, C. B.; Junger, A. S.; Jesus, D. P. de. APPLICATION OF WATER BEADS AS A NOVEL AND SIMPLE SORBENT FOR SMARTPHONE-BASED COLORIMETRIC DETERMINATION OF IRON IN WATER. *Quím. Nova* **2021**, *44*, 1360–1363.
<https://doi.org/10.21577/0100-4042.20170782>.
- (42) Sun, X.; Agate, S.; Salem, K. S.; Lucia, L.; Pal, L. Hydrogel-Based Sensor Networks: Compositions, Properties, and Applications—A Review. *ACS Appl. Bio Mater.* **2021**, *4* (1), 140–162. <https://doi.org/10.1021/acsabm.0c01011>.
- (43) Cairns, R.; Brown, J. A.; Buckley, N. A. Dangerous Toys: The Expanding Problem of Water-Absorbing Beads. *Med. J. Aust.* **2016**, *205* (11).

- (44) Richbourg, N. R.; Wancura, M.; Gilchrist, A. E.; Toubbeh, S.; Harley, B. A. C.; Cosgriff-Hernandez, E.; Peppas, N. A. Precise Control of Synthetic Hydrogel Network Structure via Linear, Independent Synthesis-Swelling Relationships. *Science Advances* **2021**, *7* (7), eabe3245. <https://doi.org/10.1126/sciadv.abe3245>.
- (45) Tomer, R.; Dimitrijevic, D.; Florence, A. T. Electrically Controlled Release of Macromolecules from Cross-Linked Hyaluronic Acid Hydrogels. *Journal of Controlled Release* **1995**, *33* (3), 405–413. [https://doi.org/10.1016/0168-3659\(94\)00115-B](https://doi.org/10.1016/0168-3659(94)00115-B).
- (46) *Swelling - Hydrogel Design*. <https://hydrogeldesign.com/swelling/> (accessed 2023-05-02).
- (47) Kim, S. J.; Park, S. J.; Kim, S. I. Swelling Behavior of Interpenetrating Polymer Network Hydrogels Composed of Poly(Vinyl Alcohol) and Chitosan. *Reactive and Functional Polymers* **2003**, *55* (1), 53–59. [https://doi.org/10.1016/S1381-5148\(02\)00214-6](https://doi.org/10.1016/S1381-5148(02)00214-6).
- (48) Vashist, S. K.; Lam, E.; Hrapovic, S.; Male, K. B.; Luong, J. H. T. Immobilization of Antibodies and Enzymes on 3-Aminopropyltriethoxysilane-Functionalized Bioanalytical Platforms for Biosensors and Diagnostics. *Chem. Rev.* **2014**, *114* (21), 11083–11130. <https://doi.org/10.1021/cr5000943>.
- (49) Hosseini, S.; Ibrahim, F.; Djordjevic, I.; Koole, L. H. Recent Advances in Surface Functionalization Techniques on Polymethacrylate Materials for Optical Biosensor Applications. *Analyst* **2014**, *139* (12), 2933–2943. <https://doi.org/10.1039/C3AN01789C>.
- (50) Howarter, J. A.; Youngblood, J. P. Surface Modification of Polymers with 3-Aminopropyltriethoxysilane as a General Pretreatment for Controlled Wettability. *Macromolecules* **2007**, *40* (4), 1128–1132. <https://doi.org/10.1021/ma062028m>.
- (51) Knorr, R.; Trzeciak, A.; Bannwarth, W.; Gillessen, D. New Coupling Reagents in Peptide Chemistry. *Tetrahedron Letters* **1989**, *30* (15), 1927–1930. [https://doi.org/10.1016/S0040-4039\(00\)99616-3](https://doi.org/10.1016/S0040-4039(00)99616-3).
- (52) Chen, Y.-H.; He, Y.-C.; Yaung, J.-F. Exploring PH-Sensitive Hydrogels Using an Ionic Soft Contact Lens: An Activity Using Common Household Materials. *J. Chem. Educ.* **2014**, *91* (10), 1671–1674. <https://doi.org/10.1021/ed400833b>.
- (53) Schwabacher, A. W.; Lane, J. W.; Schiesher, M. W.; Leigh, K. M.; Johnson, C. W. Desymmetrization Reactions: Efficient Preparation of Unsymmetrically Substituted Linker Molecules. *The Journal of Organic Chemistry* **1998**, *63* (5), 1727–1729. <https://doi.org/10.1021/JO971802O>.
- (54) Ek, S.; Iiskola, E. I.; Niinistö, L. Gas-Phase Deposition of Aminopropylalkoxysilanes on Porous Silica. *Langmuir* **2003**, *19* (8), 3461–3471. <https://doi.org/10.1021/la020869q>.
- (55) Acres, R. G.; Ellis, A. V.; Alvino, J.; Lenahan, C. E.; Khodakov, D. A.; Metha, G. F.; Andersson, G. G. Molecular Structure of 3-Aminopropyltriethoxysilane Layers Formed on Silanol-Terminated Silicon Surfaces. *J. Phys. Chem. C* **2012**, *116* (10), 6289–6297. <https://doi.org/10.1021/jp212056s>.
- (56) Zhu, M.; Lerum, M. Z.; Chen, W. How To Prepare Reproducible, Homogeneous, and Hydrolytically Stable Aminosilane-Derived Layers on Silica. *Langmuir* **2012**, *28* (1), 416–423. <https://doi.org/10.1021/la203638g>.
- (57) Munief, W.-M.; Heib, F.; Hempel, F.; Lu, X.; Schwartz, M.; Pachauri, V.; Hempelmann, R.; Schmitt, M.; Ingebrandt, S. Silane Deposition via Gas-Phase Evaporation and High-Resolution Surface Characterization of the Ultrathin Siloxane Coatings. *Langmuir* **2018**, *34* (35), 10217–10229. <https://doi.org/10.1021/acs.langmuir.8b01044>.

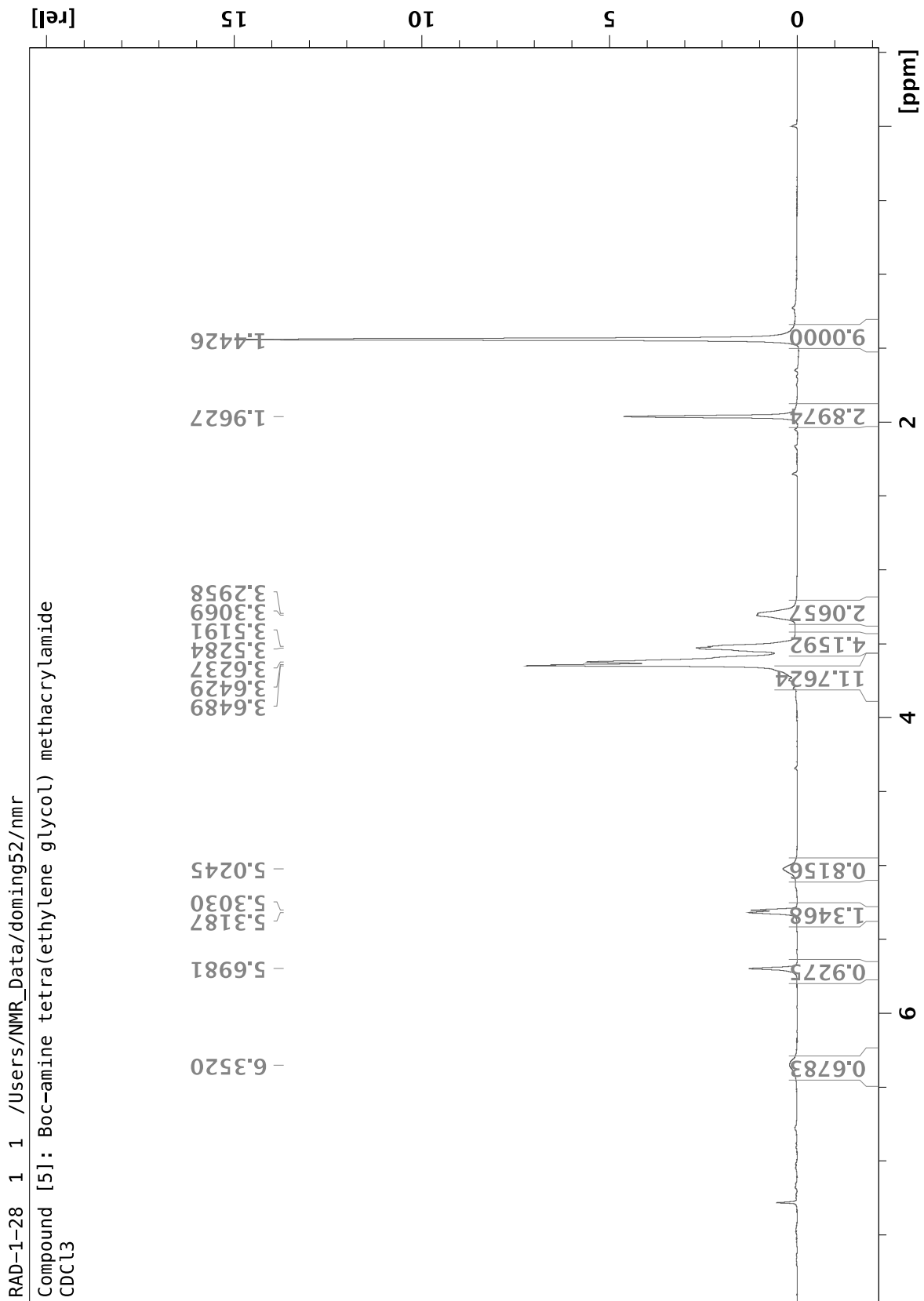
- (58) Cras, J. J.; Rowe-Taitt, C. A.; Nivens, D. A.; Ligler, F. S. Comparison of Chemical Cleaning Methods of Glass in Preparation for Silanization. *Biosensors and Bioelectronics* **1999**, *14* (8), 683–688. [https://doi.org/10.1016/S0956-5663\(99\)00043-3](https://doi.org/10.1016/S0956-5663(99)00043-3).
- (59) Ek, S.; Iiskola, E. I.; Niinistö, L. Atomic Layer Deposition of Amino-Functionalized Silica Surfaces Using N-(2-Aminoethyl)-3-Aminopropyltrimethoxysilane as a Silylating Agent. *J. Phys. Chem. B* **2004**, *108* (28), 9650–9655. <https://doi.org/10.1021/jp0499629>.
- (60) Magano, J. Large-Scale Amidations in Process Chemistry: Practical Considerations for Reagent Selection and Reaction Execution. *Org. Process Res. Dev.* **2022**, *26* (6), 1562–1689. <https://doi.org/10.1021/acs.oprd.2c00005>.

Appendix : Spectra

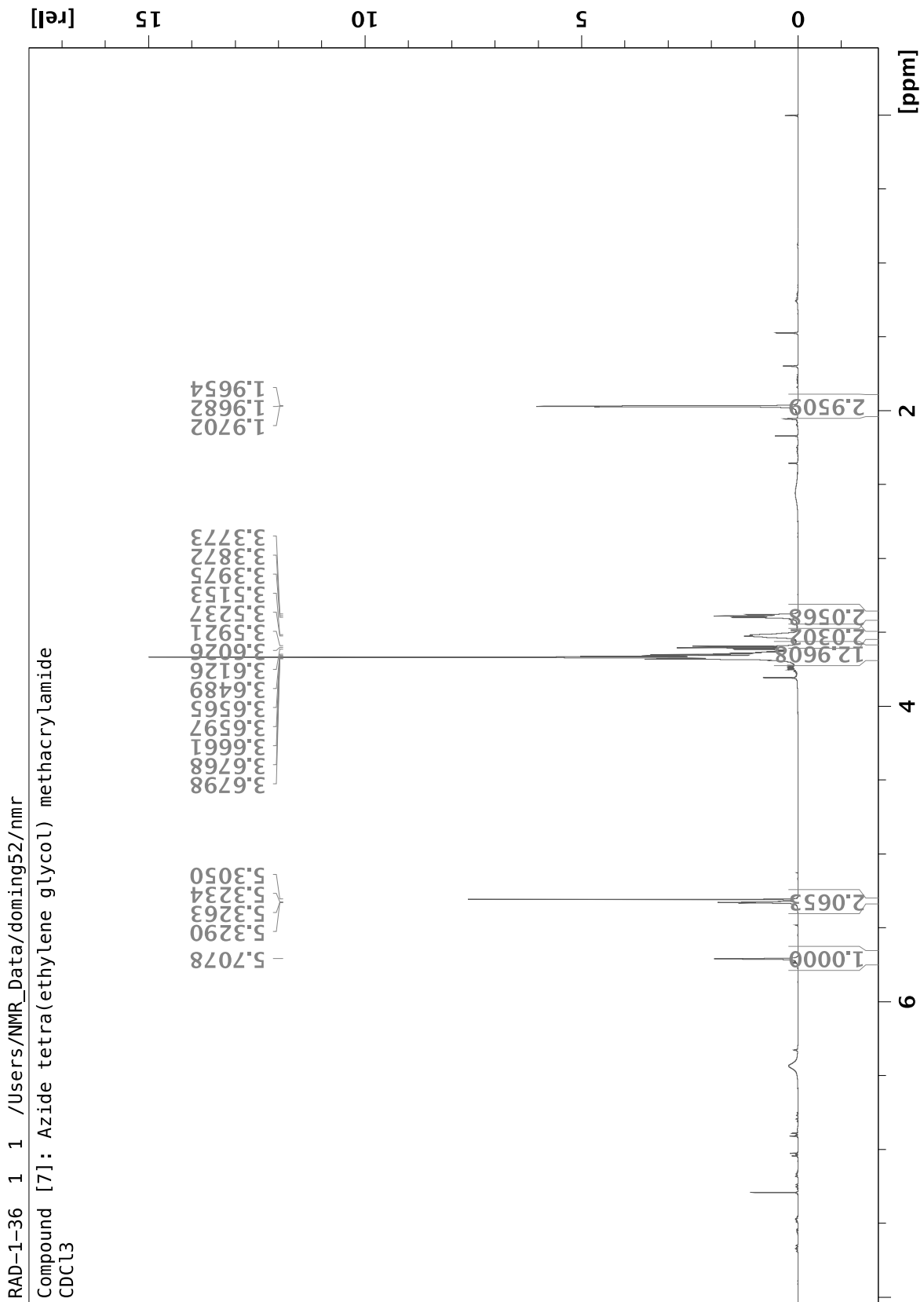
Spectrum 1: Compound [3] ¹ H NMR (500 MHz CDCl ₃).....	119
Spectrum 2: Compound [4] ¹ H NMR (500 MHz CDCl ₃).....	120
Spectrum 3: Compound [5] ¹ H NMR (500 MHz CDCl ₃).....	121
Spectrum 4: Compound [7] ¹ H NMR (500 MHz CDCl ₃).....	122
Spectrum 5: Compound [8] ¹ H NMR (500 MHz CDCl ₃).....	123
Spectrum 6: Compound [10] ¹ H NMR (500 MHz CDCl ₃).....	124
Spectrum 7: Compound [12a] 3 h ¹ H NMR (500 MHz CDCl ₃).....	125
Spectrum 8: Compound [12b] 3 h ¹ H NMR (500 MHz CDCl ₃).....	125
Spectrum 9: Compound [12a] 6 h ¹ H NMR (500 MHz CDCl ₃).....	126
Spectrum 10: Compound [12b] 6 h ¹ H NMR (500 MHz CDCl ₃).....	126
Spectrum 11: Compound [12a] 9 h ¹ H NMR (500 MHz CDCl ₃).....	127
Spectrum 12: Compound [12b] 9 h ¹ H NMR (500 MHz CDCl ₃).....	127
Spectrum 13: Compound [13] ¹ H NMR (500 MHz, DMSO-d ₆).....	128
Spectrum 14: Compound [15] ¹ H NMR (500 MHz CDCl ₃).....	129
Spectrum 15: Compound [16] ¹ H NMR (500 MHz D ₂ O).....	130
Spectrum 16: Compound [18] ¹ H NMR (500 MHz CDCl ₃).....	131
Spectrum 17: Compound [19] ¹ H NMR (500 MHz CDCl ₃).....	132
Spectrum 18: Compound [20] ¹ H NMR (500 MHz DMSO-d ₆).....	133
Spectrum 19: Compound [21] ¹ H NMR (500 MHz D ₂ O).....	134
Spectrum 20: Compound [22] ¹ H NMR (500 MHz D ₂ O).....	135
Spectrum 21: Compound [27] ¹ H NMR (500 MHz CDCl ₃).....	136
Spectrum 22: Compound [27] ¹ H NMR (500 MHz CDCl ₃) 7.15-8.05 ppm	137



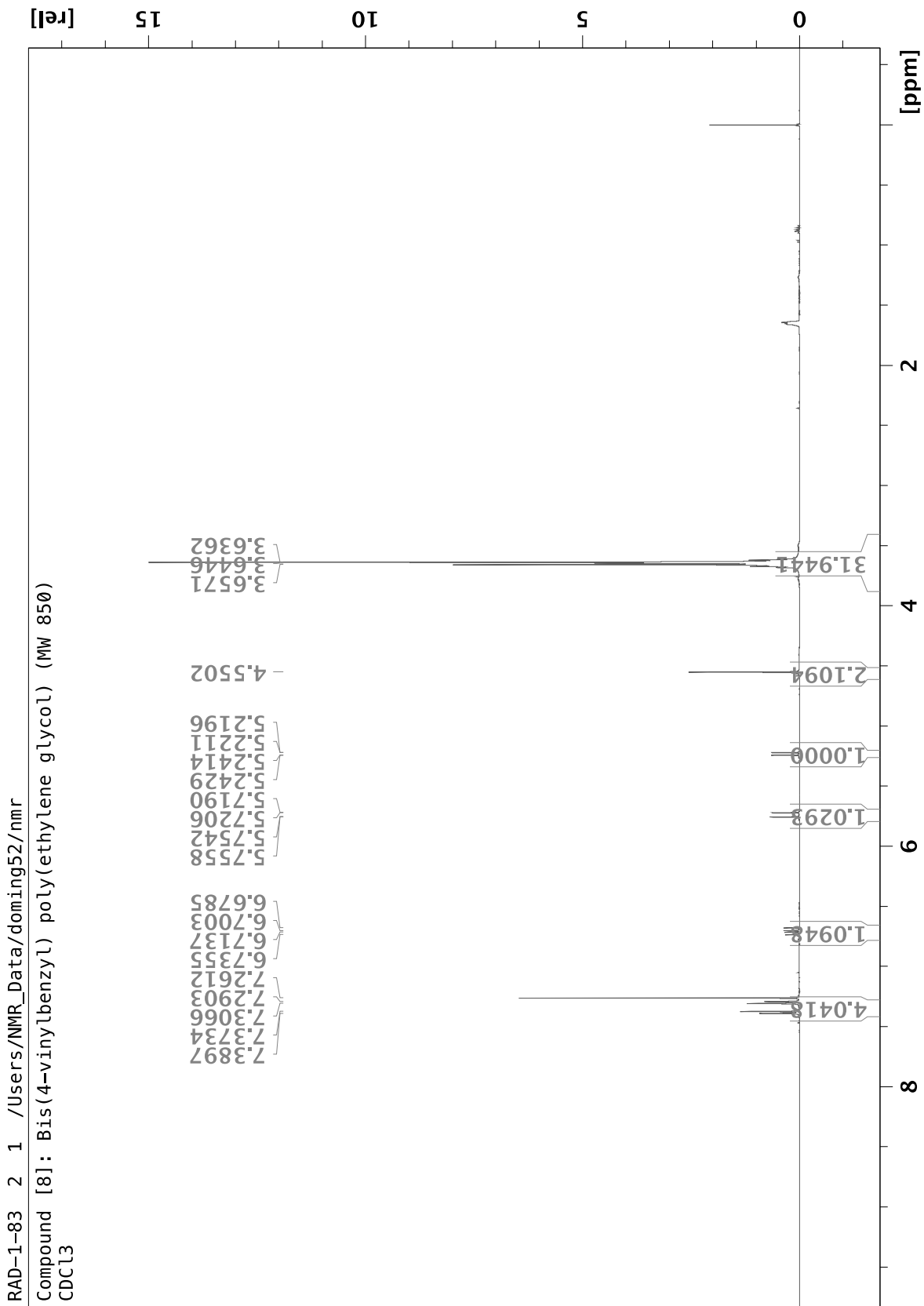
Spectrum 2: Compound [4] ¹H NMR (500 MHz, CDCl₃)



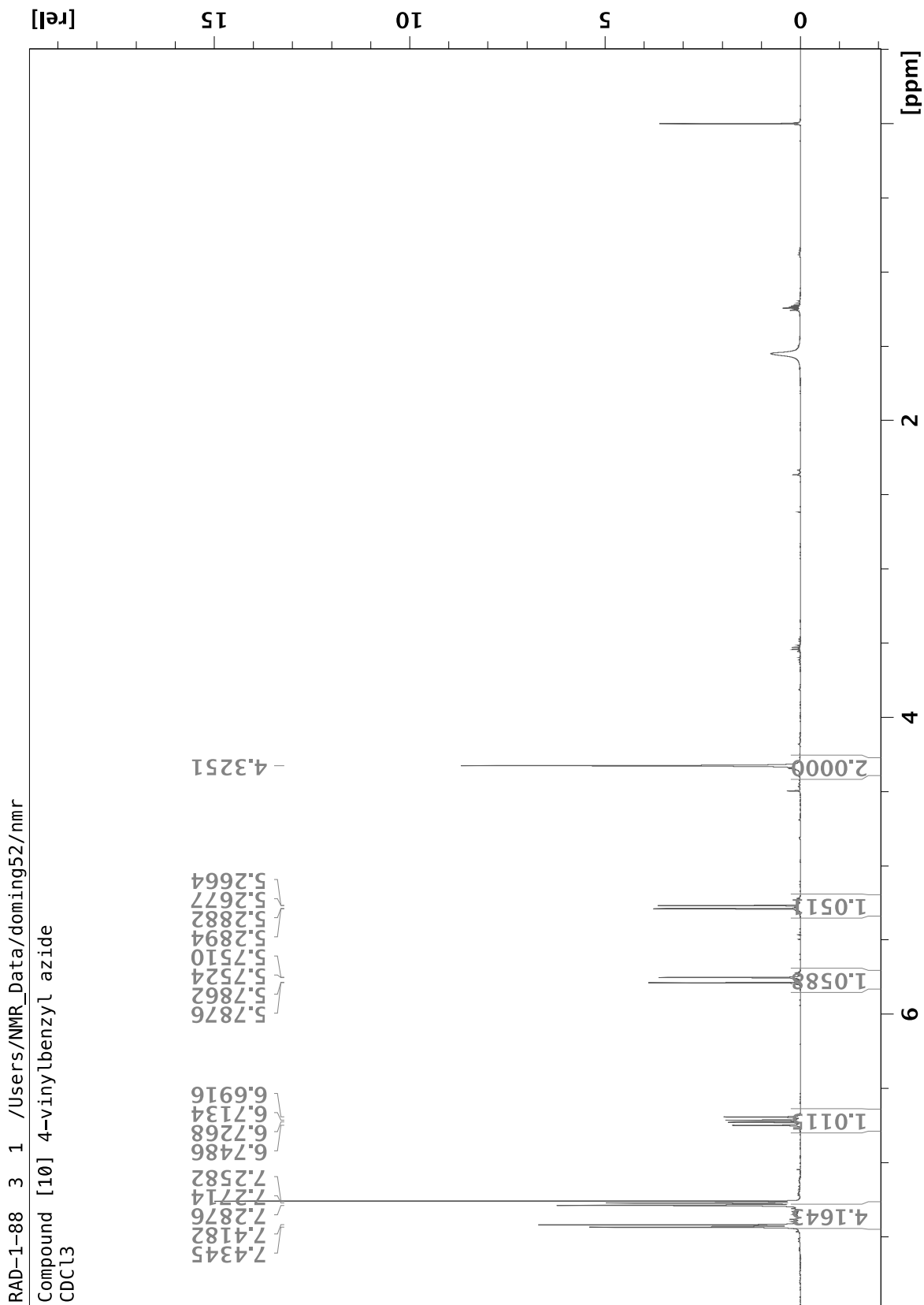
Spectrum 3: Compound [5] ¹H NMR (500 MHz, CDCl₃)



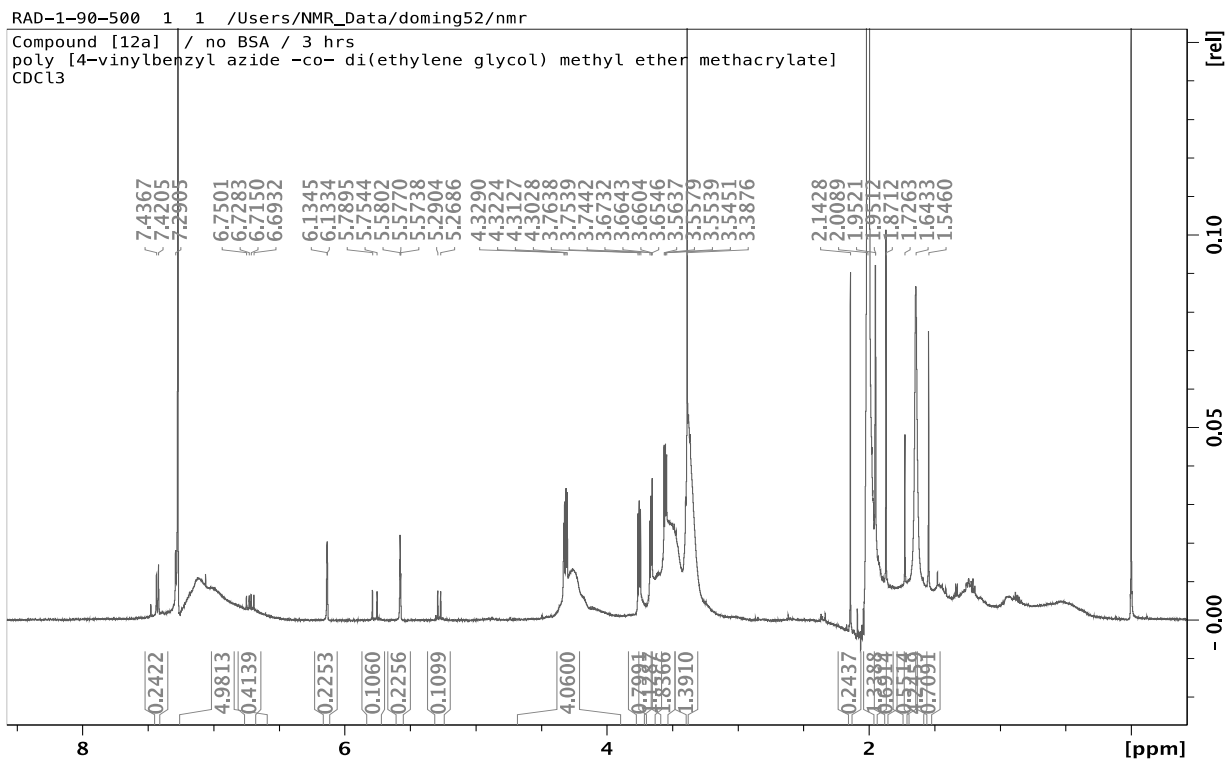
Spectrum 4: Compound [7] ¹H NMR (500 MHz, CDCl₃)



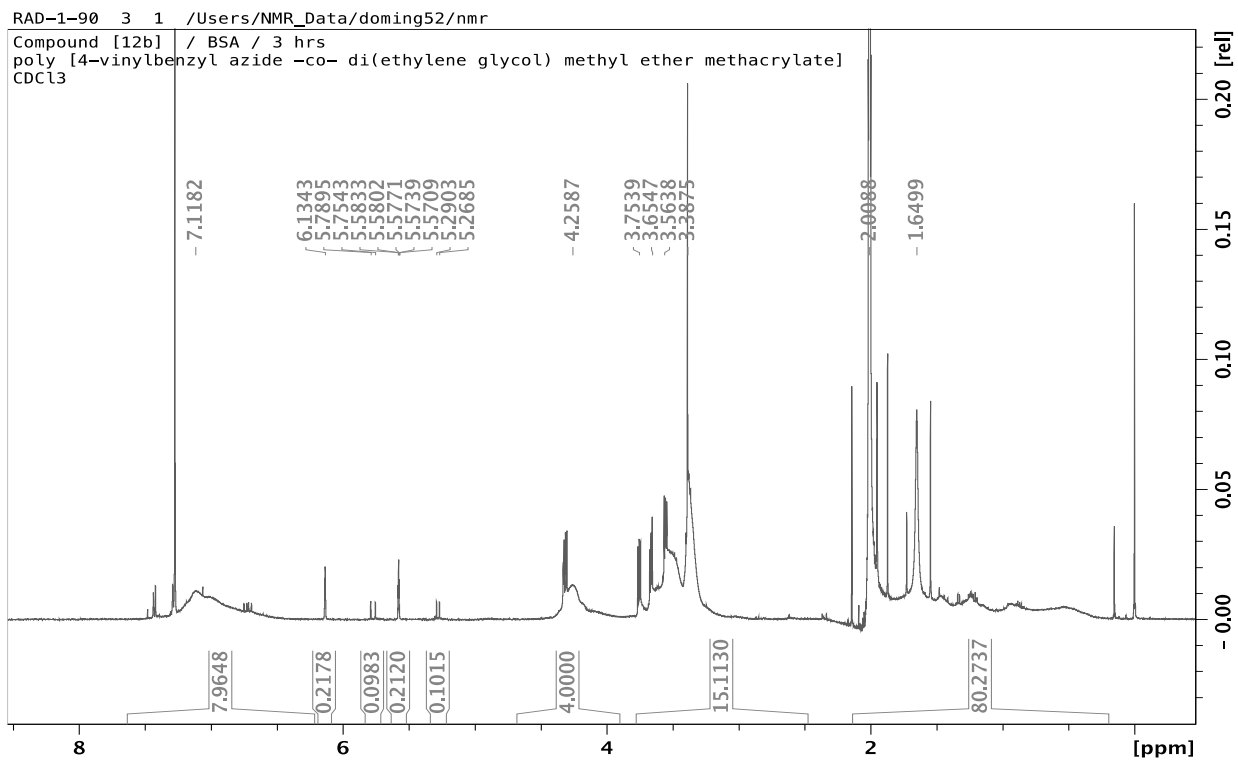
Spectrum 5: Compound [8] ¹H NMR (500 MHz, CDCl₃)



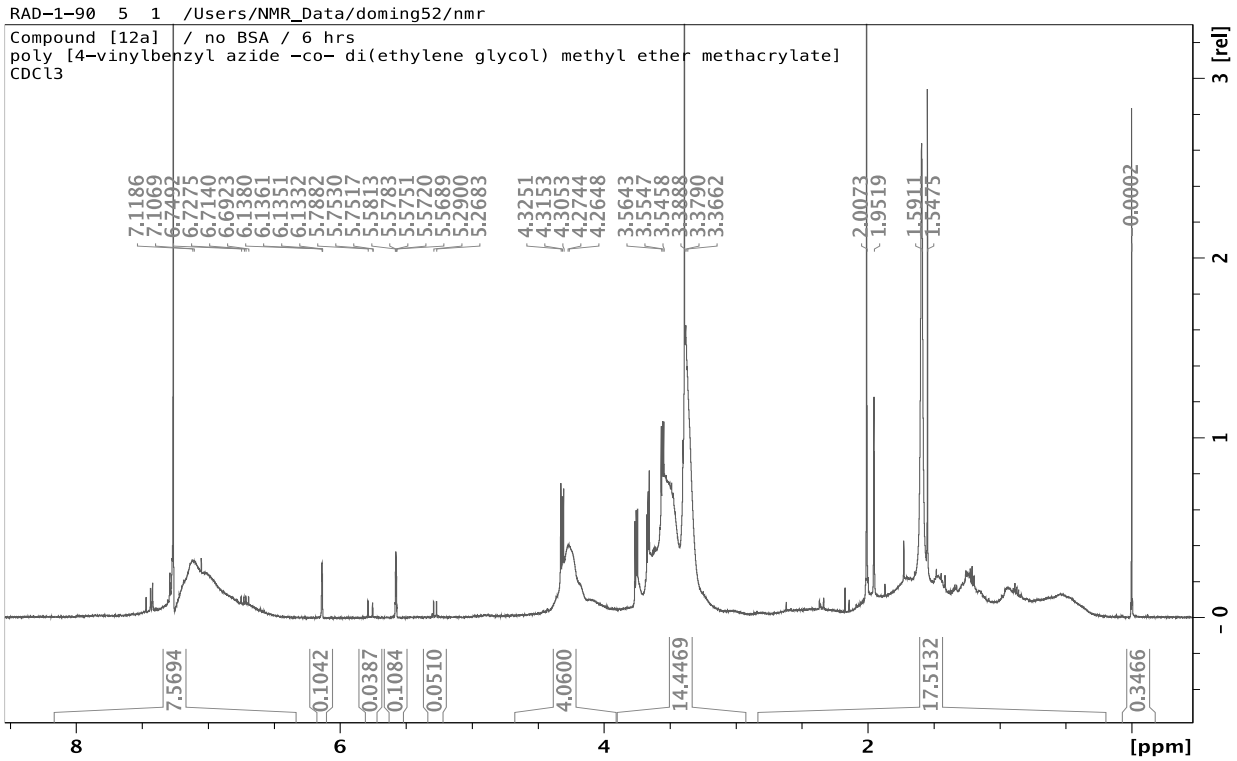
Spectrum 6: Compound [10] ¹H NMR (500 MHz CDCl₃)



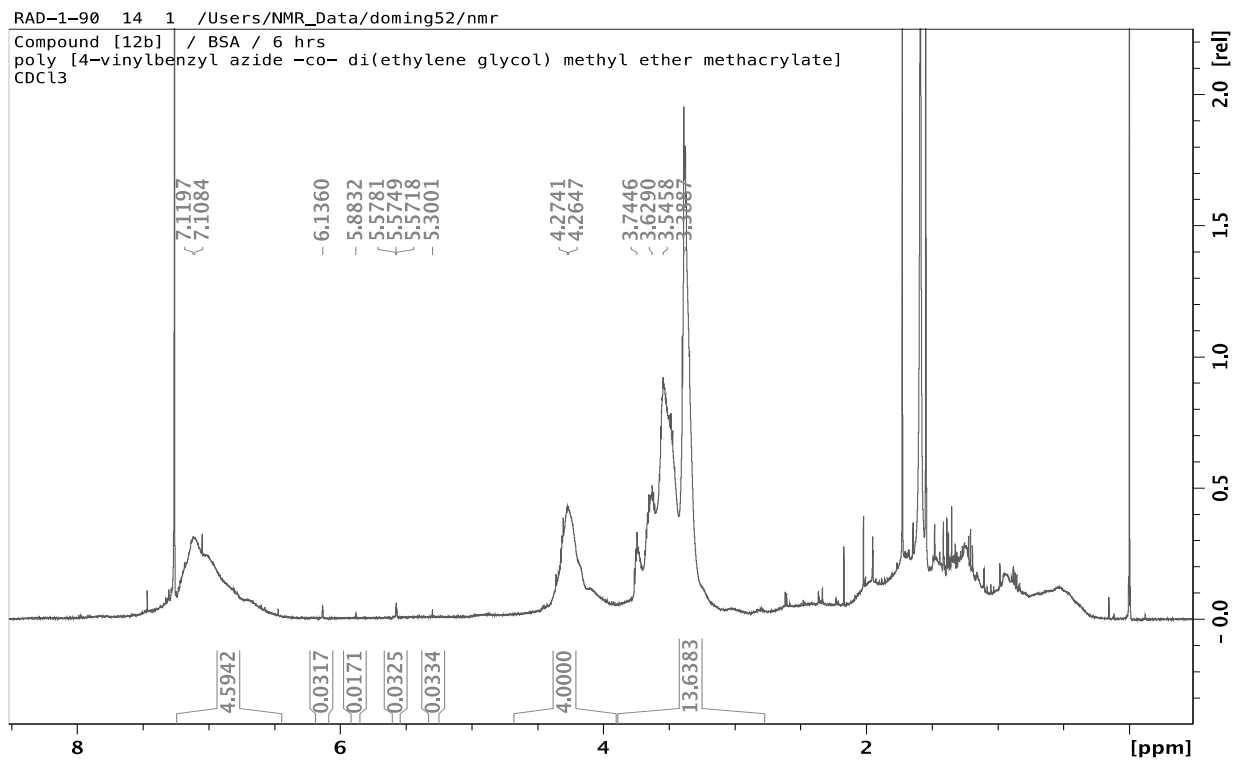
Spectrum 7: Compound [12a] 3 h ¹H NMR (500 MHz CDCl₃)



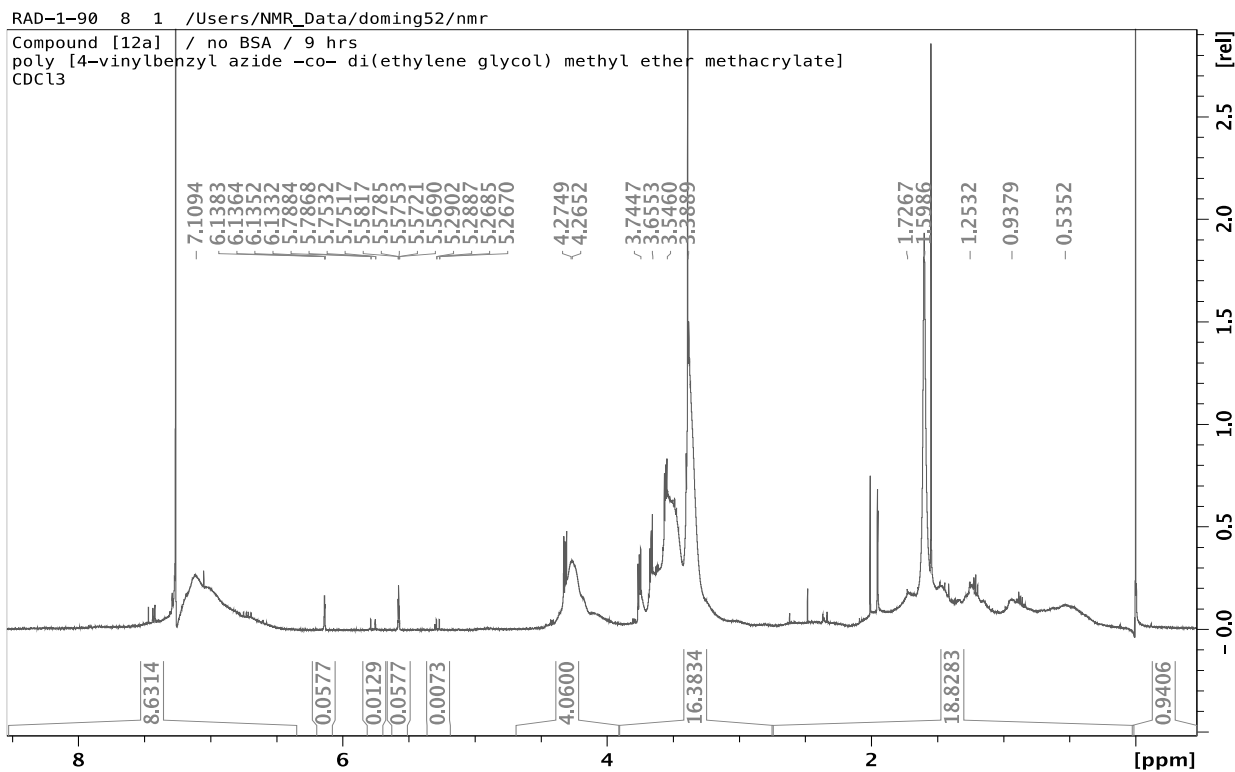
Spectrum 8: Compound [12b] 3 h ¹H NMR (500 MHz CDCl₃)



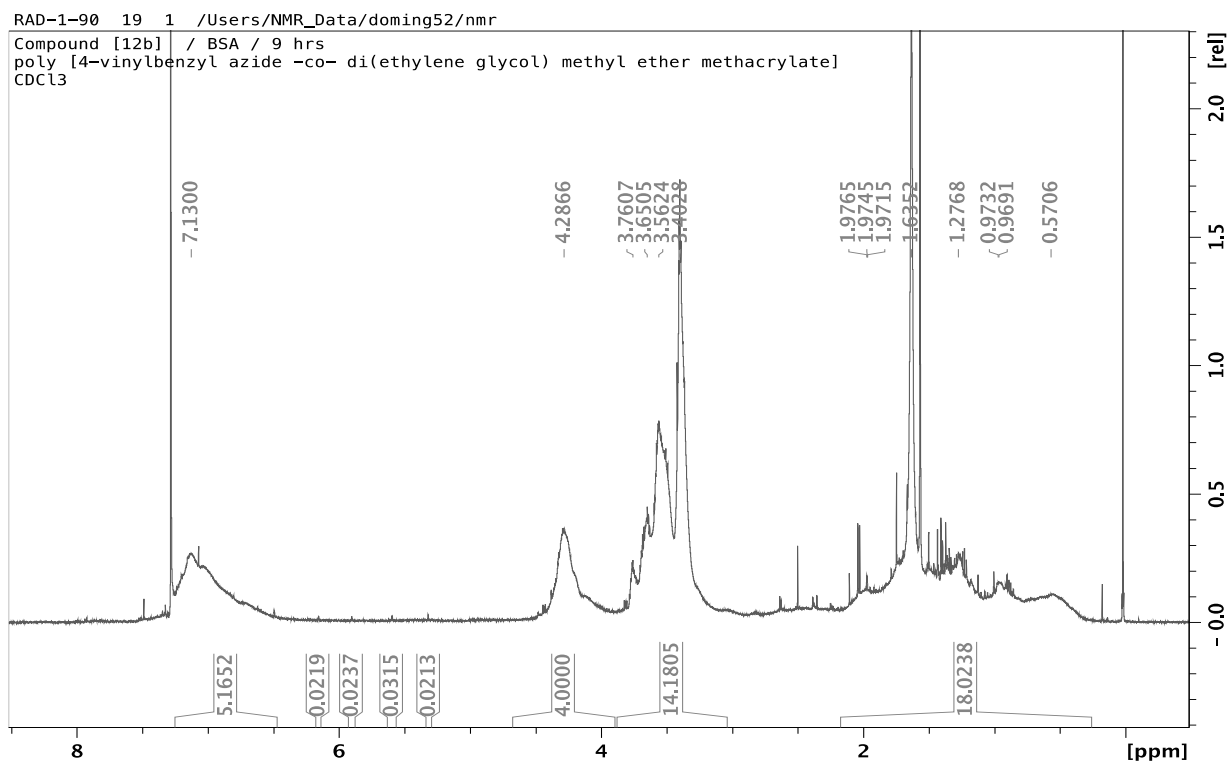
Spectrum 9: Compound [12a] 6 h ¹H NMR (500 MHz CDCl₃)



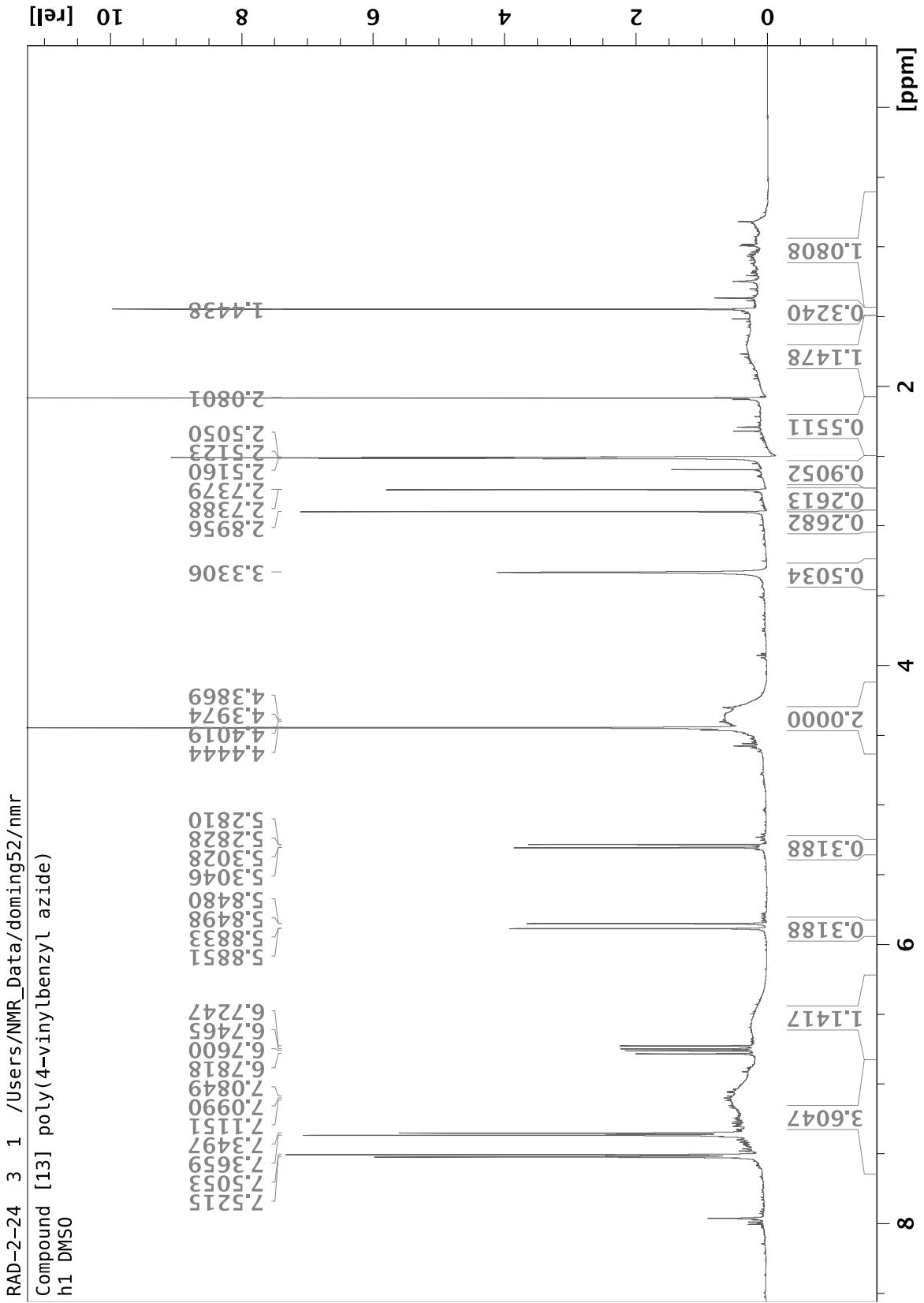
Spectrum 10: Compound [12b] 6 h ¹H NMR (500 MHz CDCl₃)



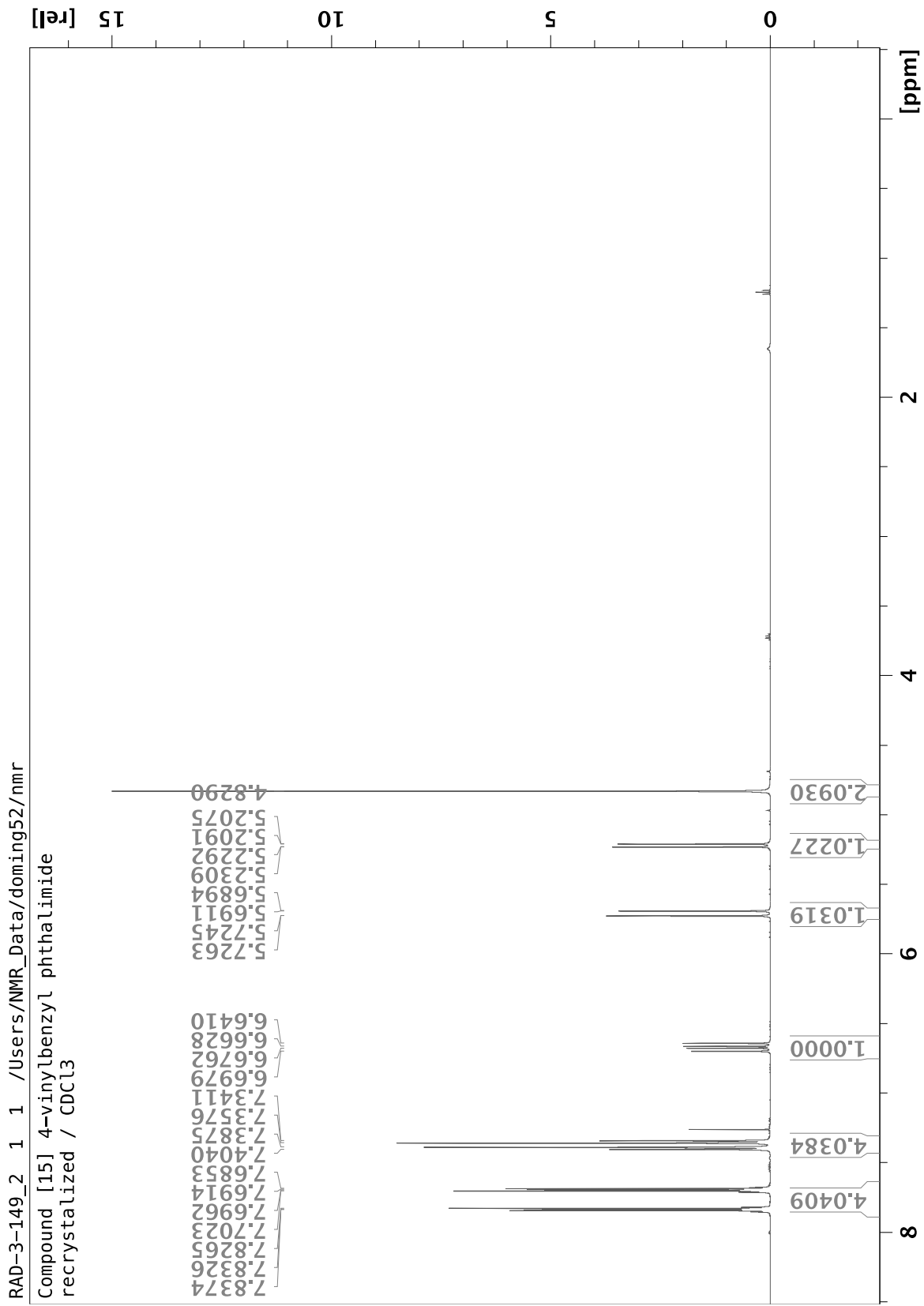
Spectrum 11: Compound [12a] 9 h ¹H NMR (500 MHz CDCl₃)



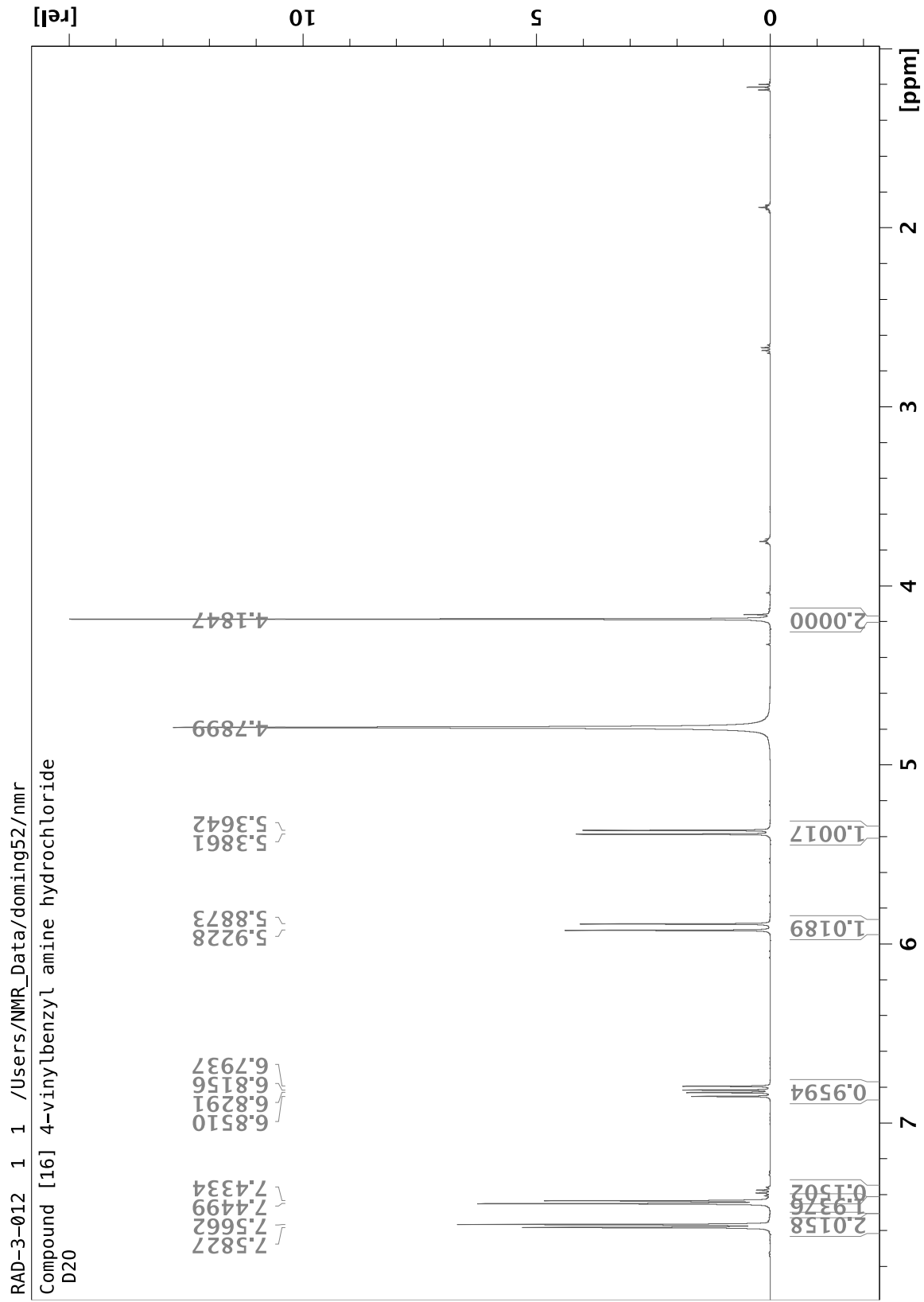
Spectrum 12: Compound [12b] 9 h ¹H NMR (500 MHz CDCl₃)



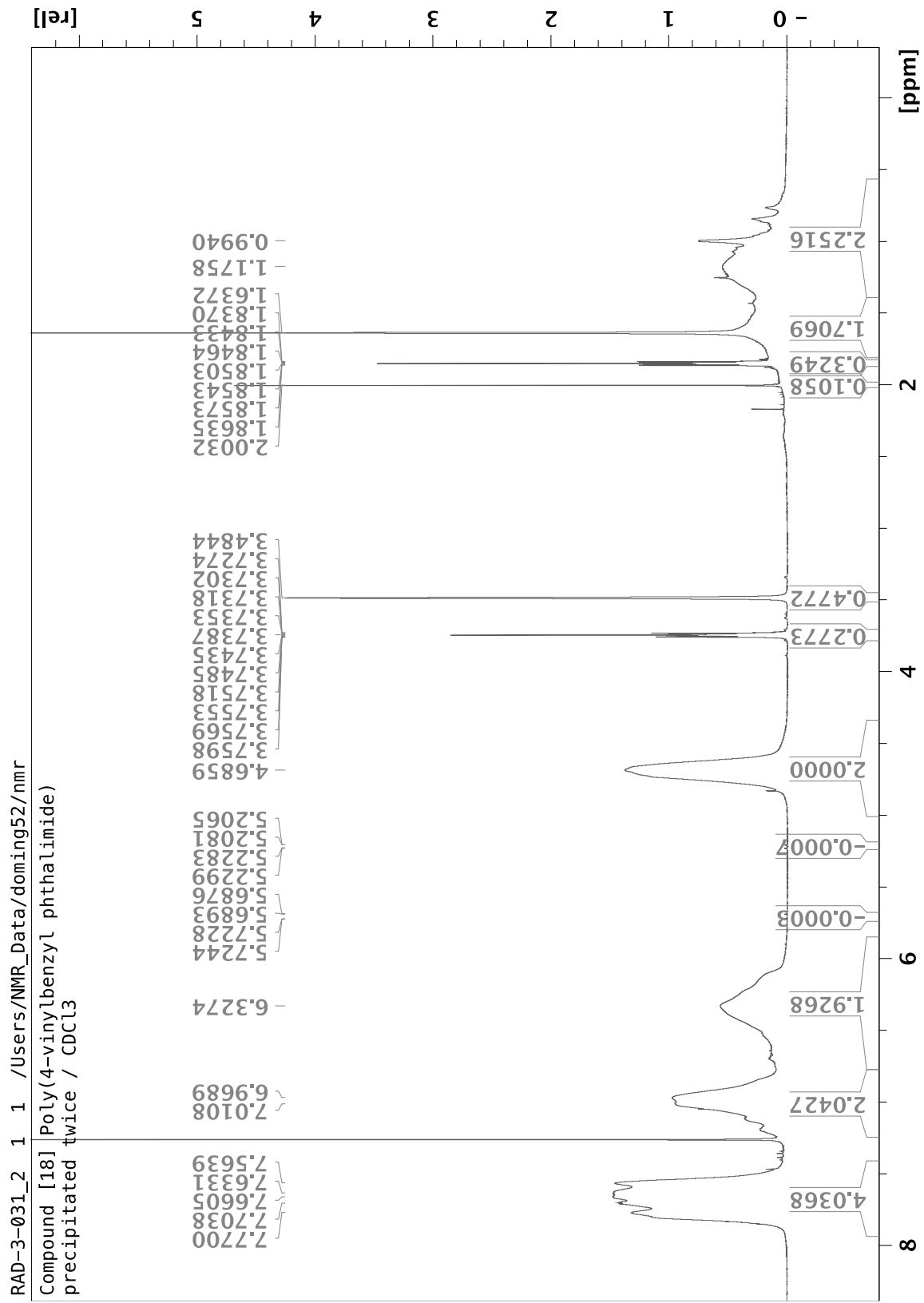
Spectrum 13: Compound [13] ^1H NMR (500 MHz DMSO- d_6)



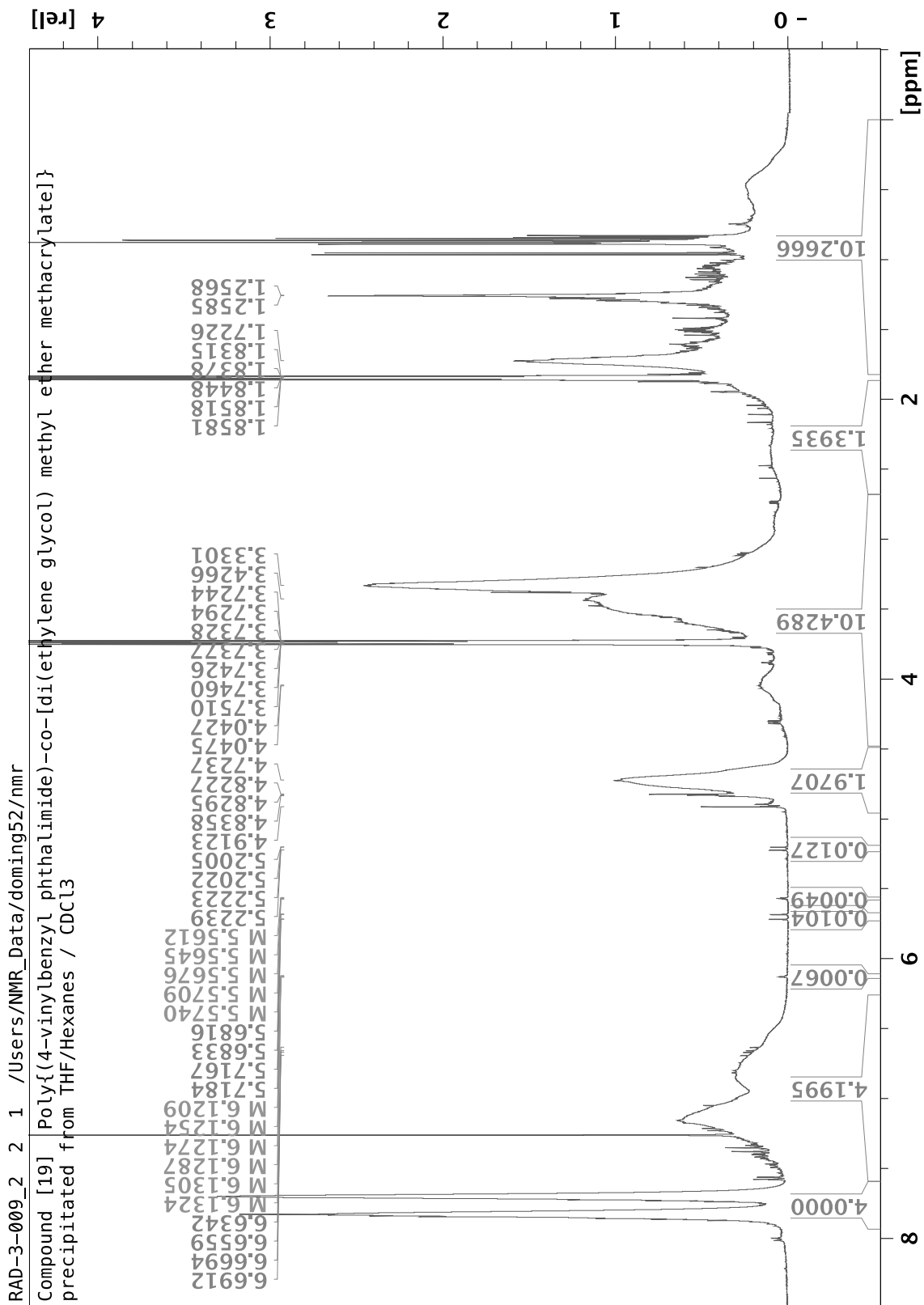
Spectrum 14: Compound [15] ¹H NMR (500 MHz, CDCl₃)



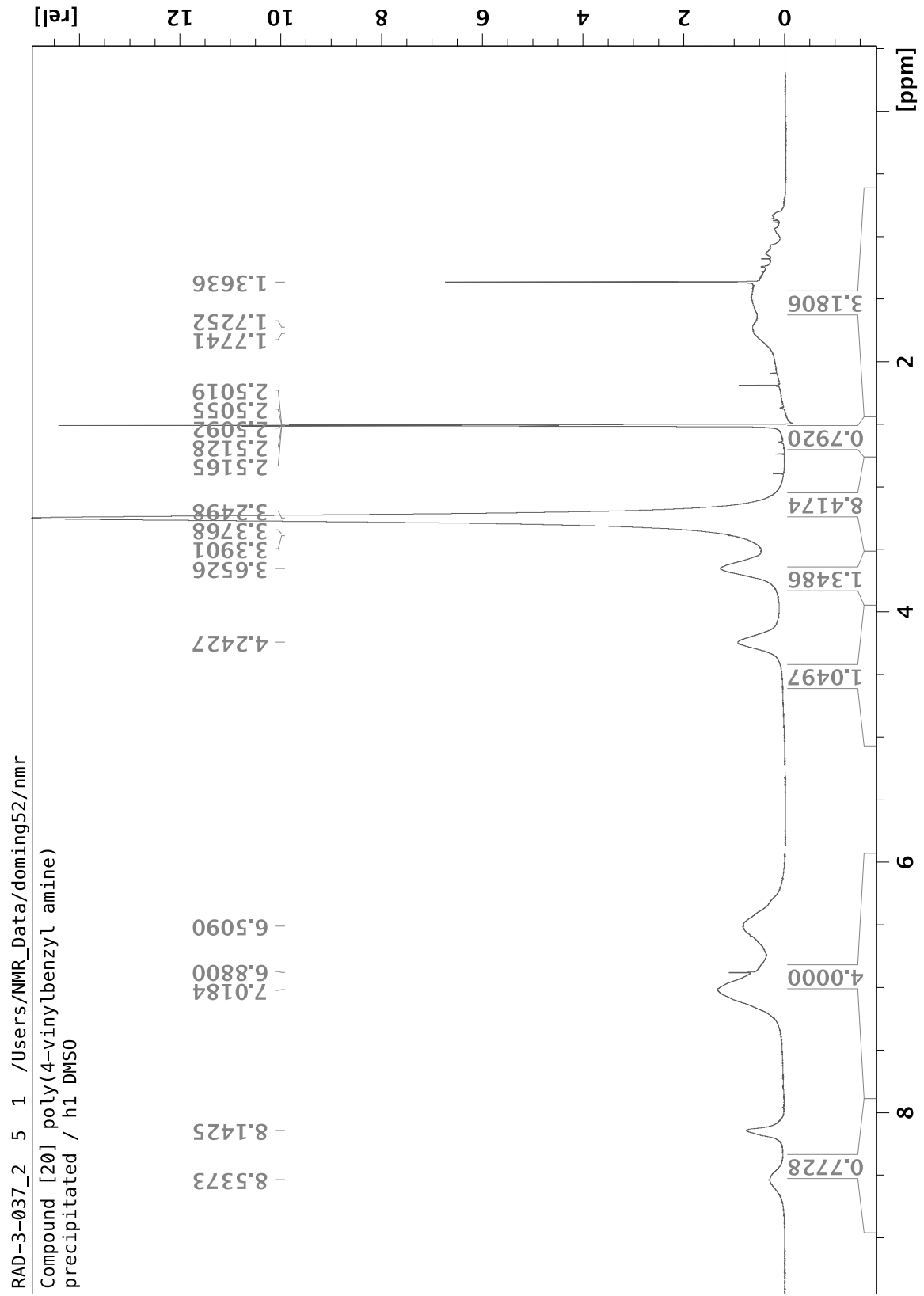
Spectrum 15: Compound [16] ¹H NMR (500 MHz D₂O)



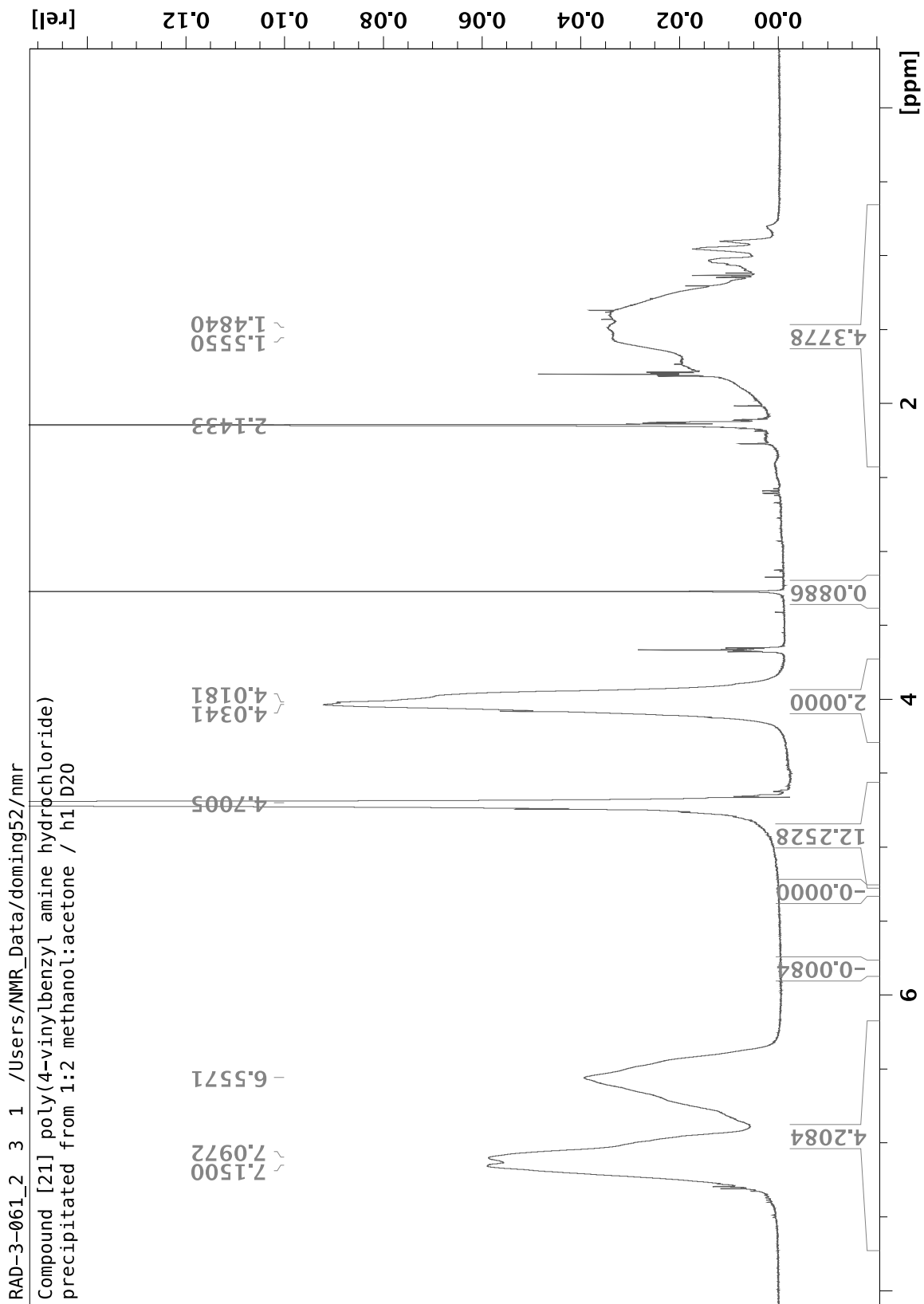
Spectrum 16: Compound [18] ¹H NMR (500 MHz, CDCl₃)



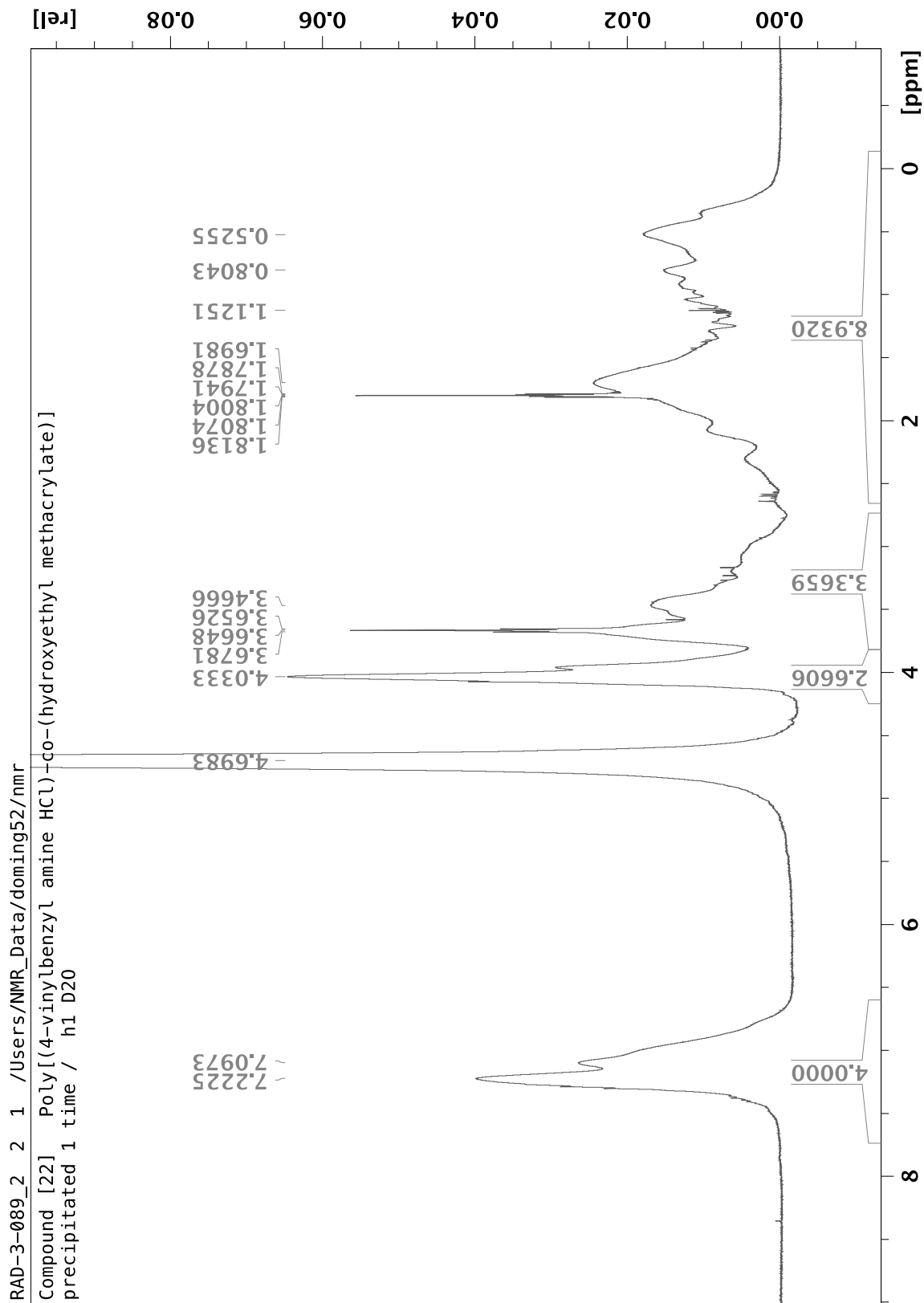
Spectrum 17: Compound [19] ¹H NMR (500 MHz, CDCl₃)



Spectrum 18: Compound [20] ¹H NMR (500 MHz DMSO-d6)

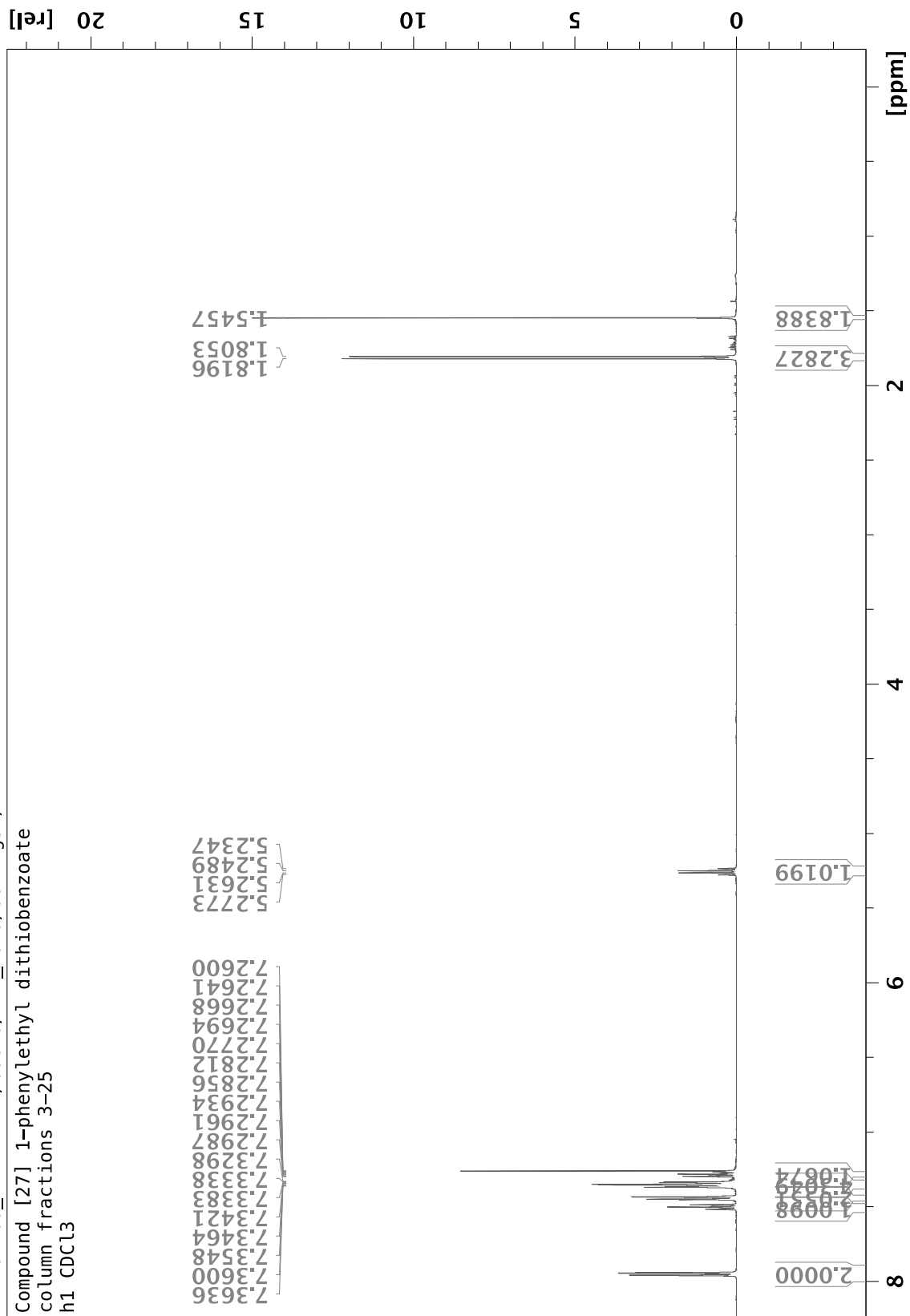


Spectrum 19: Compound [21] ^1H NMR (500 MHz D_2O)

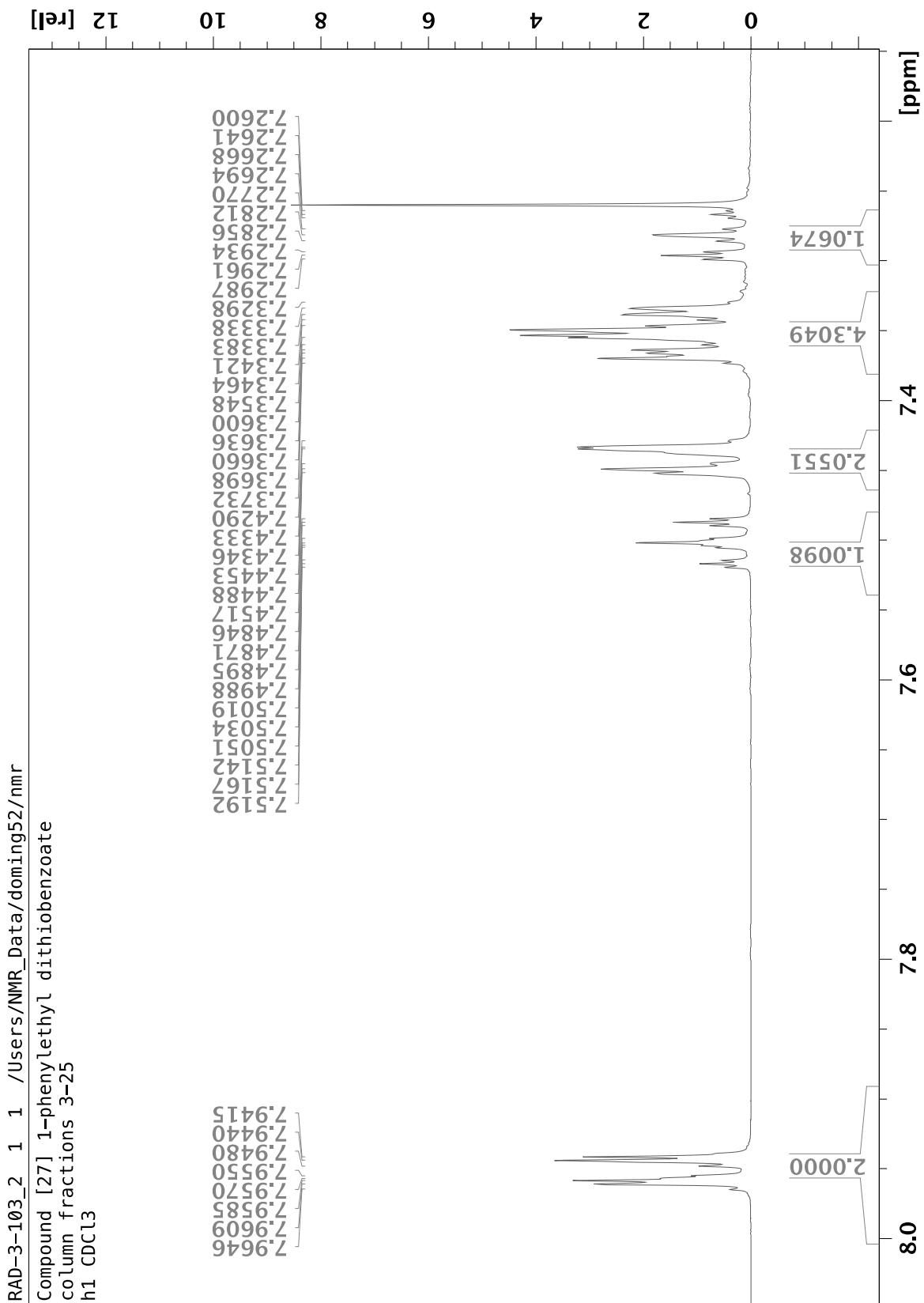


Spectrum 20: Compound [22] ^1H NMR (500 MHz D_2O)

RAD-3-103_2_1_1 /Users/NMR_Data/doming52/nmr
 Compound [27] 1-phenylethyl dithiobenzoate
 column fractions 3-25
 h1 CDCl3



Spectrum 21: Compound [27] ¹H NMR (500 MHz, CDCl₃)



Spectrum 22: Compound [27] ^1H NMR (500 MHz, CDCl_3) 7.15-8.05 ppm